7. Function

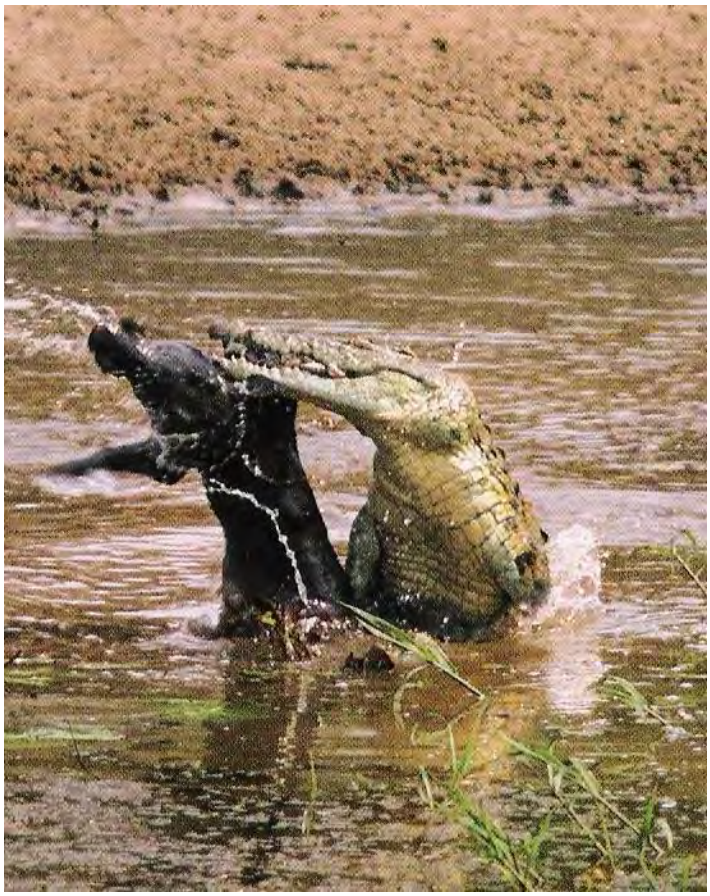

A warthog *Phacochoerus africanus* being shaken by a Nile crocodile (*Crocodylus niloticus*). Large crocodiles use violent shaking to kill or dismember certain size classes of prey – this behaviour can form the basis of a mechanical scenario within a biomechanical analysis (image taken from Ross and Garnett 1989).

"But to judge of the relative merits of conflicting analogies is one of the most delicate and difficult points of comparative anatomy".

Rev. William D. Conybeare (1822, p.104)

7.1 Form and function in *Kronosaurus queenslandicus*

The aim of this thesis is to generate a reconstruction of the feeding ecology of *Kronosaurus queenslandicus*. With living oceanic predators, feeding ecology can be described as a niche comprising quantitative and qualitative components; (1) the specific habitat(s) where feeding occurs (e.g. coastal, pelagic), (2) the type of food (e.g. plankton, fish, cephalopods), and (3) the size range of prey taken. For fossil species, habitat and prey type can be inferred on the basis of taphonomic and palaeoenvironmental data (see Chapter 8), in addition to considerations based on body size (Chapter 6). The present chapter will focus on the latter aspect of niche, i.e. prey size.

Can ecological function be predicted from biological structure?

Documenting the range of prey size in living predators is a challenging task: for example, only recently has it been evident that the African lion *Panthera leo*, one of the best studied predators, does prey upon African elephants (Hayward and Kerley 2005, Joubert and Joubert 1997). For extinct predators all of the problems associated with palaeontological datasets make the exercise even more difficult. The extent of the challenge is illustrated by considering the range of prey size taken by the species often cited as a modern analogue for large pliosaurs such as *Kronosaurus*, the killer whale *Orcinus orca*. The documented prey size for killer whales ranges from small clupeids (specifically, Atlantic herring *Clupea harengus*, which have a body mass of less than 1 kg) to the largest animal on the planet, the blue whale *Balaeonoptera musculus*, which exceeds 100,000 kg in mass (Corkeron and Connor 1999, Jefferson et al. 1991, Similä et al. 1996): this is a size range of six orders of magnitude and may be the widest range of prey size taken by any predator bar humans.

The comparison between pliosaurs and killer whales is made on the basis of body size, tooth morphology, and the overall 'robusticity' of the skull (Massare 1987). However, whether the catholic diet of killer whales should serve as a guide to reconstructions of pliosaur ecology is not clear. At both ends of its niche, the ability of killer whales to catch their prey depends as much upon complex behaviours as it does the physical characteristics of their feeding apparatus. Large whales are subdued by pack hunting techniques, whilst herring are captured through a combination of cooperative herding and strikes with the caudal flukes that stun the fish. In each situation, there is no evidence that a solitary killer whale, using only the power and speed of its jaws, would be able to catch either the very largest or the very smallest of the prey in its niche, underlining the benefits of its complex nervous system.

Of course, reconstructions of niche in extinct predators are unable to directly include details of behaviour. The importance of 'behavioural plasticity' in determining the niche realised by modern predators has been emphasised; Lauder (1995) analysed comprehensive ecological and morphological data for species of aquatic predators, including teleost fish and salamanders, and showed that the ecological function in these species could not be predicted from their morphological structure. Lauder further concluded that the plasticity of the nervous system acts as a "wildcard", limiting the extent to which ecology can be inferred from structure alone.

Lauder's analysis does not present an encouraging context for attempts, such as this one, to reconstruct ecology in fossil species; indeed, Lauder considered that attempts to predict function from structure were optimistic (Lauder 1995). The implications of Lauder's conclusions are of obvious importance to palaeobiological analyses: yet, I am not aware of any attempts to address this issue directly[1]. A critical assessment of that work is beyond the scope of the present study, but a potentially important point is the measurement of niche that Lauder focused upon in his analysis. Niche theory distinguishes between fundamental (sometimes called potential) niche, and realised niche. The realised niche is the description of the actual ecology of a sampled population, whilst the fundamental niche is the total range of ecologies that a species is theoretically capable of. It is arguable that the fundamental niche (the maximum

[1] But see Plotnick and Beaumiller (2000).

range of possible feeding ecology) will be determined by, amongst other factors, the mechanical limits of the skeleton (Wroe et al. 2005), whilst the realised niche (the actual feeding ecology observed within an individual or a population) will be determined by the environmental context and the animal's behaviour. Although this logic has not been explicitly tested, some analyses have found a relationship between fundamental niche and functional morphology; specifically, maximum recorded prey size for a species (as a proxy for the upper limit of fundamental niche) and bite force in terrestrial carnivores (Meers 2003, Wroe et al. 2005). It is possible that the difference between the optimism of a 'functionalist' paradigm of eco-morphology, and the plasticity of a 'behaviouralist' paradigm, lies at least in part with the basic ecological concepts that are examined.

For the present analysis, I assume that there is a logical link between functional morphology and fundamental niche. On the basis of that assumption, it is postulated that biomechanical analyses can be used to interpret palaeoecology. It should be emphasised that this assumption is of great potential importance to functional morphologists and ecologists, and deserves further exploration. For now, the behavioural plasticity that allows killer whales to expand the breadth of their niche is regarded as being the exception that may one day prove the rule – but first a better understanding of the rules that relate structure to function is required.

The biomechanics of feeding ecology in marine predators

The array of behaviours used by predators to catch and kill different prey is complex, and the importance of mechanical aspects in each of these varies. A systematic approach, such as the 'paradigm' analysis used by Taylor (1987) can be useful in identifying the relevant mechanics. The following overview considers the different components of predatory behaviour used by large marine/ aquatic carnivores.

Predation can be conceptualised as involving four major components; detection, capture, killing (disabling), and processing. Skull mechanics play a different role in each of these: detection typically involves the capabilities of the nervous system and sensory organs, but biomechanical factors are more important in the other phases. For a predator such as *Kronosaurus* feeding on relatively small prey (e.g., 10 kg or less),

the forces required to kill the prey are unlikely to present any difficulties in terms of skull mechanics, and as far as processing is concerned, the prey can be swallowed whole. For small prey, it is prey capture that is much more likely to be limited by mechanics; whilst the overall speed of a large predator is likely to be sufficient that prey cannot outrun it, smaller animals are usually much more agile in the water. The speed with which the feeding apparatus can be deployed depends upon its overall dimensions and hydrodynamic properties: elongate, thin jaws can be swept precisely through the water with rapid speed, increasing the ability of large predators to capture small prey. In several species of crocodile, and in bottlenose dolphins, techniques for maximising capture rate have been described, including the use of the body and tail to prevent escape by the fish in restricted waterways.

For prey at the opposite end of the size spectrum, skull mechanics is unlikely to be a limiting factor in prey capture; as long as the predator is able to get itself close to the prey, large prey are unlikely to be able to evade a strike with the jaws. The mechanical issues that are more likely to limit the ability of the predator to kill and process the prey are thus structural rather than hydrodynamic.

For killing, the range of strategies used by extant predators are illustrative: killer whales kill their largest prey, balaenopterid whales, through pack harassment of the prey and inflicting multiple bites. In some circumstances, the flukes are targeted; in others, the prey is prevented from breathing regularly; but overall the tactics used are reminiscent of the way that a wolf pack hunts large prey such as moose. In contrast, white sharks and large saltwater crocodiles are solitary hunters and maximum prey size is smaller in these species, compared with killer whales. White sharks are reputed to kill their marine mammal prey through a single, or small number, of bites that inflict a fatal wound, whilst crocodiles kill large terrestrial prey principally by drowning them.

In each case, skull mechanics are undoubtedly important: white sharks have blade-like (ziphodont) teeth which are able to cut through flesh without requiring very high bite forces (Wroe et al. 2008), allowing a large amount of flesh to be removed in one bite. In contrast, the teeth of crocodiles are conical, which have less penetration and

cutting effect for a given amount of bite force (Meers 2003), but which are better able to resist loads that are not aligned with the long axis of the tooth. In attempting to drown large quadrupeds, the jaws and teeth of a crocodile must be able to resist the forces produced by the struggling prey. In addition, crocodiles often disable or unbalance the prey by twisting their whole body rapidly around their long axis whilst holding the prey securely within the jaws (the infamous 'death roll'): this induces torsional loads to the skull and teeth (Busbey 1995, McHenry et al. 2006).

Processing of prey, i.e. reducing the carcass into portions that are small enough to swallow, presents unique challenges for an aquatic carnivore. On land, predators can remove small pieces whilst gravity holds the carcass to the ground, but in water both predator and prey are effectively weightless. The limbs of aquatic predators are often modified for aquatic locomotion and are thus unsuited for bracing the prey during attempts to tear off flesh. Consequently, aquatic predators use a number of techniques to process prey once they have made a kill. If the prey is not too large relative to the predator, it can be held up out of the water and shaken vigorously: this tactic is used by crocodiles and leopard seals. With larger prey, the inertia of the carcass can be used as an anchor: if the predator takes a bite and then moves its head rapidly relative to the prey, inertia will tend to hold the carcass in place and the predator will be able to remove a portion of flesh. The precise movements used tend to correlate with tooth morphology: white sharks feeding on a large whale carcass use rapid sideways shakes of the head which maximise the cutting action of the teeth, whilst crocodiles use the same torsional action that they also use to disable prey (but which in the context of prey processing is termed 'twist-feeding'), for which robust conical teeth are the optimal shape.

Ecological information for these species can be placed within this biomechanical context. Adult white sharks prey on pinnipeds and dolphins, but their technique for disabling marine mammals that are up to or slightly bigger than themselves is not effective against much larger animals – a single bite is not a fatal wound for a large whale. For this reason, only the infants of the large whale species are vulnerable to predation by white sharks: the sharks are, however, capable of processing a whale carcass of any size and will scavenge large whales that they have not killed

themselves. Large crocodiles (*Crocodylus porosus*, *C. niloticus*, *C. palustris*) appear to be capable of killing and processing prey at least up to their own body size, and will scavenge large elephant carcasses. For both of these large aquatic predators, maximum prey size appears to be limited by their ability to kill very large animals, rather than any limits on prey processing.

There is less information on the head movements used by killer whales to process large prey, such as a whale. Overall jaw and tooth morphology of a killer whale is more like a crocodile than a white shark, but I am unaware of any reports of twist-feeding in killer whales. Killer whales are reported to target high value portions of baleen whale carcasses, in particular the tongue, and it may be that a simple bite is sufficient for this. The details of how the feeding apparatus is used, from a functional perspective, remain unclear for killer whales.

A comparative palaeobiomechanical analysis of Kronosaurus

The biomechanics of extant aquatic predators provide a context for the reconstruction of feeding ecology in *Kronosaurus*. The approach used here will be to establish the limits of niche, in terms of prey size, using a biomechanical approach. As a starting point, the focus will be on the mechanical limits of the skull and jaws for a predator hunting on its own in open water, without considering the potential for complex behaviours to provide access to larger (e.g. pack hunting in killer whales) or smaller (pack herding, or 'body trapping', techniques used by crocodiles and various delphinids) prey than would be predicted on the basis of skull morphology alone.

Within a 'functionalist' paradigm (in the sense used above), the lower limit of prey size is likely to be determined by the hydrodynamics of the skull, whilst the upper limit can be expected to correlate with the maximum structural capacity of the jaws and teeth (McHenry et al. 2006). An analysis of the hydrodynamics of *Kronosaurus* is beyond the scope of the present work. Instead, this chapter will focus upon the use of biomechanical analysis to establish the structural capacity of the skull during simulated feeding behaviours, as a means of reconstructing maximum prey size for *Kronosaurus queenslandicus*.

The analysis will use a comparative, rather than an absolute, approach. Modelling of absolute mechanical behaviour requires detailed information on the material properties of the structure, and on the magnitude and type of loads to which the structure is exposed. From an engineering perspective, the material properties of bone are not understood in sufficient detail to permit accurate modelling of absolute mechanical performance in well studied taxa such as humans and domestic mammals, and remain largely unknown for groups such as crocodiles. Likewise, the magnitude of the loads induced by, for example, a crocodile when twist-feeding on prey of various sizes, has never been measured. In a comparative analysis, however, the absolute values of material properties and load magnitude are less important; as long as they are consistent for the structures included in the analysis, the mechanical performance of those structures can be assessed relative to each other and this approach has been used successfully in investigations of feeding ecology in various extinct and extant species of predator (McHenry et al. 2006, McHenry et al. 2007, Meers 2003, Rayfield 2005, Wroe 2007, Wroe et al. 2007a, Wroe et al. 2005). Additionally, if one or more of the specimens are from extant taxa, then the results are at least potentially testable against empirical data: this approach underlies the majority of comparative biomechanical analyses performed to date.

The comparative taxon used in this study is the saltwater crocodile *Crocodylus porosus*: in terms of basic morphology, the large species of *Crocodylus* (*C. porosus*, *C. niloticus*, *C. palustruis*, *C. acutus*) are the most similar of the living aquatic carnivores to *Kronosaurus*, and the ecology and feeding behaviour of *C. porosus* are reasonably well documented.

The structural mechanics of the skull in *Kronosaurus queenslandicus* and *Crocodylus porosus* are modelled using Finite Element Analysis (FEA), as with other recent biomechanical analyses of functional morphology in living and extinct predators and using a similar set of methods (Bourke et al. 2008, Clausen et al. 2008, McHenry et al. 2007, Moreno et al. 2008, Wroe 2007, Wroe et al. 2007a, Wroe et al. 2008, Wroe et al. 2007b). FEA of skull mechanics requires data on three components; (1) skull geometry, (2) material properties, and (3) the mechanical loads involved. The loads incurred during feeding behaviour are themselves considered in two components;

intrinsic loads, which result from biting and which are powered by the jaw adductor muscles, and extrinsic loads, which are caused by movement of the skull relative to the prey (e.g. shaking, or twist-feeding) (McHenry et al. 2007).

The details of the FEA are provided in Section 7.3 below. The calculation of intrinsic loads follows methods developed for biomechanical modelling of mammalian predators, but the present focus upon reptilian carnivores requires some modification of these techniques and these are presented in Section 7.2.

7.2 Intrinsic loads: Bite force

The bite of a predator is often its primary means of killing prey, and in various analyses of biomechanics in predatory species the loads resulting from biting are implicitly or explicitly assumed[2] to be the major source of stress upon the skull (Christiansen and Adolfssen 2005, Christiansen and Wroe 2007, Meers 2003, Thomason 1991, Wroe et al. 2005). Whatever extrinsic loads may act on a predator's skull, the cranial skeletal must be capable of handling intrinsic loads and estimates of bite force are fundamental to biomechanical analysis in predatory species.

As outlined in Chapter 2, this presents certain logistical difficulties. Outside of primates, which have been studied extensively to provide insights into human functional morphology and evolution, the most comprehensive bite force data is probably for the Virginian opossum *Didelphis virginiana* (Preuschoft and Witzel 2005, Thomason 1991, Thomason et al. 1990). Even in a relatively small animal such as this, which is amenable to laboratory based studies, obtaining reliable estimates of maximum bite force is not straightforward and often involves placing the animal under anaesthesia and then using electrical (via implanted electrodes) stimulation of the jaw muscles (Thomason et al. 1990).

Whether these methods can be extended to various species of large carnivore is unknown – the only published empirical data for non-domestic carnivorous mammals is that of Binder and van Valkenburgh for a group of captive hyaenas, where voluntary (i.e. not anaesthetised) bites were recorded (Binder and Van Valkenburgh 2000). In the absence of comprehensive empirical data, comparative analyses have used the 'dry-skull' method developed by Thomason (1991), which provides an estimate of bite force based upon skull geometry: as discussed in Chapter 2, an advantage of this method is that it can be applied to fossil and museum specimens for which soft-tissue data is lacking (Christiansen 2007a, b, Christiansen

[2] This was stated explicitly by Thomason (1991), who provided the first comparative biomechanical analysis of bite force in a range of carnivores in addition to inventing a methodological approach. Thomason contrasted the behaviour of carnivores with the various behaviours seen in horned or antlered herbivores: in the latter, intraspecific or defensive behaviours such as butting are potentially the source of the highest loads in the skull and can be expected to influence morphology. In carnivores, the forces involved with feeding are perhaps more likely to be the predominant loads acting upon the skull.

Jaw muscle (Turnbull 1970)	Functional group (Thomason 1991)
Temporalis superficialis Temporalis profundus Temporalis zygomaticus	Temporal
Masseter superficialis Masseter profundus Zygomaticomandibularis Pterygoidus internus superficialis anterior Pterygoidus internus superficialis posterior Pterygoidus internus profundus Pterygoidus externus	Masseter-pterygoid

Table 7-1: Jaw adductor muscles in carnivorans, as described in the domestic cat *Felis sylvestris catus* by Turnbull (1970) (left), and simplified for the dry-skull method by Thomason (1991).

and Adolfssen 2005, Christiansen and Wroe 2007, McHenry et al. 2007, Wroe 2007, Wroe et al. 2007a, Wroe et al. 2005).

Studies of reptile biomechanics face similar issues to those focussing on mammals. Empirical data on bite force in reptiles is scant, and generally restricted to smaller species (McBrayer and White 2002). Of the larger, predatory species, empirical data exists only for the American alligator *Alligator mississippiensis* (Erickson et al. 2003). As with the mammals, comparative studies of skull biomechanics in predator reptiles require a technique for estimating bite force based upon skull geometry – a reptilian version of Thomason's 'dry skull' method. An attempt at this is proposed here.

Methods

In creating the 'dry skull' method for mammalian carnivores, Thomason simplified the jaw adductor musculature into two major components; the temporalis, and the masseter-pterygoid (Thomason 1991). These groupings reflect the functional and geometric similarities and differences between the 10 individual jaw adductor muscles in carnivorans (Turnbull 1970) (see Table 7-1). The temporal and masseter-pterygoid groups originate from the upper and lower regions of the temporal arcade

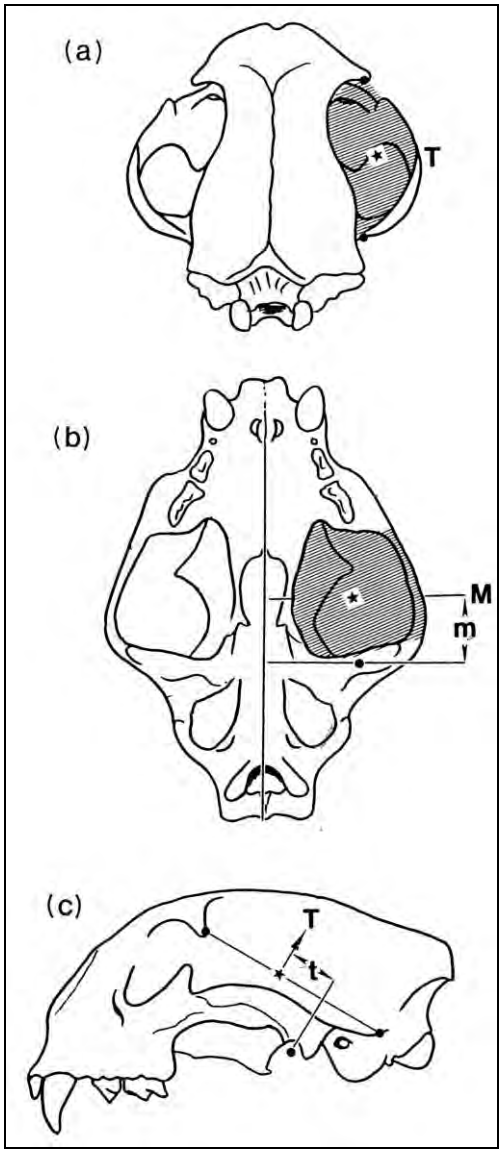

Figure 7-1: Geometric data used to calculated bite force in the dry-skull method (Thomason, 1991). (a) posterio-dorsal view showing cross-sectional area (CSA) of the temporal group: the plane of this view is normal to the vector **T** shown in (c); (b) ventral view showing CSA of masseter-pterygoid group; (c) lateral view showing skull landmarks (i.e. postorbital process, and posterior-most point on dorsal edge of zygomatic bar) used to establish the 'temporal' plane shown in (a). Stars ★ indicate centroids of muscle areas, solid circles • indicate landmarks and position of jaw joint axis. Inlevers **t** and **m** are calculated as the shortest distance between jaw axis and the centroids of the muscle CSAs for the temporal (**T**) and masseter-pterygoid (**M**) muscles respectively. Reproduced from Thomason (1991).

respectively, and so the upper and lower borders of the temporal region can be used to delineate the relevant cross-sectional areas (Figure 7-1).

For each muscle group, a plane normal to the overall line of action must be established, and the cross-sectional area (CSA) of the group is calculated in this

Jaw muscle	Abbreviation	Functional group
M. Adductor Mandibulae Externus	MAME	Temporal
M. Adductor Mandibulae Posterior	MAMP	
Pseudotemporalis	PST	
Pterygoidus Anterior	PTA	Pterygoid
Pterygoidus Posterior	PTP	
Intramandibularis	IM	not applicable
Depressor Mandibulae	DM	

Table 7-2: Jaw adductor muscles in crocodilians. Left column summarises the system used by Iordansky (1964); centre column shows the abbreviations for each muscle name used by Cleuren et al. (1995). Note that many studies (including those) subdivide the M. Adductor Mandibulae Externus (MAME) into Superficialis (MAMES), Medialis (MAMEM), and Profundus (MAMEP) portions. Right, functional groupings used to generate a dry-skull method for reptiles in this study (see text).

plane. The line of action for the temporal muscles is from the middle of the upper temporal region and runs towards the coronoid process of the lower jaw: Thomason selected a plane that passes through the postorbital process and the rear part of the zygomatic arch on each side of the skull as the best representation of the plane normal to that line of action, and one that could be established from osteological landmarks in a wide range of taxa (Figure 7-1c). The masseter-pterygoid muscles have a line of action from the lower temporal arcade towards the ventral edge of the posterior part of the mandible, and thus the basal skull plane[3] was chosen for establishing CSA of that group.

As the dry-skull method models the skull and jaws as a simple lever system, the required inputs are (1) muscle forces, (2) muscle inlever distance, and (3) bite point outlever distance. The muscle forces are calculated from the CSA of each group, multiplied by an estimate of muscle tension (Thomason used an estimate of 300 kPa, i.e. 30 N/cm^2). The inlever distances are simply the shortest distance between the centroid of each muscle group CSA and the jaw hinge axis, measured in the plane normal to each muscle group's line of action. Similarly, the outlever distance is the

[3] The basal skull plane is defined by (1) a line drawn in the sagittal plane between the anteriormost part of the premaxillae (or maxillae, if the premaxillae are not present as separate elements) and the posteriormost part of the occipital condyles, and (2) the transverse axis. The measurement Basal Skull Length (BSL) is taken in this plane.

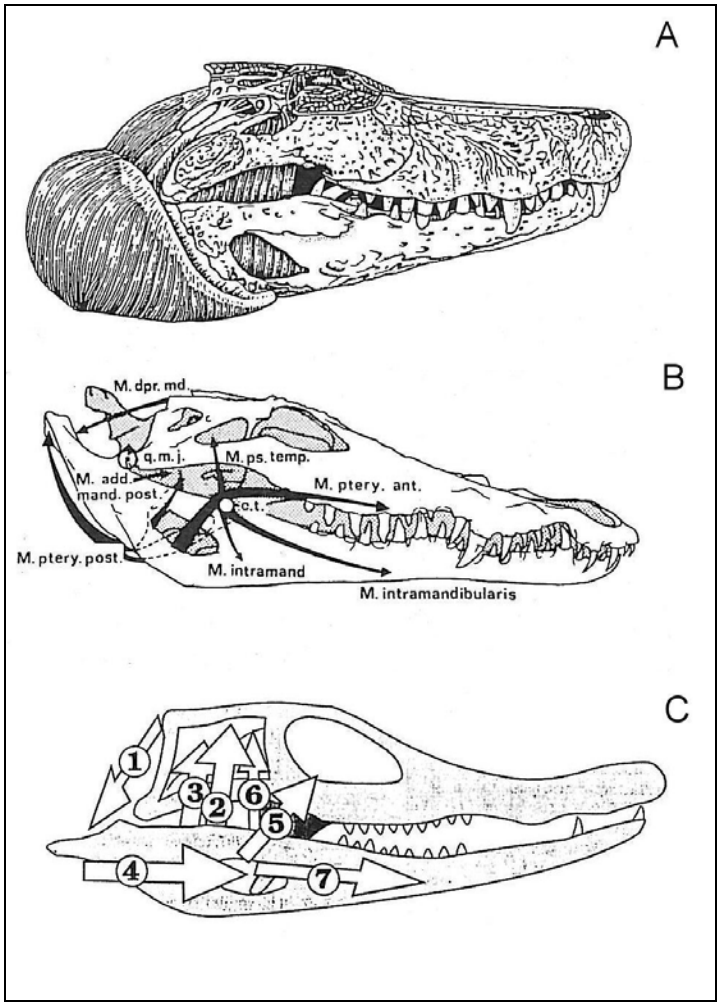

Figure 7-2: Jaw adductor muscles in crocodilians. A, the head of *Alligator* with skin removed, and with the superficial jaw muscles visible at the rear of the skull. Note the large pterygoidus muscle lying external to the retro-articular portion of the mandible. B, diagramatic view of the skull of *Crocodylus*, showing the vectors of the major muscles; q.m.j., quadrate-mandibular joint; c.t., central tendon; for full muscle names refer to Table 7-2. C, diagramatic view of the jaw muscles in *Caiman crocodilus*; 1, DM; 2, MAME; 3, MAMP; 4, PST; 5, PTA; 6, PTP; 7, IM (for muscle acronyms refer to Table 7-2. A, B, from Schumacher 1985; C, from Cleuren et al. 1995).

shortest distance from the bite point to the jaw hinge axis: these three data are sufficient to provide an estimate of bite force using lever dynamics.

To use a similar approach for reptiles, the logic underlying Thomason's approach needs to be adapted to the specific arrangement of sauropsid jaw muscles in reptiles. This study is primarily concerned with crocodilians and pliosaurs, which means that the complex arrangement in various squamates can be ignored. Despite the lack of a close phylogenetic relationship between crocodiles and pliosaurs, the basic

arrangement of the reconstructed jaw muscles in pliosaurs (Taylor 1992) is reasonably similar to that of crocodilians (Holliday and Witmer 2007, Iordansky 1964) – perhaps a result of both groups having robust, akinetic skulls that are used for feeding in the aquatic environment.

Taxa and Specimens

Ideally, a theory-based method such as this would be compared against comprehensive empirical data in order to gauge its level of accuracy. However, this empirical data is rare. In addition to the two species that will form the basis of the FEA, *Crocodylus porosus* and *Kronosaurus queenslandicus*, dry-skull bite force was calculated for additional specimens of large carnivorous reptile species for which there are published measurements or estimates of bite forces; *Alligator mississippiensis* (Erickson et al. 2003), *Caiman crocodilus* (Cleuren et al. 1995, Sinclair and Alexander 1987), *Tyrannosaurus rex* (Erickson et al. 1996, Meers 2003, Rayfield 2005), and *Varanus komodoensis* (Moreno et al. 2008).

Crocodilian jaw musculature: a functional overview

Various authors have provided nomenclatural systems for crocodilian jaw muscles: however, consistency between these has been rare [for a review of the relevant literature, see Holliday and Witmer (2007)]. The system used in this study follows that of Iordansky (1964; also used by Schumacher 1985 and Cleuren et al. 1995) for individual muscle names (Table 7-2, Figure 7-2), but groups them according to approximate lines of action into two major groupings;

- Temporal group: These muscles originate from the upper part of the adductor chamber, and have a line of action (vector) that is more-or-less vertical in lateral view, inserting onto the medial surface and dorsal edge of the mandible in front of the jaw joint.
- Pterygoid group: These muscles originate from the lower parts of the adductor chamber (mainly, the pterygoid and palatine bones of the palate), and have a vector that is oriented posterior-ventrally. They insert onto the mandible behind the jaw joint.

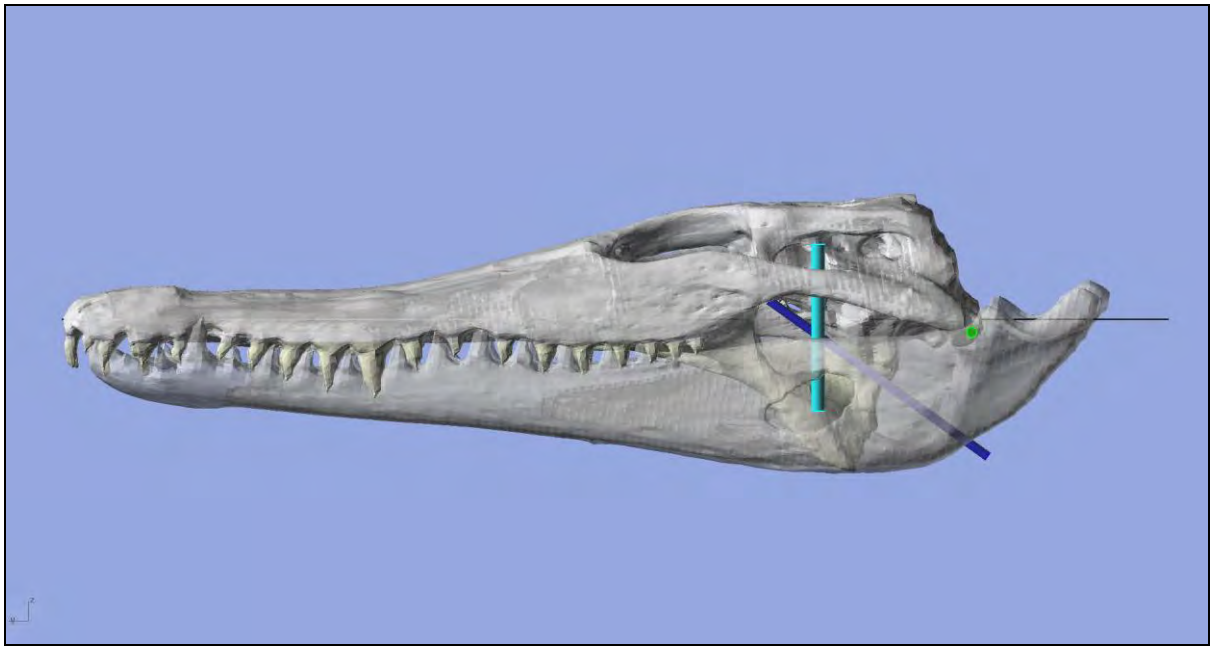

Figure 7-3: 3D model of skull of juvenile *Crocodylus porosus*, in left lateral view. The model was generated from CT scan data of an unnumbered Australian Museum (AM) specimen (BSL 18.43 cm). The skull is aligned with the longitudinal axis (premaxillae-occipital condyle) in the horizontal plane (the line of this axis is shown by the black line at the rear of the skull). The green circle marks the axis of the jaw joint (in the transverse plane), the cyan beam marks the line-of-action (vector) of the Temporal jaw muscle group, and the dark blue beam marks the line of action of the Pterygoid jaw muscle group. See text for explanation, and compare with Figure 7-2C; the Temporal muscle vector is equivalent to vectors 2, 3, 6, and the Pterygoidus to vectors 4, 5 in that diagram.

The similarity to the two muscle groups used by Thomason (1991) for the mammalian dry skull method is intentional: as with Thomason's method, this system seeks to approximate the actual complexity of the jaw muscles (which are highly complex in crocodilians) into the simplest possible geometric model, and ends up with two major groups.

Jaw muscle-group vectors

Once the major groupings of jaw muscles have been decided, the next step is to indentify their vectors. For a reptile dry-skull method, I designated this to be a line normal to the basal skull plane for the Temporal group: the basal skull plane is itself determined by the anteriormost tip of the premaxillae and the posteriormost point of the occipital condyle (Figure 7-3). The vector for the Pterygoid group was taken to

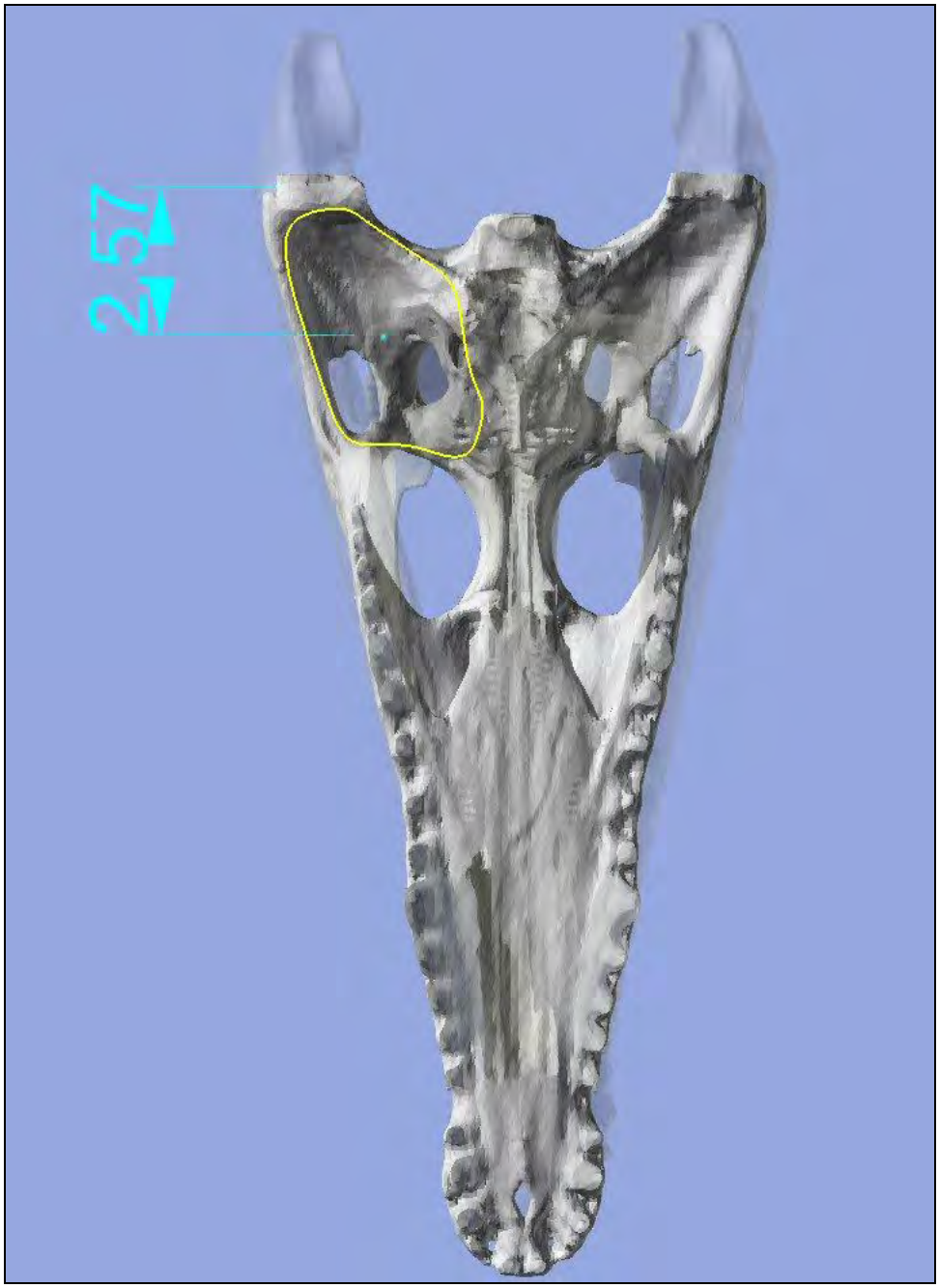

Figure 7-4: Ventral ('Temporal') view of the skull show in Figure 7-3. The view is parallel with the Temporal vector (cyan beam) shown in Figure 7-3, i.e. normal to the basal skull plane. The transparency of the lower part of the pterygoid flange and the mandible has been increased to reveal the upper part of the adductor chamber; the yellow line shows the boundary of the designated Cross Sectional Area for the Temporal muscle group (see text). The number in cyan is the shortest distance, in centimetres, from the centroid of this area (shown as a small cyan circle) and the jaw joint axis: this distance is taken as the inlever for the Temporal muscle group.

be from a point at half the cranial height at the postorbital bar, to the lower edge of the mandible directly ventral to the jaw joint when the jaw is fully closed (Figure 7-3).

Figure 7-5: An adult male *Alligator mississippiensis*, photographed at the Australian Reptile Park, Somersby, NSW. Note the large bulge of soft tissue at the side of the neck, immediately behind the rear part of the skin that is tight to the skull; this bulge is largely M. pterygoidus posterior (compare with Figure 7-2A). Photograph: C. McHenry.

As with Thomason's original version for mammals, an essential feature of the criteria used to indentify these vectors is that they can be designated consistently from osteological landmarks.

Cross-sectional areas

Similarly, the CSA for each functional group must be determined from osteological landmarks alone. For each group, the skull must be imaged as if viewed along the relevant vector; thus, for the Temporal group, the skull is imaged in ventral view. The muscles comprising the temporal group insert around the edges of the adductor chamber, specifically along the lateral edge of the braincase, the ventral surface of the postorbital and squamosal around the edge of the temporal fenestrae, the ventral surface of the quadrate, the ventral surface of the jugal (lower temporal) bar, and the

Figure 7-6: Posterior-oblique ('Pterygoid') view of the skull shown in Figure 7-3. The view is parallel with the vector for the Pterygoid muscle group (shown as a dark-blue beam in Figure 7-3). The boundary of the designated CSA for the muscle group is shown as a yellow line, which traces the margins of the pterygoid fossa and, laterally, the external edge of the mandible (see text). Due to the large proportion of the posterior pterygoidus that lies external to the osteological confines of the skull (see Figure 7-2, Figure 7-5, and text), the CSA modelled here may well be an underestimate of the actual Physiological CSA of the Pterygoid muscle group.

ventral surface of the post-orbital bar (Holliday and Witmer 2007, Iordansky 1964). These muscles do not extend beyond the osteological boundaries of the skull (Figure 7-2A). The boundary chosen to designate the CSA of the Temporal group reflects this (Figure 7-4).

The Pterygoidus muscles of crocodilians, however, quite famously exceed the bony confines of the skull. In particular, the Pterygoidus posterior (PTP) wraps around the ventral surface of the mandible underneath the jaw joint[4], and ends up with a considerable portion of its mass situated external and behind the posterior parts of the cranium and jaws (Figure 7-2A). Given the lack of bony constraint on this muscle's size, it is possible for it to become very large, and this is exactly what does happen in many species of crocodilian; the characteristic 'bulge' behind the head, clearly visible in large individuals, is all jaw muscle[5] (Figure 7-5). Whilst this is a remarkable anatomical set-up on the part of the crocodile, it makes designating a relevant CSA a little difficult, given that we must use osteological landmarks. Given this, the boundary used to designate the CSA for the Pterygoid group follows the edge of the pterygoid fossa (as viewed along the appropriate line of action) medially, dorsally, and ventrally, and the external edge of the (fully adducted) mandible laterally (Figure 7-6).

Even using the anatomical features specified above for the boundaries of the two muscle groups, it is possible to draw several different lines for each. In order to establish more precise criteria for delineating the boundaries, candidate boundary lines were drawn for both Temporal and Pterygoid groups on a model of a small *Caiman crocodilus* (Figure 7-7). The lines chosen for use here were those with areas proportionally most similar to data for calculated physiological CSA from Cleuren et al. (1995) for a similar sized *Caiman crocodilus* (Table 7-3, Table 7-4).

Inlevers

The inlever is the distance from the hinge axis that the muscle forces act on; the muscle force multiplied by the inlever distance gives the moment, or torque, generated by that muscle. With Thomason's dry-skull method for mammalian carnivores, the inlever for each muscle group is calculated as the distance from the centroid to the position of the jaw hinge axis, measured in the same plane as the

[4] Which is a major reason why this point was chosen to determine the line of action for the Pterygoid group.

[5] Exactly how this 'cheat' affects crocodile skull mechanics has yet to be determined, although a reasonable assumption is that the effect is significant.

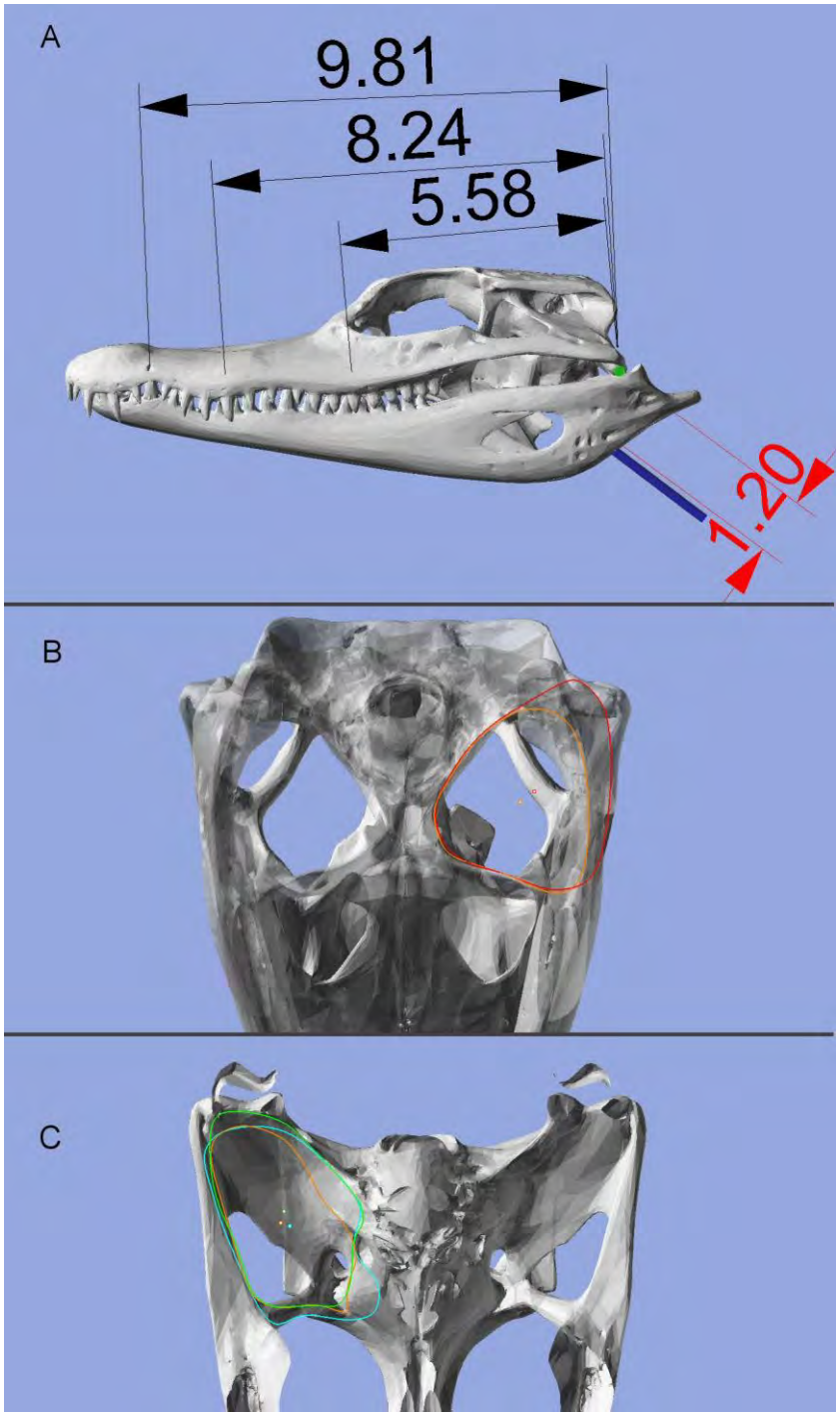

Figure 7-7: 3D model of a small *Caiman crocodilus* skull, constructed from CT scan data of FMNH 73711 produced by the Digital Morphology group at the University of Texas (www.digimorph.org). A, oblique lateral view of skull. B, Pterygoid view, showing different candidate boundaries for the Pterygoid muscle group CSA; pty 2 (orange), and pty 3 (red). C, Temporalis view, showing candidate boundary lines for Temporal muscle group CSA; temp 1 (orange), temp 2 (green), temp 3 (cyan). The combination of pty 2 and temp 3 is proportionally closest to physiological CSA data for Caiman crocodilus calculated by Cleuren et al. (1995) (see Table 7-4). The green filled circle visible in 'A' shows the jaw hinge axis; the blue bar shows the vector for the pterygoid muscle group. In 'A', the red text gives the inlever for the pterygoid system, and the black text the outlevers for front, mid, and rear bites.

		Physiological CSA		
		All muscles		Temporal + Pterygoid
Group	**muscle**	**g/cm**	**%**	**%**
Temporal	MAMES	1.77	10.2	51.8
	MAMEP	2.08	11.9	
	MAMP	2.21	12.7	
	PST	0.93	5.3	
Pterygoid	PTA	2.25	12.9	48.2
	PTP	4.25	24.4	
n/a	IM	2.65	15.2	
	DM	1.27	7.3	

Table 7-3: Jaw muscle Physiological Cross-Sectional Areas (PCSA) for small (1.00 kg) *Caiman crocodilus*, from data presented by Cleuren et al. (1995). Cleuren et al. calculated PCSA by dividing their measurements of jaw muscle volume by the fibre lengths provided by Sinclair and Alexander (1987) for a similarly sized animal – hence the units (g/cm). I used this data to calculate the ratio of PCSA for the Temporal and Pterygoid groups (right column). Note that Cleuren et al. presented data only for the M. Adductor Mandibulae Externus Superficialis (MAMES) and M. Adductor Mandibulae Externus Profundus (MAMEP); in their analysis, the PCSA for the third part of the MAME, the M. Adductor Mandibulae Externus Medialis (MAMEM), was divided in half and added to the totals for the MAMES and MAMEP.

outline		paired with				
	CSA	3.39	4.08	4.46	4.09	5.20
CSA		temp 1	temp 2	temp 3	pty 2	pty 3
3.39	temp 1				45.3	39.4
4.08	temp 2				49.9	43.9
4.46	temp 3				**52.2**	46.2
4.09	pty 2	54.7	50.1	**47.8**		
5.20	pty 3	60.6	56.1	53.8		

Table 7-4: Ratios of muscle group CSA for the three Temporal and two Pterygoid boundaries shown in Figure 7-7. The combination of the temp 3 and pty 2 outlines (bold) provided the closest match to the ratio obtained from Cleuren et al. (1995) of 51.8% Temporal and 48.2% Pterygoid (Table 7-3). Specimen size is comparable for the two datasets: the skull shown in Figure 7-7 is from a small *Caiman crocodilus* (FMNH 737311) with a BSL of 11.18 cm: Cleuren et al. (1995) based their data from a 1.00 kg *Caiman crocodilus* with a "skull length" (exact measurement type unspecified) of "approximately 10 cm" (Cleuren et al., 1995; p. 83). Figures in greyed 'CSA' column and row give absolute areas in cm^2.

muscle's CSA. Exactly the same logic as been applied here: see Figure 7-4 and Figure 7-8.

Outlevers

The outlever is simply the point on a lever arm upon which the lever's torque acts; in the present context, these are the bite points. Three possible bite points were identified; each represents the largest upper jaw tooth in the front, middle, and rear parts of the tooth row respectively (which tooth each one is applied to varies between species). For example, in the *Crocodylus porosus* model shown in Figure 7-8, these were the 4th premaxillary tooth (Pmx4) for front bites, the 5th maxillary tooth (M5) for mid bites, and the 10th maxillary tooth (M10) for rear bites. The middle of these (i.e. the M5 in *C. porosus*) is the largest tooth in the jaw, and is taken to be

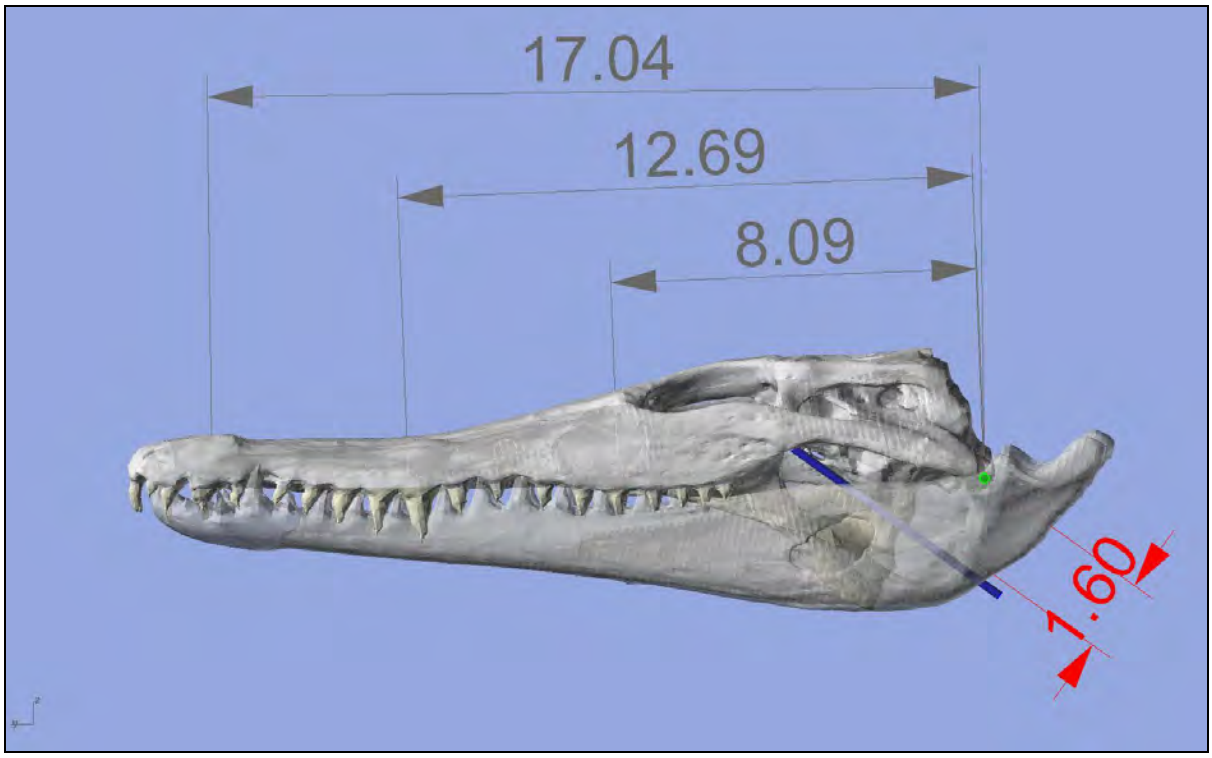

Figure 7-8: Lateral view of the 3D *Crocodylus porosus* model, showing outlever distances (grey, above the skull) and the inlever distance for the Pterygoidus muscle group (red, posterior to the skull). All distances are given in centimetres. The Pterygoid inlever distance is calculated as the shortest distance between the centroid of the Pterygoid CSA (Figure 7-6) and the jaw hinge axis, taken in the 'Pterygoid' plane (i.e. normal to the Pterygoid muscle vector shown in Figure 7-3). The outlever distances are the shortest distances (in the parasagittal plane) between the jaw hinge axis and the middle of the base of the crown of the 4th premaxillary tooth (Pmx4), the 5th maxillary tooth (M5), and the 10th maxillary tooth (M10) for 'front', 'mid', and 'rear' bites respectively.

functionally equivalent to the M4 in *Alligator* and *Caiman*, M7 in *Varanus komodoensis*, M1 in *Kronosaurus*, and M4 in *Tyrannosaurus* (Table 7-6): these are comparable to the canines of carnivorous mammals, in that they are teeth with a 'fang-like' morphology that are predicted to be used in killing prey. These bite points are hereafter referred to as 'front', 'mid', and 'rear' bite positions. The outlever distance for each bite point was measured as the shortest distance between the middle of the base of the respective tooth crown, and the jaw hinge axis, viewed in the parasagittal plane (Figure 7-8).

Muscle force

Following Thomason (1991) and others (McHenry et al. 2007, Moreno et al. 2008, Wroe 2007, Wroe et al. 2007a, Wroe et al. 2005, Wroe et al. 2007b), the tension developed by muscle was assumed to be 300 kPa (i.e., a force of 30 N per square centimetre of muscle CSA).

Morphometrics and body mass

To examine the scaling relationships of calculated bite force across the sampled taxa, several measurements were taken from each skull model used: these are detailed in Table 7-5 and Table 7-6. Estimates of mass were made from (1) reported values for specimens used (*Tyrannosaurus rex*, from Erickson et al. 2004); (2) by assuming isometric similarity with similar sized specimens for which body mass data exists (*Caiman crocodilus*, from Cleuren et al. 1995); (3) data on the regression of body mass to skull measurements for statistically significant samples of extant species (*Alligator mississippiensis*, from Farlow et al. 2005, Hurlburt et al. 2003; *Crocodylus porosus*, from Webb and Messel 1978); (4) data on the regression of body mass to limb bone dimensions (*Varanus komodoensis*, from Blob 2000); (5) estimates made from estimates of whole-body volume (*Kronosaurus queenslandicus*, Chapter 6). The skull models for each of these specimens are shown in Figures 7-10–7-13.

Measurements of the skull are based on those used in Tucker et al. (1996), specifically; Dorsal Cranial Length (DCL), measured from the tip of the premaxillae to the posterior margin of the supraoccipital in the sagittal place, and also termed

Specimen	taxon	ref	BSL (cm)	DCL (cm)	CW (cm)	Skull vol (cm^3)	Body Mass (kg)
AM (no #)	*Crocodylus porosus*	C.p-1	18.43	17.92	8.77	126.3	5.2
NU (no #)	*Crocodylus porosus*	C.p-2	42.79	41.39	19.93	1,949.8	110.4
FMNH 73711	*Caiman crocodilus*	Ca.c	11.18	11.24	6.31	33.9	1.6
TMM M-983	*Alligator mississippiensis*	A.m	37.03	36.48	19.46	1170.8	88.3
FMNH PR2081	*Tyrannosaurus rex*	T.r	149.66	151.37	89.21	158,061.0	5,654.0
QM F10113	*Kronosaurus queenslandicus*	K.q	187.57	184.45	91.72	113,403.8	5,781.0
AM R106933	*Varanus komodoensis*	V.k	12.29	11.22	6.66	39.4	6.3
rescaled	*Kronosaurus queenslandicus*	K.q(r)	48.41	47.61	23.67	1,949.8	99.4

Table 7-5: Reptile specimens, and major skull dimensions, used to generate 'dry skull' predictions of bite force. BSL, Basal Skull Length; DCL, Dorsal Cranial Length; CW, Cranial Width. The 'rescaled' *Kronosaurus queenslandicus* 'K.q(r)' is the FE model used in the comparative FEA in Section 7.3, scaled to the same volume as the model based upon the 'C.p-2' specimen of *Crocodylus porosus*. The abbreviations in the 'ref' column are hereafter used to reference the specimens.

ref	Temporal (unilateral)		Pterygoid (unilateral)		Bite points					
	CSA (cm^2)	inlever	CSA (cm^2)	inlever	front		mid		rear	
					tooth	outlever	tooth	outlever	tooth	outlever
C.p-1	10.06	2.57	11.68	1.6	Pmx4	17.04	M5	12.69	M10	8.09
C.p-2	54.88	6.01	67.29	3.53	Pmx4	37.87	M5	29.92	M10	18.11
Ca.c	4.461	1.67	5.204	1.2	D4	9.81	M4	8.24	M10	5.58
A.m	43.504	5.27	49.457	3.5	D4	33.44	M4	29.19	M11	18.04
T.r	1375.89	23.11	533.197	9.59	M1	131.5	M4	115.53	M9	84.88
K.q	1119.1	32.54	667.45	10.56	Pm4	171.92	M1	159	M14	94.09
V.k	6.45	1.8	4.57	0.44	M3	11.55	M7	9.74	M9	8.68
K.q(r)	74.55	8.4	44.46	2.73	Pm4	44.37	M1	41.04	M14	24.28

Table 7-6: Measurements used in the 'dry skull' calculations of bite force for the reptile specimens listed in Table7.5. Cross-sectional area (CSA) for the Temporal and Pterygoid muscle groups are based upon the outlines shown in Figure 7-4–Figure 7-13; note these are the areas corresponding to one side of the skull only (unilateral). The distances for the inlevers and the outlevers are in cm. Specified teeth are identified by element and the count of tooth positions from the front of that element, i.e.; premaxillary (Pmx), maxillary (M), and dentary (D). See Table7.5 for abbreviations in 'ref' column.

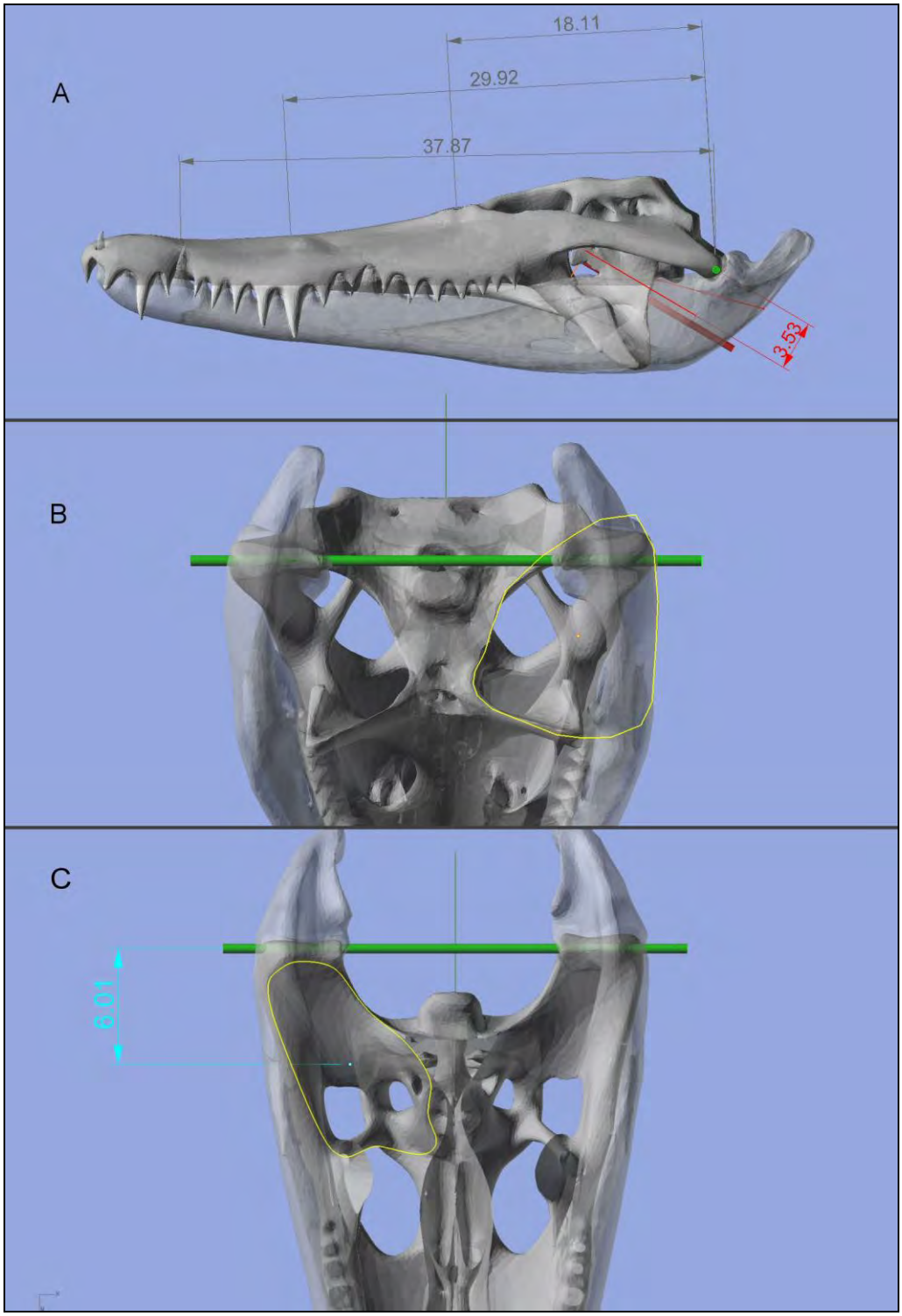

Figure 7-9: 3D model of the large *Crocodylus porosus* specimen ('C.p-2'), in (A) lateral, (B) 'pterygoid', and (C) 'temporal' views. The green bar (visible end-on in 'A') shows the jaw hinge axis; the red bar in 'A' shows the vector for the pterygoid muscle group. In 'A', the red text gives the inlever for the pterygoid system, and the grey text the outlevers for front, mid, and rear bites. The yellow lines in 'B' and 'C' denote the outlines used to measure cross-sectional area of the pterygoid and temporal respectively; the blue text in 'C' shows the inlever for the temporal group. The lower jaw is shown as partially transparent, as is the lower half of the cranium in 'C'.

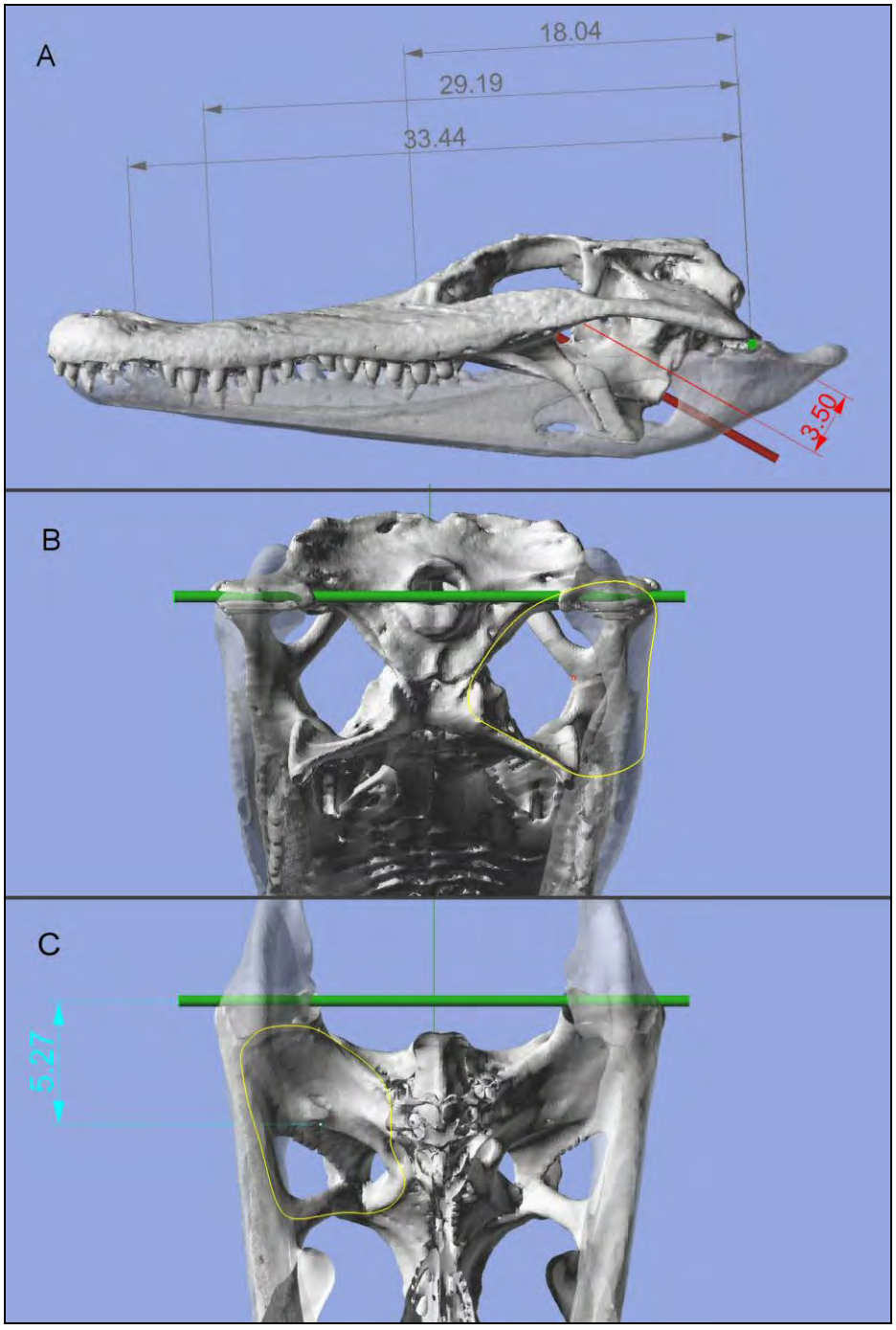

Figure 7-10: 3D model of *Alligator mississippiensis*, constructed from CT scan data of TMM M-983 and produced by the Digital Morphology group at the University of Texas (www.digimorph.org), in (A) lateral, (B) 'pterygoid', and (C) 'temporal' views. The green bar (visible end-on in 'A') shows the jaw hinge axis; the red bar in 'A' shows the vector for the pterygoid muscle group. In 'A', the red text gives the inlever for the pterygoid system, and the grey text the outlevers for front, mid, and rear bites. The yellow lines in 'B' and 'C' denote the outlines used to measure cross-sectional area of the pterygoid and temporal respectively; the blue text in 'C' shows the inlever for the temporal group. The lower jaw is shown as partially transparent, as is the lower half of the cranium in 'C'.

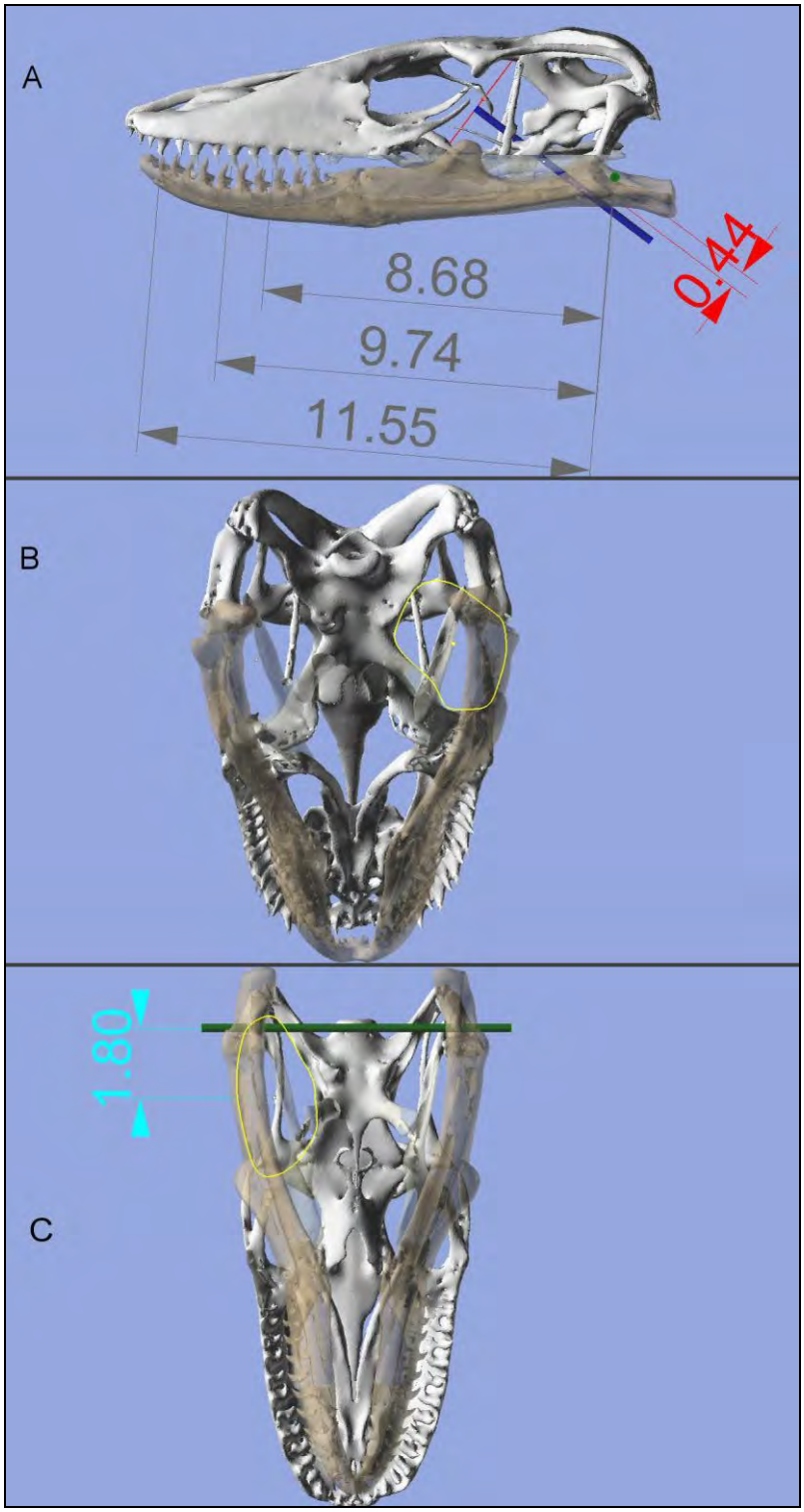

Figure 7-11: 3D model of *Varanus komodoensis*, in (A) lateral, (B) 'pterygoid', and (C) 'temporal' views. The green bar (visible end-on in 'A') shows the jaw hinge axis; the blue bar in 'A' shows the vector for the pterygoid muscle group. In 'A', the red text gives the inlever for the pterygoid system, and the grey text the outlevers for front, mid, and rear bites. The yellow lines in 'B' and 'C' denote the outlines used to measure cross-sectional area of the pterygoid and temporal respectively; the blue text in 'C' shows the inlever for the temporal group. The lower jaw is shown as partially transparent.

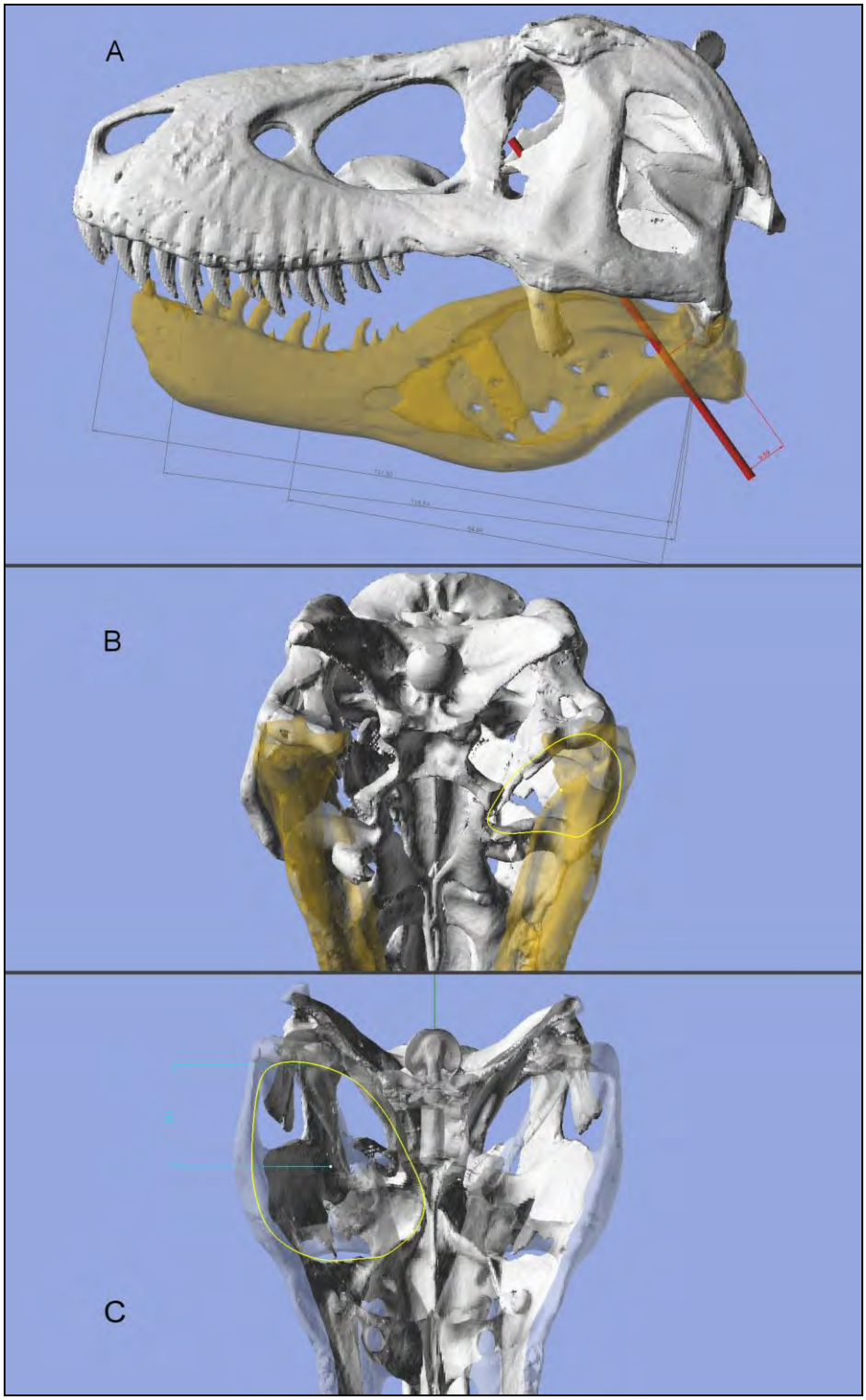

Figure 7-12: 3D model of *Tyrannosaurus rex*, based upon CT data provided by Eric Snively of the scale sculpted created by Brian Cooley, in (A) lateral, (B) 'pterygoid', and (C) 'temporal' views. The green bar (visible end-on in 'A') shows the jaw hinge axis; the red bar in 'A' shows the vector for the pterygoid muscle group. In 'A', the red text gives the inlever for the pterygoid system, and the grey text the outlevers for front, mid, and rear bites. The yellow lines in 'B' and 'C' denote the outlines used to measure cross-sectional area of the pterygoid and temporal respectively; the blue text in 'C' shows the inlever for the temporal group. The lower jaw is shown as partially transparent, as is the lower half of the cranium in 'C'.

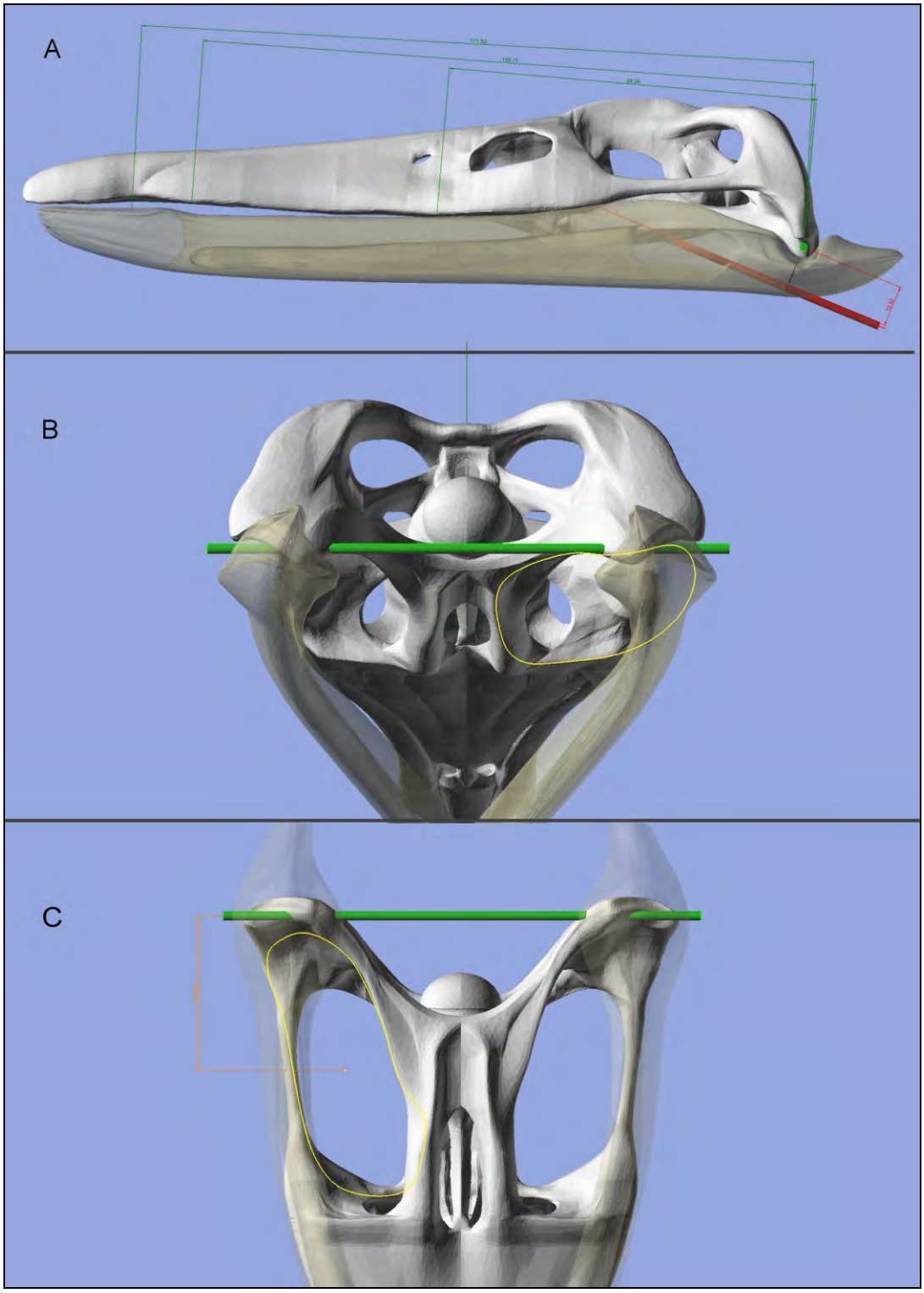

Figure 7-13: 3D model of *Kronosaurus queenslandicus*, in (A) lateral, (B) 'pterygoid', and (C) 'temporal' views. The green bar (visible end-on in 'A') shows the jaw hinge axis; the red bar in 'A' shows the vector for the pterygoid muscle group. In 'A', the red text gives the inlever for the pterygoid system, and the green text the outlevers for front, mid, and rear bites. The yellow lines in 'B' and 'C' denote the outlines used to measure cross-sectional area of the pterygoid and temporal respectively; the orange text in 'C' shows the inlever for the temporal group. The lower jaw is shown as partially transparent, as is the lower half of the cranium in 'C'.

Head Length (Erickson et al. 2003), SKULL (Farlow et al. 2005), and Total Length of Head (Webb and Messel 1978); and Cranial Width (CW), measured across the lateral extremities of the quadrates, and also termed Maximum Head Width (Webb and Messel 1978). Also measured was Basal Skull Length (BSL), taken from the anterior tip of the premaxillae to the posteriormost apex of the occipital condyle.

Results

Table 7-5 shows the skull dimensions for the six reptile specimens, along with the body size estimates calculated for each. Although estimated body mass for the *Tyrannosaurus rex* specimen was slightly less than for the *Kronosaurus queenslandicus* specimen (5,654 vs 5,781 kg), skull volume in the *T. rex* is considerably larger than for the *K. queenslandicus* (158 vs 113 litres respectively). Conversely, the *Varanus komodensis* specimen was of a similar body mass to one of the *Crocodylus porosus* specimens (6.3 and 5.2 kg respectively), but skull volume in the komodo dragon was much less than for the crocodile (39 vs 126 cm^3).

The calculated bite forces for 'front', 'mid', and 'rear' bites for the six specimens are shown in Table 7-7. Predicted bite force results for the *Kronosaurus queenslandicus* and

ref	Bilateral muscle force (N)		Torque (Ncm)	Bite force (N)		
	Temporal	Pterygoid		front	mid	rear
C.p-1	604	701	2,673	157	211	330
C.p-2	3,293	4,037	34,042	899	1,138	1,880
Ca.c	268	312	822	84	100	147
A.m	2,610	2,967	24,142	722	889	1,338
T.r	82,553	31,992	2,214,611	16,841	19,169	26,091
K.q	67,146	40,047	2,607,827	15,169	16,401	27,716
V.k	387	274	817	71	84	94
K.q(r)	4473	2667.6	44,856	1,011	1,093	1,847

Table 7-7: Estimates of muscle force, torque, and bite force estimates for reptile specimens using the 'reptile' dry skull method.

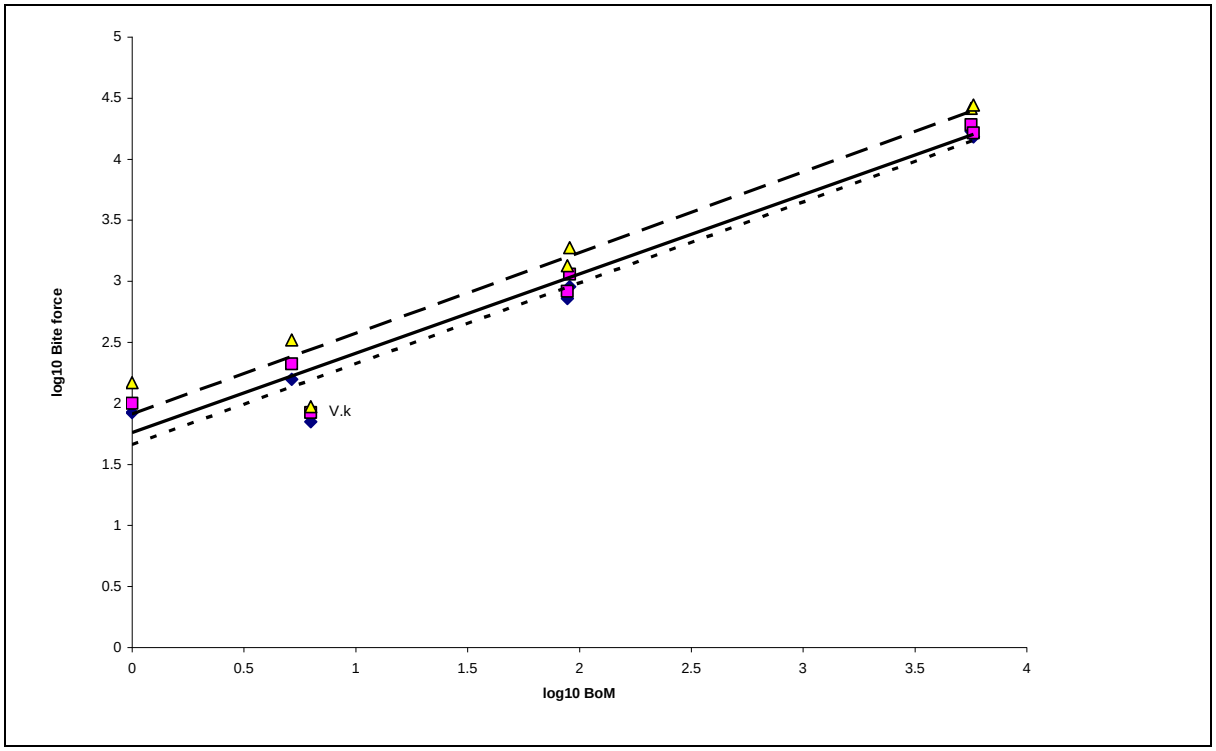

Figure 7-14: Bite force plotted against body mass (BoM), plotted as log10 values for bite force (N) and body mass (kg). Data for front bites (solid diamonds, regression line shown as short dashes), mid bites (squares, solid regression line), and rear bites (triangles, long dashes). Equations for linear regressions; rear bites, y = 0.661x + 1.91; mid bites, y = 0.649x + 1.76; front bites, y = 0.662x + 1.66. *Varanus komodoensis* (V.k) has a weak predicted bite for its body mass; bite force in the other specimens scales more or less isometrically.

Tyrannosaurus rex specimens were similar: 16.4 and 19.2 kN respectively for a 'mid' bite. The torque applied to the jaw joint was highest for *K. queenslandicus*, 26.1 vs 22.1 kNm, but the outlever is considerably shorter in *T. rex* for the front and mid bites.

The predicted bite force in *K. queenslandicus* is, when size is accounted for, similar to the predicted value for *Crocodylus porosus*, as shown by the values for the 'rescaled' *Kronosaurus queenslandicus* skull (which has been scaled isometrically to the same volume as the 'C.p-2' specimen) in Table 7-7.

The scaling relationships of bite force are shown as log–log data, plotted against body mass (Figure 7-14) and skull volume (Figure 7-15). The values for slopes and intercepts of the log–log data for bite force and torque at the different bite positions, against body mass, skull volume, and linear measurements of skull size are shown in

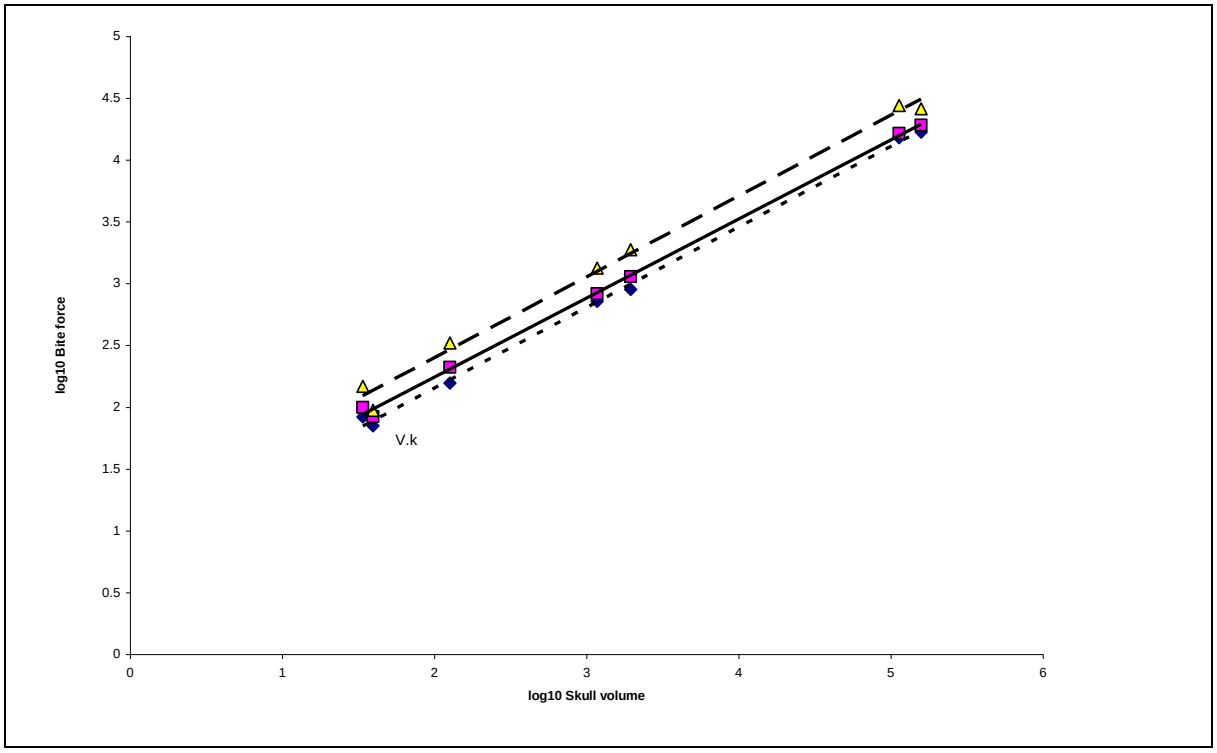

Figure 7-15: Bite force plotted against skull volume, plotted as log10 values for bite force (N) and skull volume (cm^3). Data for front bites (solid diamonds, regression line shown as short dashes), mid bites (squares, solid regression line), and rear bites (triangles, long dashes). Equations for linear regressions; rear bites, y = 0.654x + 1.09; mid bites, y = 0.640x + 0.96; front bites, y = 0.652x + 0.85. Bite force in these reptiles scales close to isometrically with respect to skull volume, including in *Varanus komodoensis* (V.k), for which the low predicted bite force for its body mass appears to be a result of a relatively small head.

Table 7-8. Scaling relationships (slopes) are very similar for 'front', 'mid', and 'rear' bites. For the volume based measurements of body size (body mass and skull volume), the slope of the bite force regression lines are close to the predicted value for isometry, 0.67. Likewise, the slopes of the bite force regression lines, plotted against linear skull measurements (BSL, DCL, QQ) are close to the predicted value for isometry (2.00).

Comparing body size with torque at the jaw joint removes potential complications from variation in outlever lengths between species. Torque is the product of area (force of the jaw muscles correlates with cross-sectional area) and linear distance of the inlever, and under isometry should thus be expected to scale to linear measurements of body size by an exponent of 3, and to volume-based measurements

		Bite Force				Torque	
		isometry	**front**	**mid**	**rear**	**isometry**	**data**
BoM	slope	0.67	0.66	0.65	0.66	1.00	0.99
	intercept	–	1.66	1.76	1.91	–	2.59
Skull volume	slope	0.67	0.65	0.64	0.65	1.00	0.97
	intercept	–	0.85	0.96	1.09	–	1.39
DCL	slope	2.00	1.99	1.95	2.00	3.00	2.97
	intercept	–	-0.23	-0.10	-0.01	–	-0.24
BSL	slope	2.00	2.01	1.97	2.02	3.00	3.01
	intercept	–	-0.29	-0.16	-0.06	–	-0.33
CW	slope	2.00	2.01	1.97	2.02	3.00	3.00
	intercept	–	-0.25	-0.15	-0.08	–	-0.29

Table 7-8: Slope and intercepts for log–log plots of bite force and torque against different measures of skull and body size. Predicted values for slopes for scaling by isometry are indicated (see text).

of body size by an exponent of 1. The results in Table 7-8 indicate that torque scales isometrically across the reptile specimens sampled here.

When plotted against body mass (Figure 7-14), the result for the *V. komodoensis* specimen is an obvious outlier – it has a comparatively weak result for its size – but when bite force is plotted against skull volume (Figure 7-15) the *V. komodoensis* result is much closer to the regression line, indicating that the weak bite force in this taxon may simply be a function of its smaller relative head size.

Discussion

A key question in comparative studies of bite force based upon morphological data is how well these methods predict actual bite force. *In vivo* data is restricted to a small number of species; in the absence of a broad basis of empirical data, some insight into this question can be gained by placing the estimates generated here into the context of recent work on bite force in various groups. Table 7-9 lists the slopes and intercepts of regression lines for log-log data from various studies that have

presented comparative analysis of how bite force scales with body mass in mammalian and reptilian predators.

For a given slope, the intercept can be used to rank bite strength between different groups: for example, both the dry skull data for reptilian 'mid' bites from the present study, and for carnivoran canine bites from Wroe et al. (2005), have slopes near 0.67 (0.65 and 0.67 respectively): the intercept of 1.91 for the reptiles, compared with 1.71 for the mammals, suggests that the reptiles have a stronger bite, at the teeth used as killing fangs, for their body size.

Source	taxon	method	slope	intercept	*n*
Meers 2003	all predators (rear bites?)	various	0.92	1.90*	17
Meers 2003	crocodilians (rear bites)	various	0.79	2.34*	2
Erickson et al. 2003	*Alligator miss.* (rear bites)	observed	0.79	2.06†	41
Present study	reptiles (mid bites)	dry skull	0.65	1.76	7
Present study	reptiles (rear bites)	dry skull	0.66	1.91	7
Meers 2003	mammals (rear bites)	various	0.73	2.19*	11
Wroe et al. 2005	extant mammals	dry skull	0.60	1.71	31
Wroe et al. 2005	extant dasyurids	dry skull	0.70	1.88	3
Wroe et al. 2005	extant carnivorans	dry skull	0.67	1.60	28
Wroe et al. 2005	extant felids	dry skull	0.72	1.55	10
Wroe et al. 2005	extant canids	dry skull	0.85	1.46	10
Wroe et al. 2005	*Vulpes vulpes*	dry skull	0.81	1.49	6
Eliis et al. 2008‡	*Canis lupus familiaris*	dry skull	0.83	1.36	19
Eliis et al. 2008‡	*Canis lupus familiaris*	observed	0.63	1.90	19
Eliis et al. 2008‡	*Canis lupus familiaris*	CB_M	0.72	1.72	19

Table 7-9: Values for slopes and intercepts for log–log plots of bite force (N) vs. Body mass (kg) from various studies. All data for canine bites unless indicated otherwise. *, intercepts from Meers (2003) were originally stated as functions of natural logarithms and have been converted here by dividing by ln(10). †, intercept from Erickson et al. (2003) converted from value given, -0.31, which was for body mass in grams. ‡, data derived by removing 'dog 2' (not 'dog 3') from raw data presented by Ellis et al. (2008). CB_M is the conversion of dry skull estimates of canine bite force (CB_S) according to measured physiological cross-sectional area of the jaw muscles given by Thomason (1991); $\log(CB_M) = 0.858 \log(CB_S) + 0.559$.

The majority of the slopes listed in Table 7-9 are close to the isometric value, 0.67. The exceptions are; Meers (2003), all predators; Meers (2003), crocodilians; Erickson et al. (2003), *Alligator mississippiensis*; Wroe et al (2005), extant mammals; and all of the dry skull datasets focusing on canids, i.e. Wroe et al. (2005), extant canids; Wroe et al. (2005), *Vulpes vulpes*; and Ellis et al. (2008), *Canis lupus familiaris*.

For the Meers (2003) data, the dataset for crocodilians had $n = 2$ and the larger of these values was the maximum observed bite force reading from Erickson et al. (2003), so these studies are not completely independent – that latter value was at the upper range of body size in Meers' 'all predators' dataset and appears to have had a significant effect on the resulting slope (compare with the slope for mammals from Meers' data, which is 0.73 for $n = 11$). The Erickson et al. data (slope = 0.79) strongly suggests allometry of bite force in *Alligator mississippiensis*, and this may be a result of the allometric increase in head size with body size in this species (Farlow et al. 2005).

The Wroe et al. 'extant mammals' set included dasyurids and carnivorans; in that dataset, the dasyurids have both a higher average bite force and a smaller average body mass and their inclusion acts to reduce the slope (and increase the intercept) of the 'all mammals' regression: note that the regression for carnivorans in the Wroe et al. data ($n = 28$) has a slope of exactly 0.67. The same dataset found that the slope for felids ($n = 10$) was close to isometry, but for canids was markedly higher (0.85, $n = 10$), and that a high slope also characterised a within-species subset of the data (*Vulpes vulpes*). Likewise, Ellis et al. (2008) also found a high slope (0.83) for dry skull estimated bite force within one species of canid, the domestic dog, although the same study found a very different slope (0.63) for observed *in vivo* data from the same specimens.

The discrepancy between dry skull derived estimates of bite force, and observed values for the same taxa, is especially important. In all cases, observed bite force exceeds the predictions based upon the dry skull method; for example, the *Alligator* specimen (Figure 7-10) predicted in the present study to have a bite force of 1338 N at the rear bite position (Table 7-7) should have an in vivo bite force of 3900–4500 N

according to Erickson et al.'s data. Ellis et al. (2008) recorded a canine bite of 859 N in a 40 kg dog which has a dry skull predicted bite force of 451 N. Individual data points from studies on other taxa, such as the spotted hyaena *Crocuta crocuta* (Binder and Van Valkenburgh 2000), also point to a much larger *in vivo* bite force than the value predicted from the dry skull method.

However, dry skull derived estimates are potentially useful if the discrepancy is consistent. There is reason to think that the discrepancy between dry skull estimates and in vivo measurements is a result of two factors; (1) the 2D dry skull method underestimates the effective inlever of the jaw muscles, and (2) the measurement of cross-sectional area (CSA) of jaw muscles used in the dry skull method does not account for muscle pennation and therefore underestimates physiological cross-sectional area (PCSA). Evidence for the first comes from the 3D FE models constructed by McHenry et al. (2007) and Wroe et al. (2007); for the lion *Panthera leo*, the dingo *Canis lupus dingo*, and the thylacine *Thylacinus cynocephalus*[6], the bite force from the 3D models was considerably greater than that derived from the same specimens using the 2D approach. Since the principal difference between the 2D and 3D models is the estimation of the jaw muscle inlevers – the 3D models approximate the actual geometry of the jaw muscle fibre bundles – it is tempting to conclude that this factor may be an important component of the difference between the 2D dry skull and the *in vivo* results.

Thomason (1991) measured PCSA in a number of carnivoran heads and derived a regression-based correction factor for dry skull estimates that accounts for pennation in the jaw muscles; applying this to Ellis et al's (2008) dry skull data results in a regression line that is closer to that for their *in vivo* data in both slope and intercept (Table 7-9). When sufficient data from 3D models is available, it will be interesting to test whether the combination of improved estimates for the muscle inlever and PSCA are sufficient to bring dry skull based estimates close to the *in vivo* data. Note that discrepancies due to inlever geometry and muscle pennation probably apply to most taxa, but may be particularly important for crocodilians and carnivorans; the

[6] Note that the 3D estimate for *Smilodon fatalis* was lower than the 2D derived result, but this is for reasons – principally, the very reduced coronoid process of the sabre-tooth cat – that are unique to *Smilodon* in the present context (McHenry et al. 2007).

former, because of the extreme development of the pterygoidus noted earlier, and the latter because the increased length of the temporalis muscle will exacerbate the importance of PCSA vs CSA of that muscle.

If the discrepancy between dry-skull and *in vivo* data can be resolved into mechanically relevant factors such as jaw muscle geometry, then dry skull estimates of bite force are potentially useful tools for biomechanical analyses, especially within a comparative context. The possibility that a complex biological property of predatory animals, which must logically be a product of skeletal morphology (including hard and soft tissues) and behavioural factors, can be understood through simple mechanical paradigm is of interest and potential importance. As more data becomes available, these ideas can be tested further – the next few years promise to be interesting ones for the study of skull biomechanics

7.3 Finite Element Analysis

Methods

Solid mesh

The finite element model of *Crocodylus porosus* was constructed as part of a final year project in the Bachelor of Engineering degree at the University of Newcastle (Ingle 2007), from CT data of a 3.1 m (Total Length) individual that was killed as part of the Northern Territory crocodile management program and made available by Adam Britton. CT scanning was performed at the Newcastle Mater Misericordae Hospital using a Toshiba Aquilion 16 slice scanner. The CT data was processed in MIMICS, and the bone of the skull was masked from the soft-tissues of the head to produce a separate surface mesh for the cranium and mandible. These meshes were exported into STRAND7, and were converted into solid meshes comprising four-noded tetrahedral ('tet4') elements; 754,083 tet4s for the mandible, and 832,613 for the cranium.

The *Kronosaurus queenslandicus* model was generated from the surface meshes produced in Chapter 5: as with the *Crocodylus porosus* model, these were exported from MIMICS from STRAND7 and converted to solid meshes of 450,563 tet4 elements for the mandible and 940,455 for the cranium.

Material properties

Although the factors that determine material properties in bone are complex, the density of the bone, i.e. the extent to which it is mineralised, has a strong effect. Density varies throughout each bone, in particular between regions of spongy and cortical bone, but can be imaged and quantified using CT data, where the CT attenuation (or CT density) is strongly influenced by actual density.

As discussed in Chapter 5, the relationship between CT density and actual density is also complex and depends on the type and absolute quantity of material and the setup of the instrumentation. Data on CT density and actual density for the Toshiba scanner used in this study were collated from samples of bovine rib bones as part of

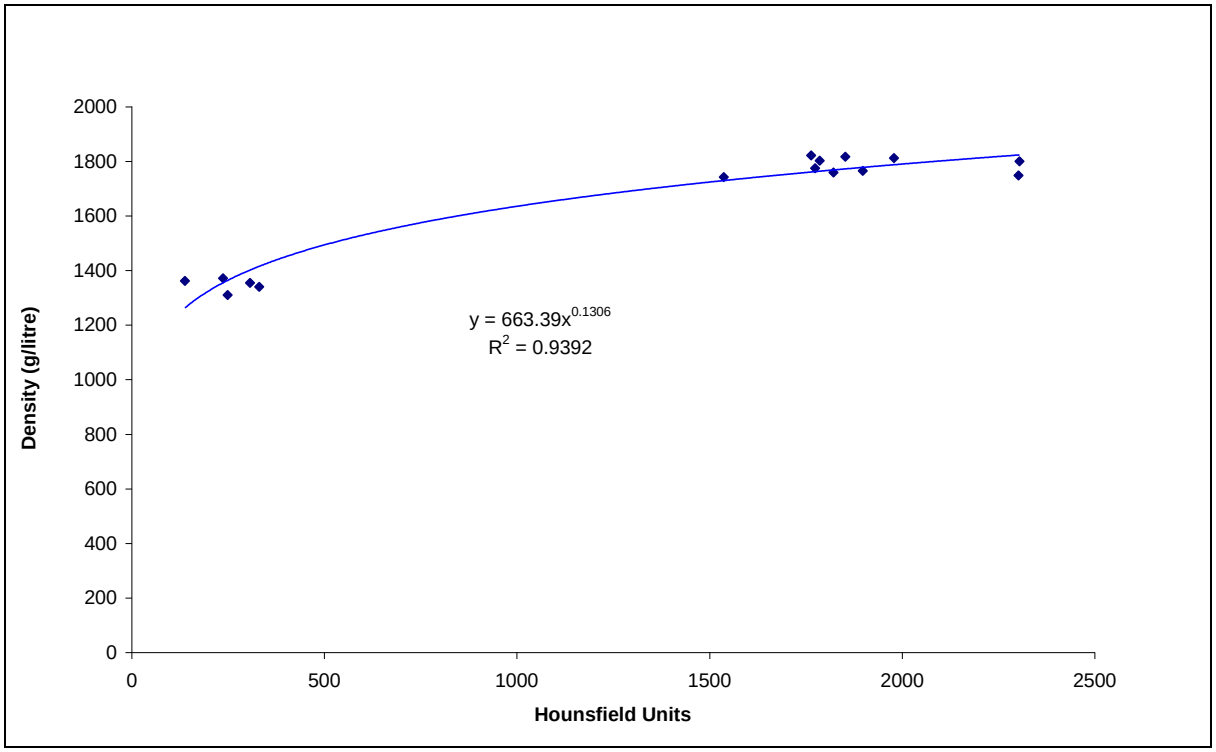

Figure 7-16: CT density (measured in Hounsfield Units – see Chapter 5) vs true density (grams/litre) for samples of bovine rib bone. The equation for the polynomial line of best fit to the data is shown on the chart, along with the value for the R^2. Note that the data is strongly bimodal, corresponding to values for spongy bone (<500 HU) and cortical bone (>1500 HU). Data from McLellan (2007).

another final year project (McLellan 2007). For the range of densities present in the bovine samples, a polynomial equation describing the relationship between CT density and absolute density was derived (Figure 7-16). The bovine samples had a minimum CT density of ~300 Hounsfield Units (HU – see Chapter 5), whereas a typical CT scan has minimum HU values of -1000: for the lower end of the Hounsfield range, the standardised Hounsfield values for air (-1000 HU) and water (0 HU) were combined with the bovine bone sample data to describe an idealised relationship between CT density and real density for scans of bony tissue (Figure 7-17).

Modelling techniques previously developed (McHenry et al. 2007, Wroe et al. 2007b) allow material properties for each individual element with the FE model to be assigned on the basis of the CT density of the corresponding voxel of the scan data. This allows the construction of a heterogeneous model, which includes a number of material property types that is set by the user. In this study, each element in the

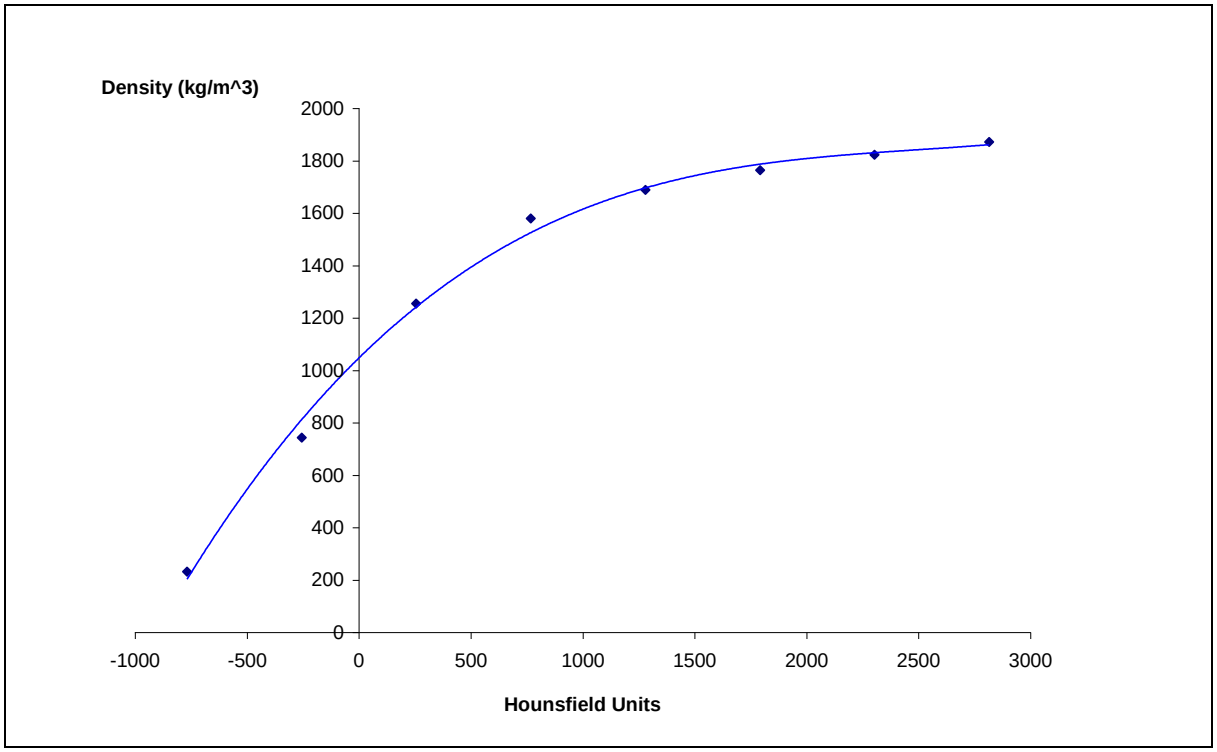

Figure 7-17: Idealised relationship between CT density and actual density, incorporating data from Figure 7-16. The solid diamonds indicate the values for each of the eight material property types used in the heterogeneous models (Table 7-10).

Crocodylus porosus model was assigned to one of eight material property types: the average CT density for each type was used to assign the absolute density for that property type as outlined above. For each property type, Young's modulus $\boldsymbol{E}$ was assigned on the basis of absolute density $\boldsymbol{\rho}$ by the equation $\boldsymbol{E} = 0.23\ \boldsymbol{\rho}^{1.49}$, using data from Keller et al. (1990) as reviewed by Rho et al. (1995)[7] (Table 7-10).

Because the *Kronosaurus queenslandicus* model was not constructed directly from CT data, the techniques used to create the heterogeneous *Crocodylus porosus* model cannot be applied. The *K. queenslandicus* model was therefore homogeneous, i.e. the modelled bone was assigned a single set of material properties, and so that the mechanics of the two models could be compared a homogeneous version of the *Crocodylus porosus* model was also created. For the homogeneous models, Young's modulus was assigned on the basis of average density of the *C. porosus* heterogeneous model (1.59

[7] In the caption for their Figure 2, Rho et al. (1995) specified that the equation derived by Keller et al. (1990) as $\boldsymbol{E} = 6.4\boldsymbol{\rho}^{1.54}$, but this does not match the graphed data in that figure. The equation from the graph is used here.

Material property #	Median HU	Density	*E*
		kg/litre	GPa
1	-768	0.232	0.749
2	-256	0.744	4.236
3	256	1.256	9.226
4	768	1.580	12.977
5	1279	1.689	14.330
6	1791	1.765	15.298
7	2303	1.823	16.063
8	2815	1.872	16.701
Homogeneous	-	1.593	13.145

Table 7-10: Values of density and Young's modulus (*E*) for the eight material property types used in the heterogeneous model, and for the single material property type used in the homogeneous models.

kg/litre) using the equation specified above, giving a value ***E*** of 13.1 GPa (Table 7-10). The mechanical performance of the heterogeneous and homogeneous versions of the *C. porosus* model were compared to gauge the affect of the different material property sets on the final results.

Axes

For each model, the Global Axes were aligned so the Z was the longitudinal axis of the skull, the X was the transverse (medial-lateral) and the Y was the vertical (dorso-ventral) (Figure 7-18A). The longitudinal axis was defined as the basal skull axis, i.e. the line from the anterior-most tip of the premaxillae to the posterior-most apex of the occipital condyle.

Scaling

Size is an important part of mechanical performance and where, as in the present study, the original size of the models is very different, size must be accounted for. The *Kronosaurus queenslandicus* model was scaled so that it had the same volume as the *Crocodylus porosus* model: the linear scaling factor required was 0.258. With homogeneous models of uniform density and material property, the biomechanical

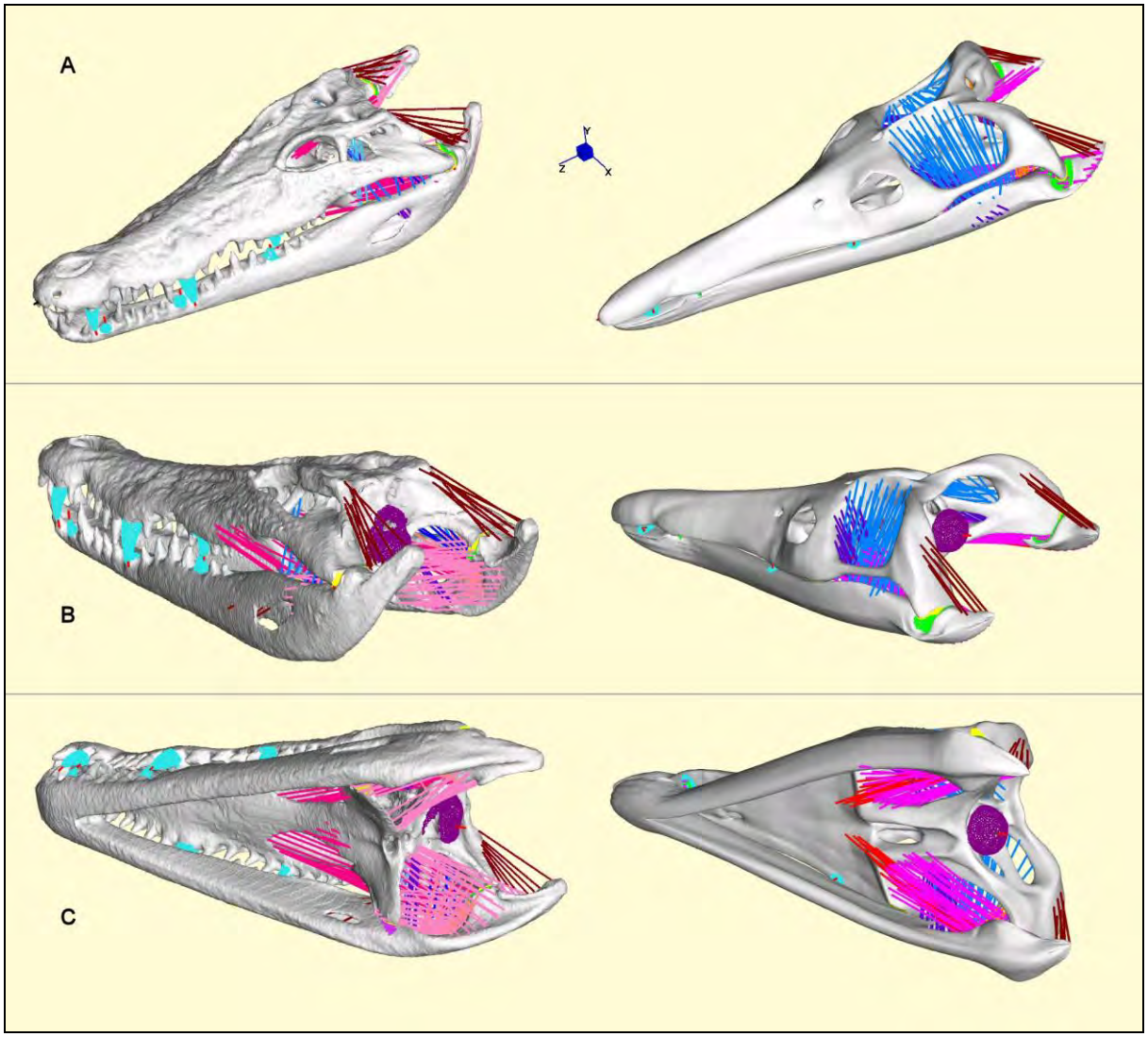

Figure 7-18: Finite Element Models of *Crocodylus porosus* (left) and *Kronosaurus queenslandicus* (right) in oblique dorsal (A), posterior (B) and ventral (C) views. Models are not shown to scale. The Global axis system for both models is shown in A: the Global Z axis corresponds with the longitudinal axis of each skull (see text for definition). The brick (tet4) elements are shown in white; the other coloured elements are beams: at the tooth margins, the beams tessellating each bite point are in cyan, and short beams that mark the nodes at which bite point restraints are placed are in red (these latter have no structural effect on the models). The 'muscle' beams in the posterior parts of the skull include the 'temporal' (shades of blue) and 'pterygoid' (red/pink) muscle systems discussed in the text: the Depressor Mandibulae is shown in dark brown. Beams tessellating the jaw joint surfaces (yellow and green) and occipital condyle (purple), like the cyan beams at the bite points, are added to prevent artificial strain concentrations: the beams tessellated to the muscle attachment areas (see text and Table 7-11) are not shown. The short red beam at the posterior apex of the occipital condyle marks the node that was used to restrain the skull (except in the 'twist' load cases, where a moment was applied to this node).

analysis then becomes an assessment of mechanical performance for a given amount of structural material, which is a mechanically and biologically relevant approach. The calculated jaw muscle forces, which are determined by cross sectional

area, were scaled by the square of the linear scaling factor and the muscle loads applied to the model were adjusted accordingly (Table 7-7).

Joints

Each jaw joint was modelled as a very stiff, short beam, oriented in the transverse (Global X) axis. The medial end was connected, via a link element (an infinitely stiff beam) to the cranium, and the lateral end to the mandible. The lateral end of the jaw beam was set to allow rotation along its own long axis: this allows the beam to work as a hinge. The articular surfaces of the joint on the mandible and cranium, which would in life hold the joint capsule, were tessellated with a network of beam elements; this allowed loads transmitted through the joint hinge to be distributed evenly over the biological joint surface (Table 7-11, Figure 7-18).

In all the extrinsic and extrinsic simulations, the occipital condyle was used either to restrain the skull in space (necessary to prevent free body rotation), or in the 'twist' load case as a point to apply a moment to the skull about the global Z axis. The restraints/moments were applied to the node on the posterior apex of the condyle. The surface of the condyle was tessellated with stiff beam elements, so that loads would be distributed evenly across the condyle (Figure 7-18).

An unusual feature of crocodilian skulls is the presence of smooth hyaline cartilage on the lateral surface of the pterygoid flanges, similar to the cartilage that typically

	E (GPa)	**diameter (mm)**
Jaw hinge axis beam	200	10.00
Bite point surfaces	100	3.00
Occipital condyle	100	3.00
Jaw joint surfaces	100	3.00
'Pterygoid' joint	100	3.00
Muscle beams (intrinsic)	0.0001	10.95
Muscle beams (extrinsic)	0.015	10.95
Muscle attachments	10	1.00

Table 7-11: Young's modulus (*E*) and geometry for the beam elements used in the FE models.

lines synovial joints. When the mandible is fully adducted, the apposing surface of the lower jaw presses very tightly to this lateral surface of the pterygoid, and previous modelling (Ingle 2007) suggests that the apposition of the pterygoid and mandible surfaces is important in preventing medial bending of the mandible during biting that would otherwise result from the strong medially-directly component of the force vector of the adductor musculature: this was also suggested by Busbey (1995). In this way, the pterygoid flange appears to act as an 'open' joint, that is lined with cartilage, but which lacks joint capsule ligaments and a synovial membrane and fluid. Although smaller than the structure in crocodilians, pliosaurs also possess a lateral pterygoid buttress which closely apposes the mandible (Taylor 1992, Taylor and Cruickshank 1993) and given the morphology described in Chapters 4 and 5 a similar joint can be inferred for *Kronosaurus queenslandicus*. The mechanical effect of this 'joint' in bracing medial bending of the mandible was simulated by connecting the pterygoid flange to the apposing surface of the mandible with a 'master-slave' link element that was set up to transmit all loads in the Global X (transverse) axis, but which did not transmit loads in the Y or Z axes. The surface of the bone surrounding the link was tessellated with stiff beam elements to avoid artificial concentration of loads (Table 7-11).

Muscle geometry

For each model, attachment areas for the jaw muscles listed in Table 7-2 were identified using data from Iordansky (1964) and Holliday and Witmer (2007) for crocodilians, and from Taylor (1992) for pliosaurs. Jaw muscles were modelled using truss elements (Figure 7-18), as has been described previously (McHenry et al. 2007, Wroe et al. 2007b). The models also included trusses representing the Depressor Mandibulae (both models) and the Intramandibularis (*Crocodylus porosus* model only). The Young's modulus of the muscle beams was given a low value for instrinsic load cases, to minimise reduction in the effective force provided by the beam pretensions, and a higher value for extrinsic load cases to simulate the isotonic contraction of muscles that are bracing the jaw system without causing adduction (Table 7-11 – see McHenry et al. 2007).

The surface of the models corresponding to the muscle attachment areas were tessellated with beam elements, to simulate the broad attachment of the adductor

muscles on the bone and to minimise artefacts arsing from the attachment of a relatively smaller number of beams simulating muscle fibres (Table 7-11).

Bite points

Nodes corresponding to the front, mid, and rear bite points detailed in Section 7.2 were identified on each side of the cranium and mandible (Figure 7-18). For each of the intrinsic and the 'twist' load cases, the relevant four nodes were fixed. For each of the 'shake' load cases, a laterally directed force was applied to each relevant node. The elements surrounding each bite point were tessellated with stuff beams to prevent artificial concentrations of load (Table 7-11, Figure 7-18). All load cases involved equal restraint/ forcing of the bite points of both sides of the skull, simulating bilateral bites.

Intrinsic loads

For intrinsic loads, muscle forces were modelled as pretensions on each truss element: the magnitude of the pretension was determined by the total forces calculated for each adductor muscle group (i.e. temporal and pterygoid) in Section 7.2, and the total number of truss elements (Table 7-12). The trusses representing the Depressor Mandibulae and (in the *Crocodylus porosus* model) the Intramandibularis were not assigned pretensions.

In Finite Element Analysis over-restraint of the model can lead to artefacts and misleading results. When a predator bites down on prey, there is a complex interplay between the hard tissues of the predator's teeth, and the hard and soft tissues of the prey's body: the actual effect of the prey in resisting the predator's teeth (which results in the development of the reaction forces that are termed 'bite force') is highly non linear and is a complex modelling challenge beyond the scope of the present analysis.

The action of the prey's body in resisting the predator's teeth is here approximated by restraining the respective four nodes for each of the front, mid, and rear bites. This is a simplification of a complex mechanical situation; previous work has

muscle	*Kronosaurus queenslandicus*					*Crocodylus porosus*		
	n	original		rescaled		n	F/beam	F
		F/beam	F	F/beam	F			
MAME	74	500.9	37067	33.38	2470	34	48.4	1646
MAMP	14	500.9	7013	33.38	467	34	48.4	1646
PST	46	500.9	23041	33.38	1535	10	48.4	484
PTA	54	500.9	27049	33.35	1801	35	39.6	1385
PTP	26	500.9	13023	33.35	867	67	39.6	2652
IM	12					10		
DM						16		
Total								
Temporal	134		67121		4473	78		3777
Pterygoid	80		40072		2668	102		4037

Table 7-12: Muscle beam forces in the FE models for intrinsic load cases. Total force for each muscle (F) is a product of the number of beam elements (n) and the pretension applied to those beams (F/beam). See Table 7-3 for muscle abbreviations and composition of 'Temporal' and 'Pterygoid' muscle groups. Forces given in Newtons.

suggested that restraining each of these nodes from movement in the θ (Theta) axis of a cylindrical coordinate system aligned to the jaw joint does not lead to over-constraint of the model. The effect of this type of constraint is to prevent the bite-point nodes from being adducted together, although they are not constrained from moving in the direction of the jaw joint's radius, or in the transverse axis, and rotations in all axes are permitted. In order to gauge the effects of different restraints upon the results, for the *Kronosaurus queenslandicus* model the intrinsic load cases were solved with each of the bite points restrained in θ of the jaw axis only (partially restrained), and in all axes (fully restrained).

Extrinsic loads

Although extrinsic loads are undoubtedly an import component of skull biomechanics in predatory mammals and reptiles, quantitative data is lacking. Examples of extrinsic loads include a rabbit being shaken by a dog, a buffalo bucking whilst being bitten by a lion, or a crocodile performing a 'death roll' on a zebra; all of these have the potential of generating high loads upon the predator's skull. Whether these loads exceed the intrinsic forces has not been tested, although Preuschoft and Witzel (2005) calculated the extrinsic loads induced by a dog shaking a 2kg rabbit are

of the same order as the intrinsic forces in a canine bite (approximately 300 N for a 18 kg dog), and several recent studies have assumed that extrinsic loads match intrinsic forces (McHenry et al. 2007, Wroe 2007, Wroe et al. 2007a).

Two classes of extrinsic loads were considered; 'twisting' loads, as might be produced by the predator rolling about its long axis while firmly gripping the prey, and 'shaking' loads, where the prey is held in the jaws and shaken violently from side to side. The magnitude of these loads were calculated using standard engineering formulae, applied to the following hypothetical situations;

1. Twist loads: A 105 kg predator, with an average radius of 0.2 m, twists around its own axis – from a standing start it completes a 360° turn in 0.5 seconds. The prey is held in the jaws, and is assumed to have sufficient mass that its inertia effectively fixes it in space.

   The torque produced in this scenario is given by the product of the moment of inertia **I** about the transverse axis **zz**, and the angular acceleration **α**:

   $$\text{Torque} = \mathbf{I_{zz}} * \boldsymbol{\alpha}$$

   $\mathbf{I_{zz}}$ is calculated from the radius **r** and mass **m** (assuming it is a solid cylinder) and is given by

   $$\mathbf{I_{zz}} = \tfrac{1}{2}\,\mathbf{m} * \mathbf{r}^2$$

   Here $\mathbf{I_{zz}}$= 2.1 kgm^2 for the values of **m** and **r** specified above. Assuming constant angular acceleration, **α**, during the twist, this can be found using

   $$\boldsymbol{\theta} = \boldsymbol{\omega}_0\mathbf{t} + \tfrac{1}{2}\,\boldsymbol{\alpha}\mathbf{t}^2$$

   where **θ** is the total angular movement in radians and **t** is the time in seconds taken to achieve this movement. Because the twist is being made from a standing start, $\boldsymbol{\omega}_0$ =0, then for a 360° rotation (2π radians) **α** is given by

   $$\boldsymbol{\alpha} = 2\boldsymbol{\theta}/\mathbf{t}^2 = 50.272 \text{ rad/s}^2$$

   Thus the torque required to achieve this motion is

   $$\text{Torque} = 2.1 \text{ kgm}^2 * 50.27 \text{ rad/s}^2$$

As (1kg * 1m)/1 second^2 is a Newton, and the angular units (radians) are not included in the measurement of torque, then the torque

$$\text{Torque} = 105.56 \text{ Nm}$$

This load was simulated by fully restraining the bite points, as specified for the above, and applying a moment of 105.56 Nm in the Z (longitudinal) axis to the same posterior apical node of the occipital condyle that was used to fully restrain the skull in the intrinsic load cases. For each model, three 'twist' simulations were run, with the front, mid, and rear bite points restrained respectively.

2. Shake loads: A predator shakes a 20 kg prey repeatedly from side to side, from an angle ($\boldsymbol{\theta}$) of 45° from the left of the predator's long axis to 45° to the right. The prey is held in the jaws, at a radius **r** from the point (in the neck) about which the head is being rotated from side to side. The prey is being shaken rapidly, so that to move the prey all the way from one side to the other (through an arc of $2\boldsymbol{\theta}$) takes 0.125 seconds. The torque **T** to be produced by the predator's postcranial musculature acting upon its skull is given by;

$$\mathbf{T} = \mathbf{I_{xx}} * \boldsymbol{\alpha}$$

where $\boldsymbol{\alpha}$ is the maximum angular acceleration during the shaking process, and $\mathbf{I_{xx}}$ is the moment of inertia of the prey. If we consider the mass of the prey to be a point mass, then the moment of inertia is the product of the prey's mass **m** and the square of the radius **r**;

$$\mathbf{I_{xx}} = \mathbf{m} * \mathbf{r}^2 = 20(\mathbf{r}^2) \text{ kgm}^2$$

Note in this analysis the mass of the predator's own skull is ignored. Here it is assumed the sideways shaking motion is sinusoidal in the time domain. The angular displacement, $\boldsymbol{\theta}$, is therefore given by

$$\boldsymbol{\theta} = \sin(f\,\mathbf{t})$$

where f is the periodicity of shaking. As the angular velocity and acceleration are first and second time derivatives of the angular displacement respectively, then

$$\boldsymbol{\omega} = -\cos(f\,\mathbf{t})$$
$$\boldsymbol{\alpha} = f^2 \sin(f\,\mathbf{t})$$

For this particular case, $f = 4\,\pi$ rad/sec ($\pi/2$ radians in 0.125 seconds), therefore, for $\mathbf{t} = 1$, the maximum value of $\boldsymbol{\alpha}$ is given by

$$\alpha = 16\ \pi^2 \text{rad/sec}^2$$

and the torque is given by

$$\mathbf{T} = 20\mathbf{r}^2 * 16\ \pi^2 \text{ Nm}$$

The value for **r** is determined by the position in the tooth row that the prey is being held. For each of the two models, values were calculated for shakes where the prey was held at the front, mid, and rear of the tooth rows, as defined for the intrinsic bites (see above). The point of rotation in the neck, about which the predator shakes its head from side to side, was assumed to be in line with the jaw joints, i.e. slightly behind the cervical-cranial joint at the occipital condyle.

For each bite position, the calculated torque was divided by the moment arm to give a laterally directed force **F** acting at the appropriate part of the tooth row (Table 7-13). The sideways shakes were then simulated by restraining the occipital condyle (i.e. preventing translations or rotations about the apical node of the condyle, as for the intrinsic load cases) and applying a force in the positive X (i.e. left) direction to each of the four nodes corresponding to a bite point: these were the same nodes used to restrain the skull in the intrinsic load cases. The force applied to each node was **F**/4, so that the total force in each load case was equal to the total force **F** calculated for each bite position in Table 7-13). For each model, three 'shake' load cases were run, simulating prey being held in the front, mid, and rear tooth positions respectively.

model	bite position	radius (cm)	Torque (Nm)	Force (N)
C.p-2	front	38	136	358
	mid	30	67	223
	rear	18	14	80
K.q-r	front	44	211	480
	mid	40	159	397
	rear	24	34	143

Table 7-13: Calculated torque generated at different bite positions by 'shaking' extrinsic loads. For a prey of 20 kg, an arc of 90°, and a time of 0.125 seconds, the torque is dependent on the radius of the bite position from the pivot about which the head is being shaken. Dividing the torque by the radius gives a laterally directed force acting on the predator's skull at the bite point. The calculated force was applied to each model for the different 'shake' load cases.

Measurements

For each model, strain data was collected as visual output from the post-processor. Both von Mises strain and principal strain were recorded: von Mises strain is a summation of the strain resulting from compression, tension, and shear, and provides a useful overall summary of the response of a structure to load, while principal strains can identify the specific compressive, tensile, and shear components. For each tetrahedral element – which is termed a 'brick' in Strand7 – there are three axes which are not necessarily aligned with the surfaces, and as principal strains are output with respect to axis systems, plotting principal strains for brick elements can be complex. For this reason, the surfaces of each model were tessellated with three-noded plate elements (thickness = 0.25 mm, E = 1 MPa), and the local x axes of the plate elements were aligned with the Global Z (i.e. longitudinal) axis; this allows the compressive and tensile strain components to be plotted in just two local axes for the plates ('xx' and 'yy'), which are both aligned with the surface of the structure. Von Mises strains are independent of axis systems and can be shown with a single plot based on brick strain.

In addition to strain data, bite reaction forces were collected from the nodes used to restrain the bite points for each of the front, mid, and rear bites, and the reaction forces from the FE models ('3D') were compared with the predictions derived from the dry skull method in Section 7.2 (2D). For both fully restrained and partially restrained models, reaction forces were measured in terms of displacement in θ ('DT' in Strand7) of the jaw hinge axis only. Jaw reaction forces were collected as end forces in the beams used as the jaw hinges; forces were collected in the three axes of these beams and summed to give resultant vectors.

Results

Bite reaction forces are shown in Table 7-14. For the full-sized *Kronosaurus queenslandicus* model (K.q), the rescaled *Kronosaurus queenslandicus* model (K.q-r), and the *Crocodylus porosus* model (C.p-2), the bite forces from the 3D models were higher than those derived from the 2D dry skull method. The reaction forces were also greater for the fully restrained compared with the partially restrained models, although the difference between these was greater for the K.q and K.q-r models than for the C.p-2 model (Table 7-15). The visual plot of strain fields differed slightly between the two restraint types, but qualitative patterns of strain were similar (Figure 7-19). There was no appreciable difference between bite reaction forces for the homogeneous and heterogeneous versions of the C.p-2 model (Table 7-14), and the strain fields are nearly identical (Figure 7-20).

Model	method	restraint type	Bite position		
			front	mid	rear
K.q (full size)	2D – dry skull	–	15,169	16,401	27,716
K.q (full size)	3D - FEA	partially fixed	18,445	20,801	35,541
K.q (full size)	3D - FEA	fully fixed	21,579	23,668	38,023
K.q-r (rescaled)	2D - dry skull	–	1011	1093	1847
K.q-r (rescaled)	3D - FEA	partially fixed	1225	1384	2373
K.q-r (rescaled)	3D - FEA	fully fixed	1504	1654	2683
C.p-2	2D – dry skull	–	899	1138	1880
C.p-2	3D - FEA (Hom)	partially fixed	1005	1320	2000
C.p-2	3D - FEA (Het)	partially fixed	1006	1320	2000
C.p-2	3D - FEA (Het)	fully fixed	1030	1359	2041

Table 7-14: Bite forces results (in Newtons) for *Kronosaurus queenslandicus* ('K.q') and *Crocodylus porosus* (C.p), using 2D dry skull and 3D finite element analysis (FEA) modelling. Bite positions for each model are specified in Section 7.2 (see Table 7-6). Data is presented for 'full size' and 'rescaled' versions of the *Kronosaurus* model, and for homogeneous ('Hom') and heterogeneous ('Het') material property sets of the *Crocodylus* model (see text).

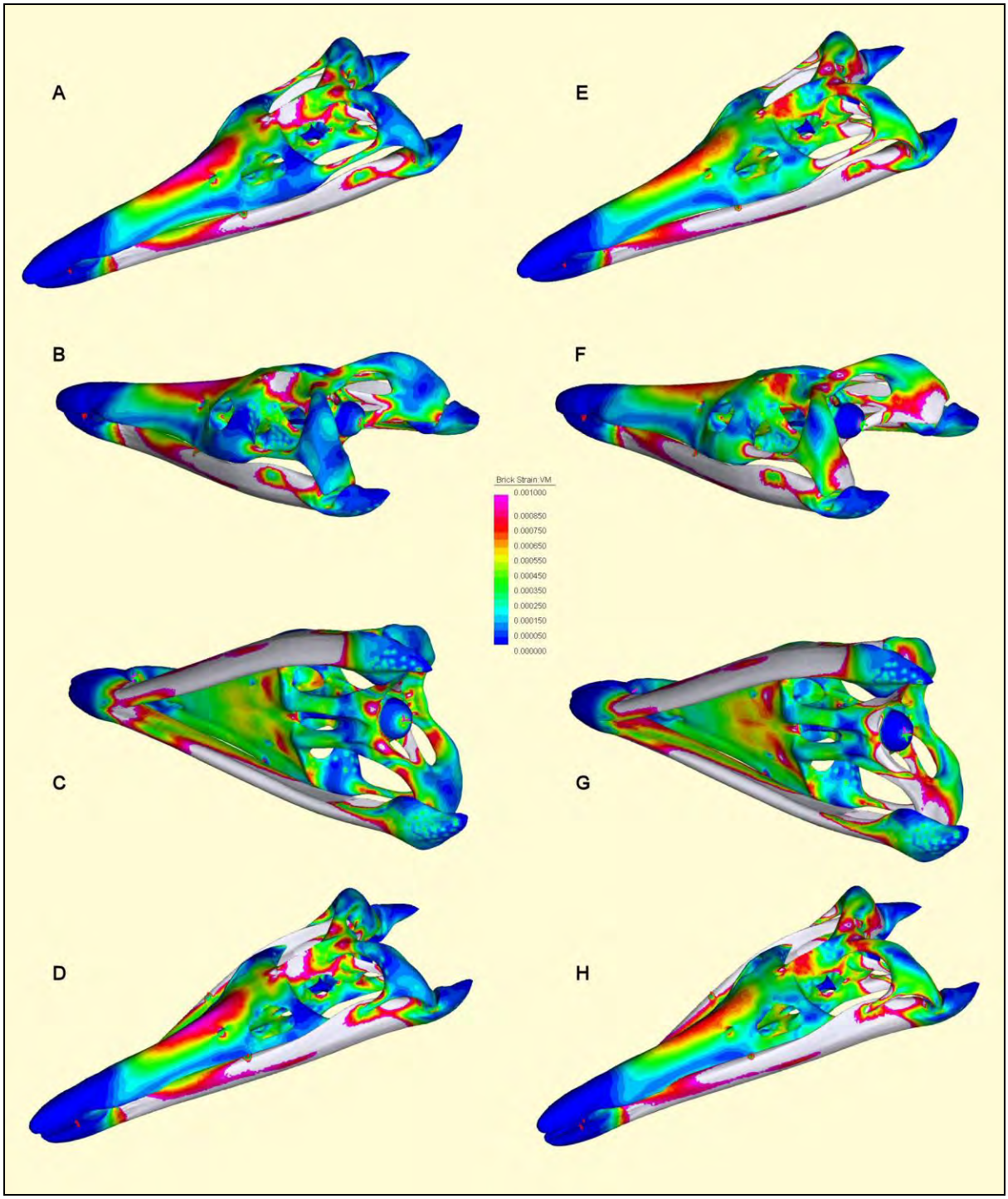

Figure 7-19: Von Mises (brick) strain for fully fixed (A-D) and partially fixed (E-H) variants of the rescaled *Kronosaurus queenslandicus* model, for mid bites. Areas of low strain are shown as blue: increments in strain are shown as various colours through to red, as per the legend. The legend shows strain figures to 6 decimal places; if the decimal point is ignored, this also allows the numbers to be read as figures of microstrain. Strains exceeding 0.001 (i.e. 1000 microstrain) are shown as white. D and H show the skull in the same view as A and E, but with displacements exaggerated to illustrate the distortion of the skull under load.

Model	method	restraint type	Bite position		
			front	mid	rear
K.q (full size)	3D - FEA	partially fixed	1.22	1.27	1.28
K.q (full size)	3D - FEA	fully fixed	1.42	1.44	1.37
K.q-r (rescaled)	3D - FEA	partially fixed	1.21	1.27	1.28
K.q-r (rescaled)	3D - FEA	fully fixed	1.49	1.51	1.45
C.p-2	3D - FEA (Hom)	partially fixed	1.12	1.16	1.06
C.p-2	3D - FEA (Het)	partially fixed	1.12	1.16	1.06
C.p-2	3D - FEA (Het)	fully fixed	1.15	1.19	1.09

Table 7-15: Ratios of various estimates of bite force using 3D FEA modelling to the respective 2D results given in Table 7-14, for specified bite positions.

In the rescaled version of the *Kronosaurus queenslandicus* model (K.q-r), the jaw muscle forces were scaled from the full sized model by the second power of the linear scaling factor, i.e. by 0.0666. The resultant bite forces in the K.q-r model would thus be expected to be 0.0666 of the forces in the full sized K.q model. For the partially restrained K.q-r model, the resultant forces were close to 0.0666^{8} times the full sized model; for the fully fixed model the factors deviated slightly more from that number (Table 7-16).

restraint type	front	mid	rear
partially fixed	0.0664	0.0665	0.0668
fully fixed	0.0697	0.0699	0.0706

Table 7-16: Scaling factors for bite force results in the *Kronosaurus* FEA models, given as ratios of 'rescaled' to 'full size', for front, mid, and rear bite positions. As the rescaled model was 0.2581 the length of the full sized models, and the bite force results are expected to scale by the second power of the linear scaling factor, the predicted ratio should be 0.0666 for all load cases.

[8] The similarity between this number and the isometric ration for surface to volume, 0.666, is a coincidence.

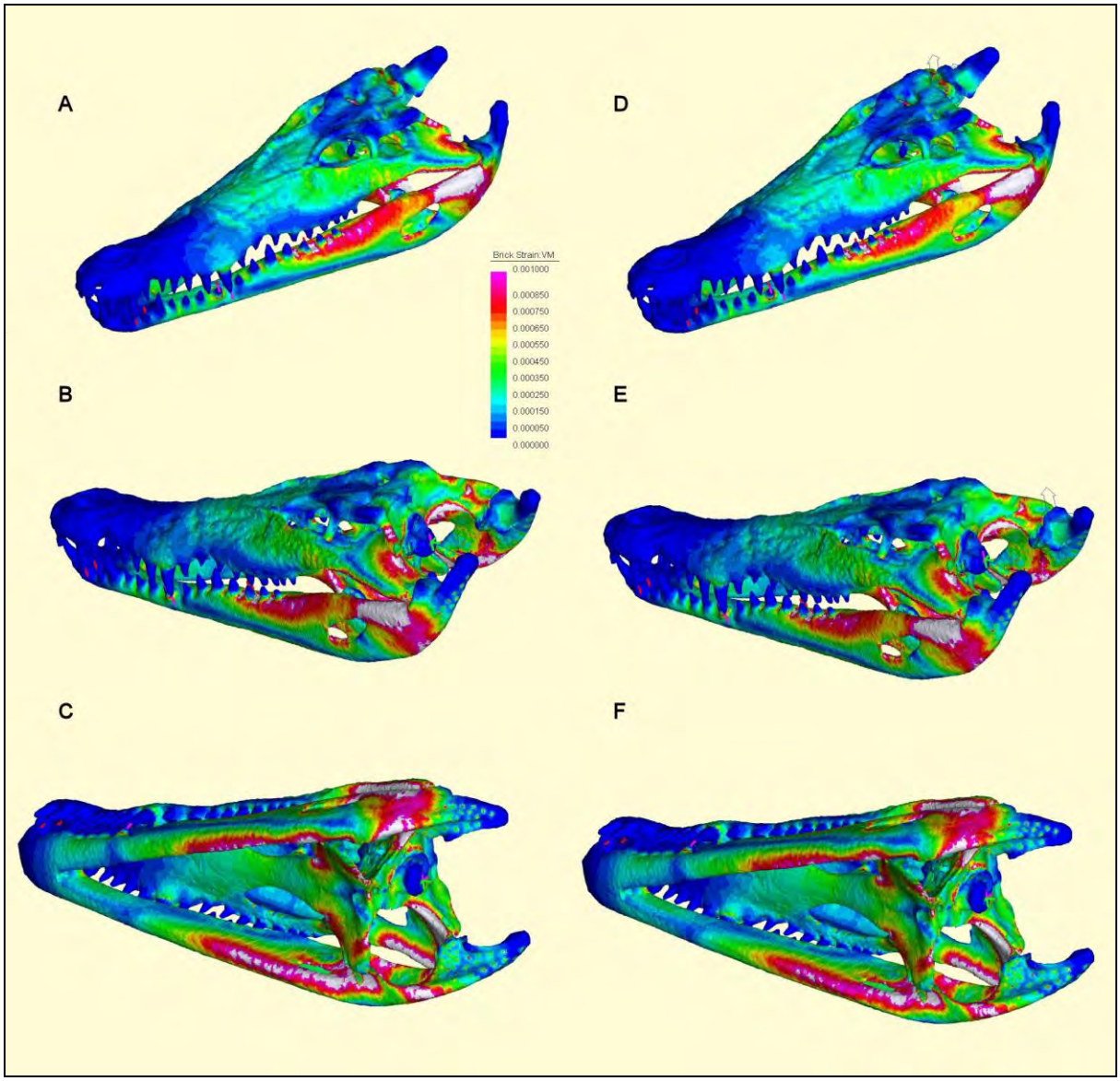

Figure 7-20: Homogeneous (A-C) vs Heterogeneous (D-F) versions of the *Crocodylus porosus* model, showing von Mises brick strain results from FEA. See Figure 7-19 for explanation of colour output and legend.

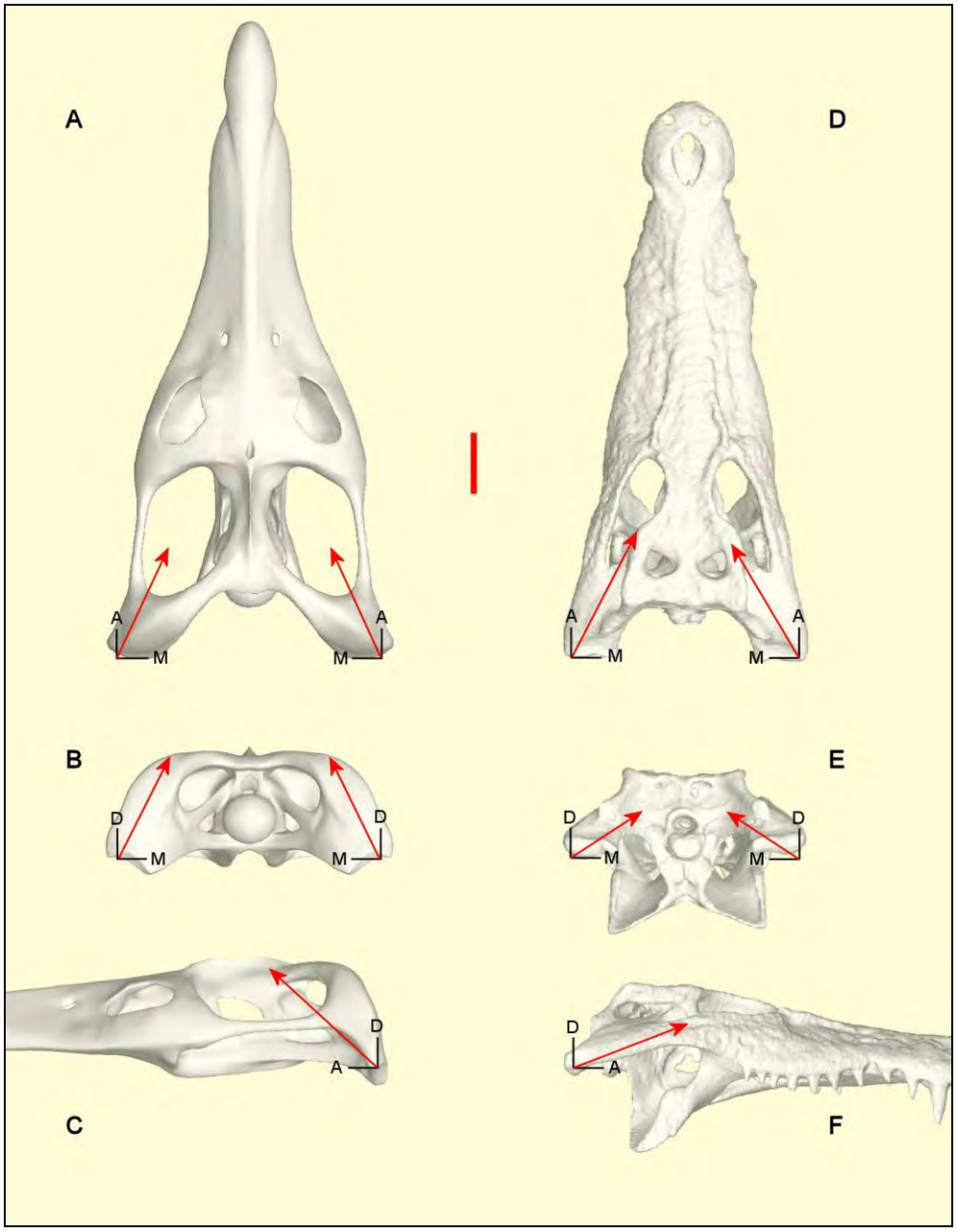

Figure 7-21: Joint forces acting on the cranium of the K.q-r (A-C) and C.p-02 (D-F) models, for mid bites under partially fixed restraints. The force vector components are shown as red arrows in dorsal (A, D), posterior, (B, E) and lateral (C, F) views: arrows are scaled to force magnitude, the solid red bar indicating 1000 N. The black lines indicate the relevant axes of the vector components (axis labels as for Table 7-17).

model	bite position	A	D	M	ADM
C.p-2	front	1598	1502	727	2310
C.p-2	mid	1602	1464	740	2293
C.p-2	rear	1627	1221	836	2199
K.q-r	front	1789	710	1009	2173
K.q-r	mid	1772	643	988	2128
K.q-r	rear	1749	479	964	2054

Table 7-17: Joint forces acting on the crania of the *Crocodylus porosus* (C.p-2) and rescaled *Kronosaurus queenslandicus* (K.q-r) models, for load cases with partially fixed restraints. Joint forces are given as vector components in the anterior-posterior (A), dorsal-ventral (D), and lateral-medial (M) axes of the jaw joint, so that a positive number indicates anteriorad, dorsad, and mediad oriented forces respectively. The magnitude of the resultant 3D force vector is given in the column 'ADM': see Figure 7-21 for illustration of the force vectors for the mid bites of each model. All forces shown in Newtons, and are averaged across left and right sides of the crania.

The joint forces were of a similar magnitude in the K.q-r and C.p-2 models, being slightly larger in the crocodile (Table 7-17). For both models, total magnitude of the joint force was highest for front bites and lowest for rear bites. The vectors for the joint forces changed slightly between front, mid, and rear bites, but were essentially oriented so that the joint forces acting on the cranium vectored anteriorly, dorsally, and medially in both models (Figure 7-21). The C.p-2 model had a larger anteriorly directed component, and the K.q-r model a larger dorsally directed component: the resultant vectors are strongly aligned with the quadrate in the C.p-2 model, and are less well aligned with the K.q-r model.

The effects of bite position on the strain fields for the *Crocodylus* and *Kronosaurus* models are shown in Figure 7-22 and Figure 7-23 respectively (for the partially fixed tooth restraints, and for the homogeneous version of the C.p-2 model). In both cases, changing bite position had a large effect on the strain fields of the rostrum, but a much smaller effect upon the strain in the temporal and occipital regions of the skull. Overall strain is higher in the K.q-r model than in the C.p-2 model, particularly in the mandible.

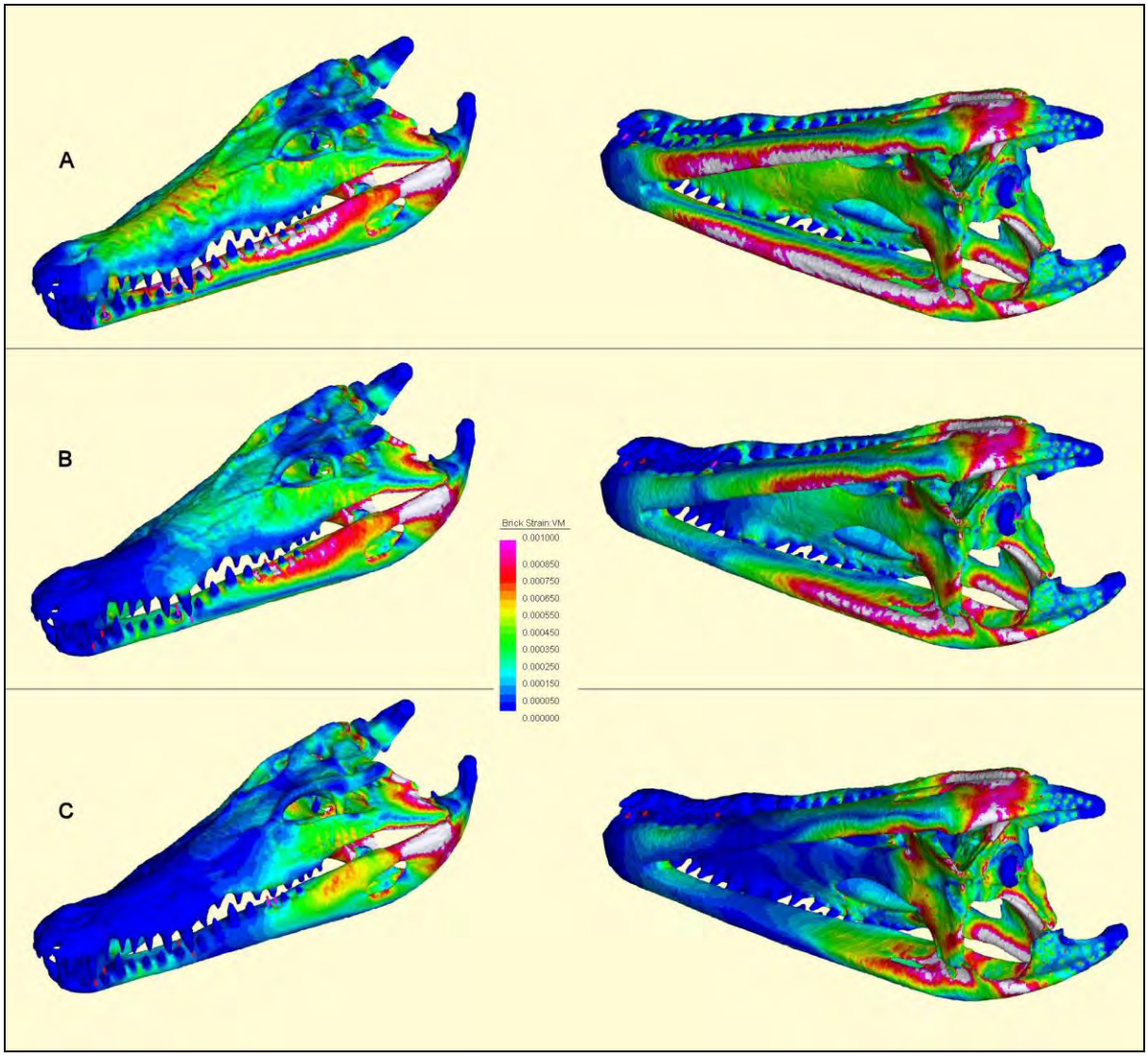

Figure 7-22: Von Mises (brick) strain results in the homogeneous *Crocodylus porosus* model for front (A), mid (B), and rear (C) bites, using partially fixed tooth restraints (see text). For explanation of colours and legend see Figure 7-19.

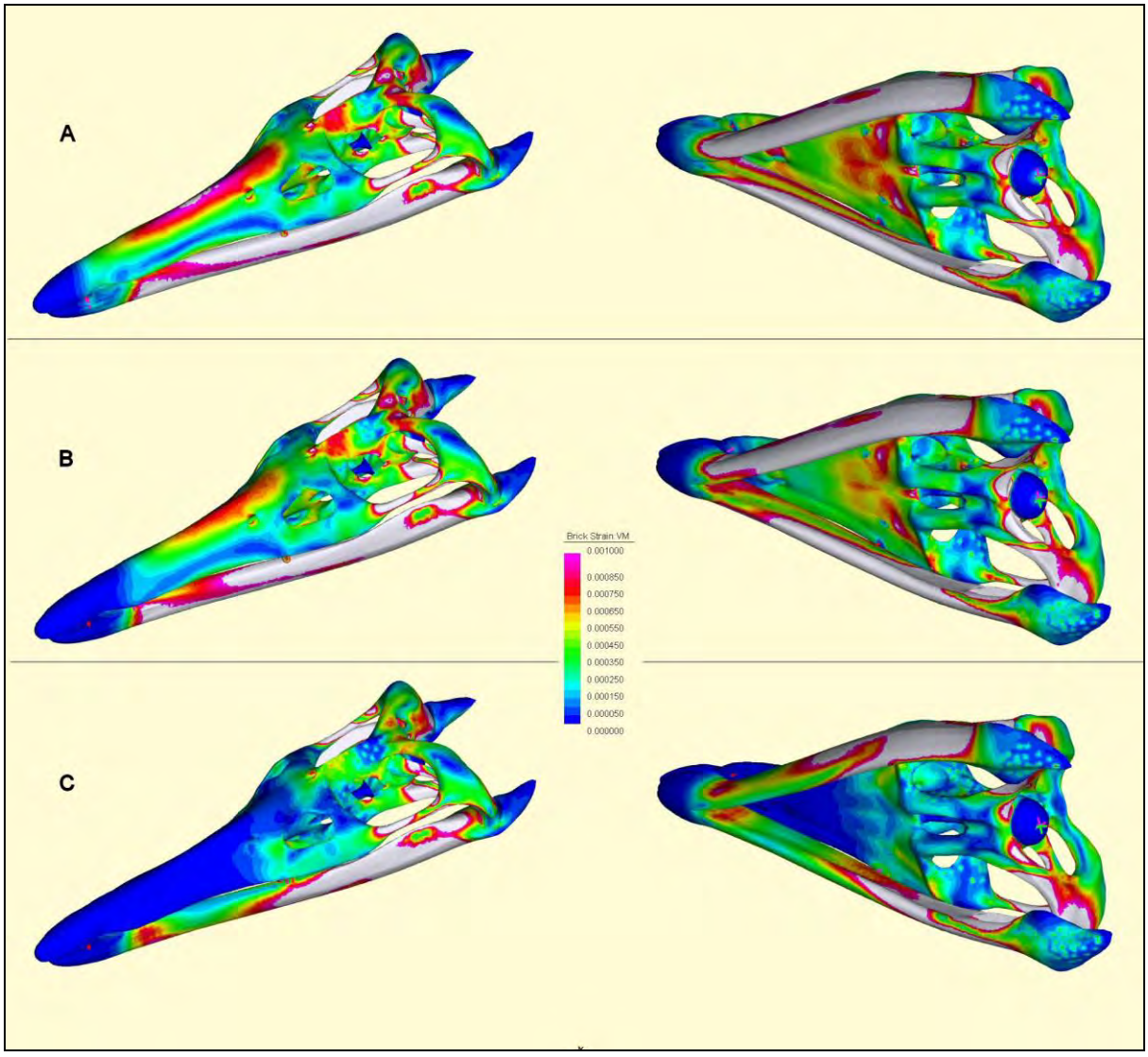

Figure 7-23: Von Mises (brick) strain results in the rescaled *Kronosaurus queenslandicus* model for front (A), mid (B), and rear (C) bites, using partially fixed tooth restraints (see text). For explanation of colours and legend see Figure 7-19.

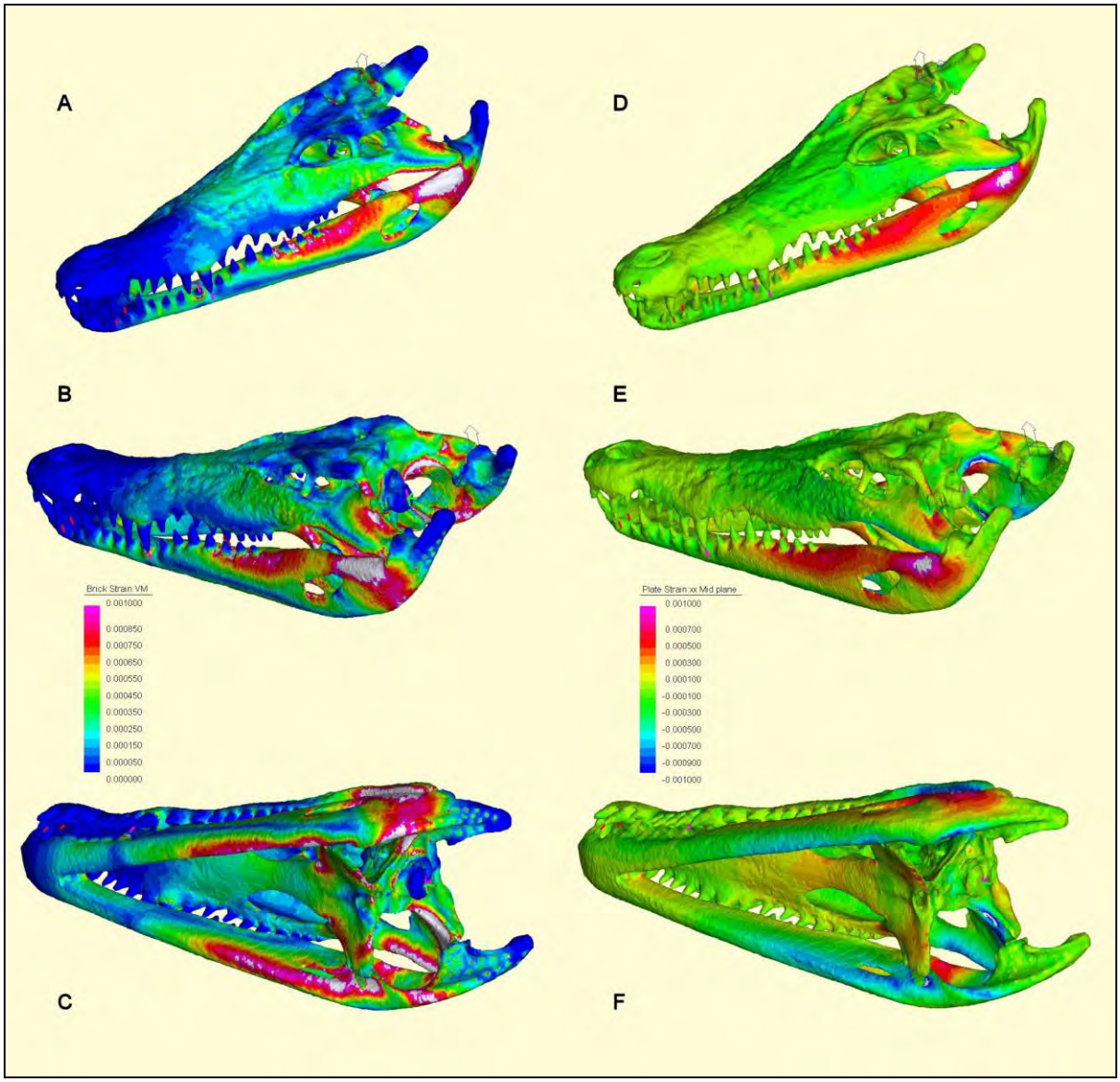

Figure 7-24: Von Mises brick strain (A-C) and principal plate strains (D-F) for the homogeneous *Crocodylus porosus* model, for a partially fixed mid bite. The principal plate strains are shown for the local xx axis of plates tessellated to the surface of the skull model; the xx axis of the plates have been aligned to the global Z (longitudinal) axis of the model. Negative principal strain, i.e. compression in the xx axis, are shown as shades of dark greens to blues; positive principal strain (tension in the xx axis) are shown as yellows to reds. The plot allows the components of the overall strain, show as von Mises strain, to be visualised; for example, the rear part of the mandible is under large amounts of overall strain and a large part of this is evidently due to compression and tension in the longitudinal axis of the skull. In D, the dorsal surface of the skull is under very slight compression (dark green), but overall stress in this part of the skull are low in any case (A).

The compressive/ tensile components of the strain about the longitudinal axis of the skull are shown in Figure 7-24 for the C.p-2 model and in Figure 7-25 for the K.q-r model, for mid bites using partially fixed restraints and the homogeneous version of the crocodile model. For both skulls, the tooth bearing sections of the rostrum and

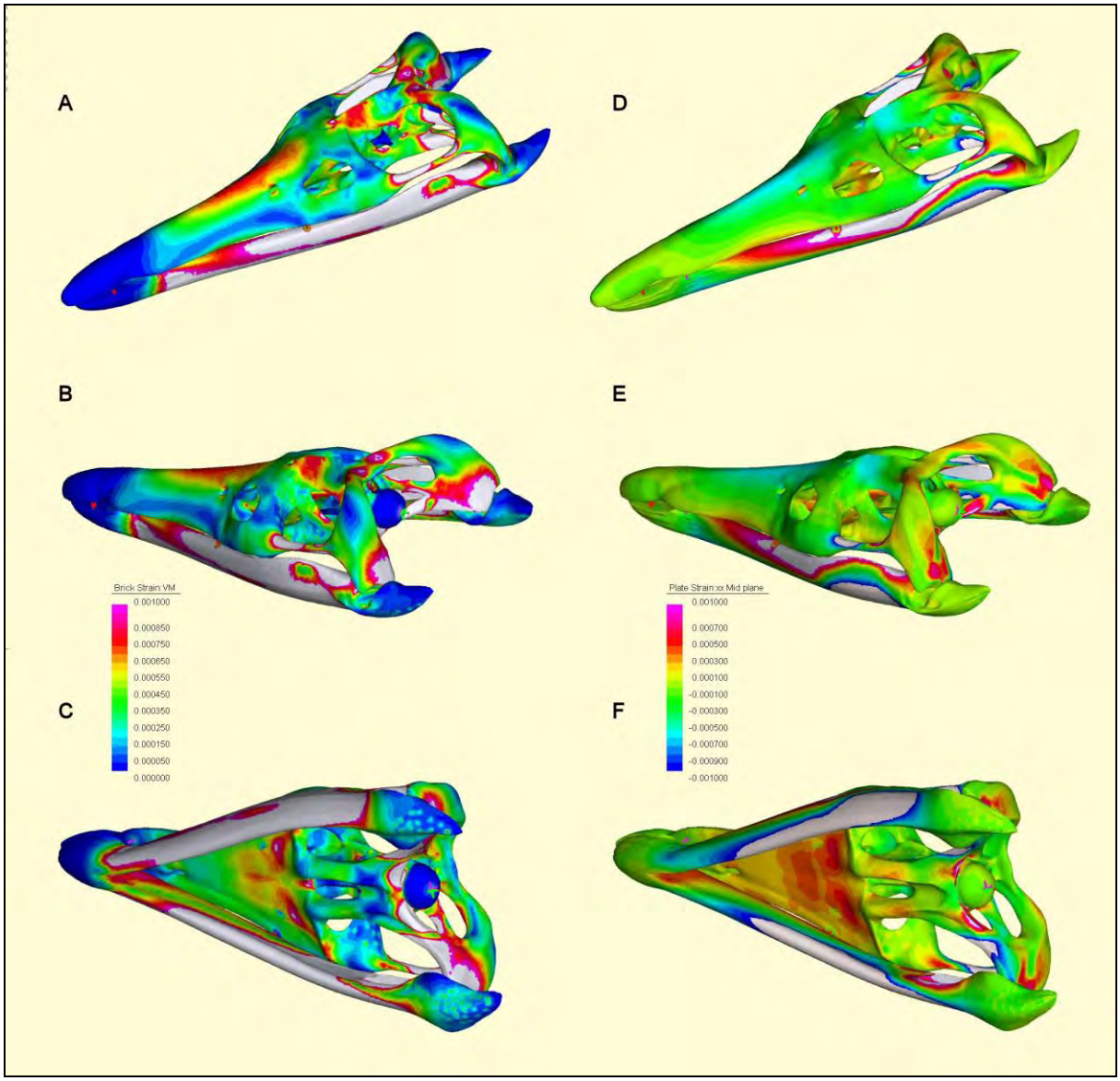

Figure 7-25: Von Mises brick (A-C) and principal plate (D-F) strains for the rescaled *Kronosaurus queenslandicus* model, for a partially fixed mid bite. Principal plate strains are shown for the local xx axis of the plates – see Figure 7-24 for explanation. The high levels of overall strain on the dorsal median ridge of the posterior rostrum (A) are shown to have a large component of compression in the longitudinal axis (D), as would be expected from beam theory.

mandible act as beams, with the dorsal side of the rostrum and the ventral edge of the mandible under compression, and the palatal surface and dorsal edge of the mandible under tension. The magnitudes of compressive and tensile components appear to be greater for the K.q-r model, although this may be a result of the higher overall strain this model, rather than the rostrum in *Kronosaurus* necessarily behaving more like a beam.

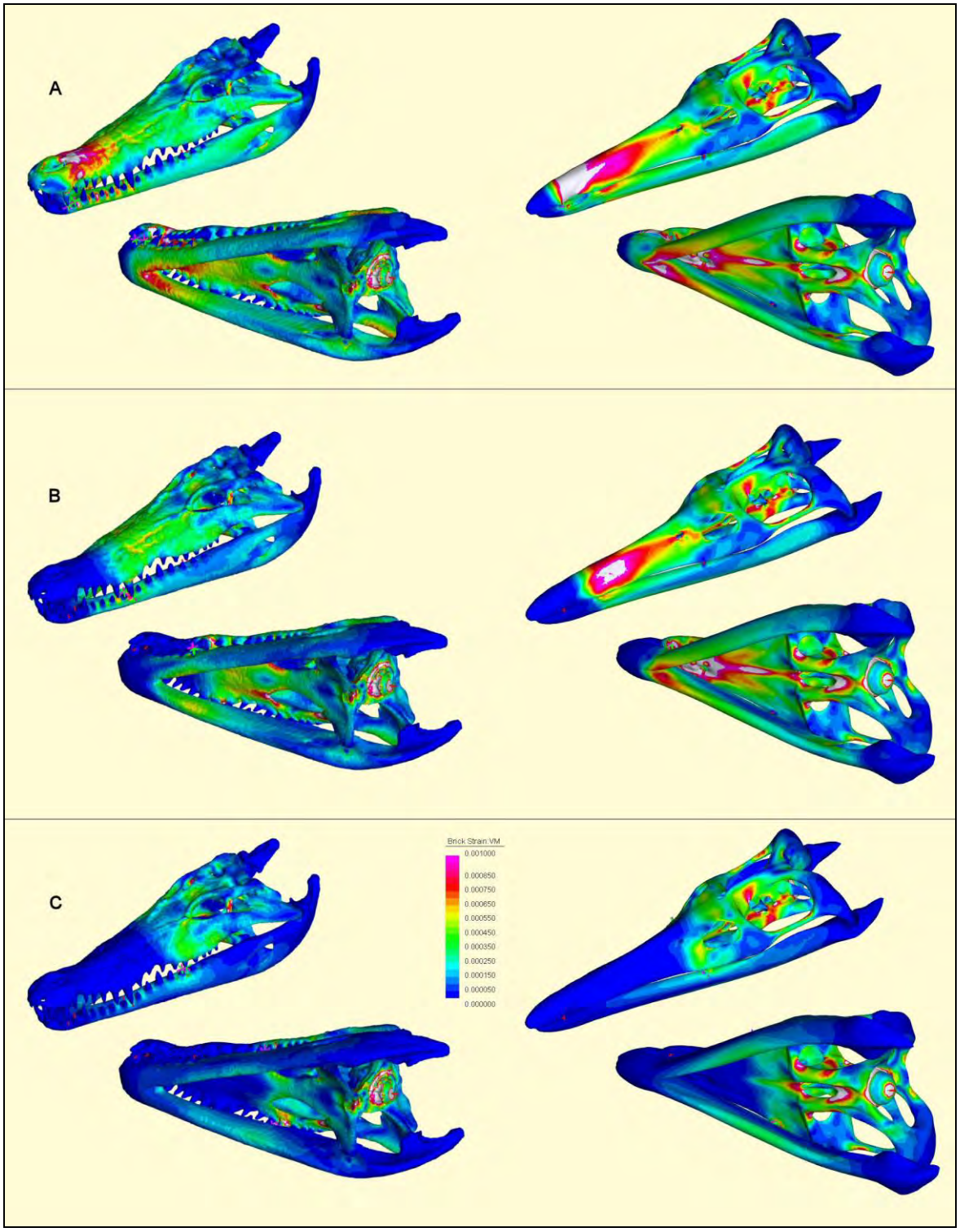

Figure 7-26: Von Mises brick strains for the homogeneous *Crocodylus porosus* and the rescaled *Kronosaurus queenslandicus* models during twist loads, for front (A), mid (B), and rear (C) bite positions. Each skull is shown in oblique dorsal and ventral views; the *Crocodylus* model is on the left and the *Kronosaurus* is on the right. For explanation of colours and legend, see Figure 7-19.

The response of the models to extrinsic loads are shown in Figure 7-26 for twist loads, and Figure 7-27 for shake loads. In both types of intrinsic loads, for both

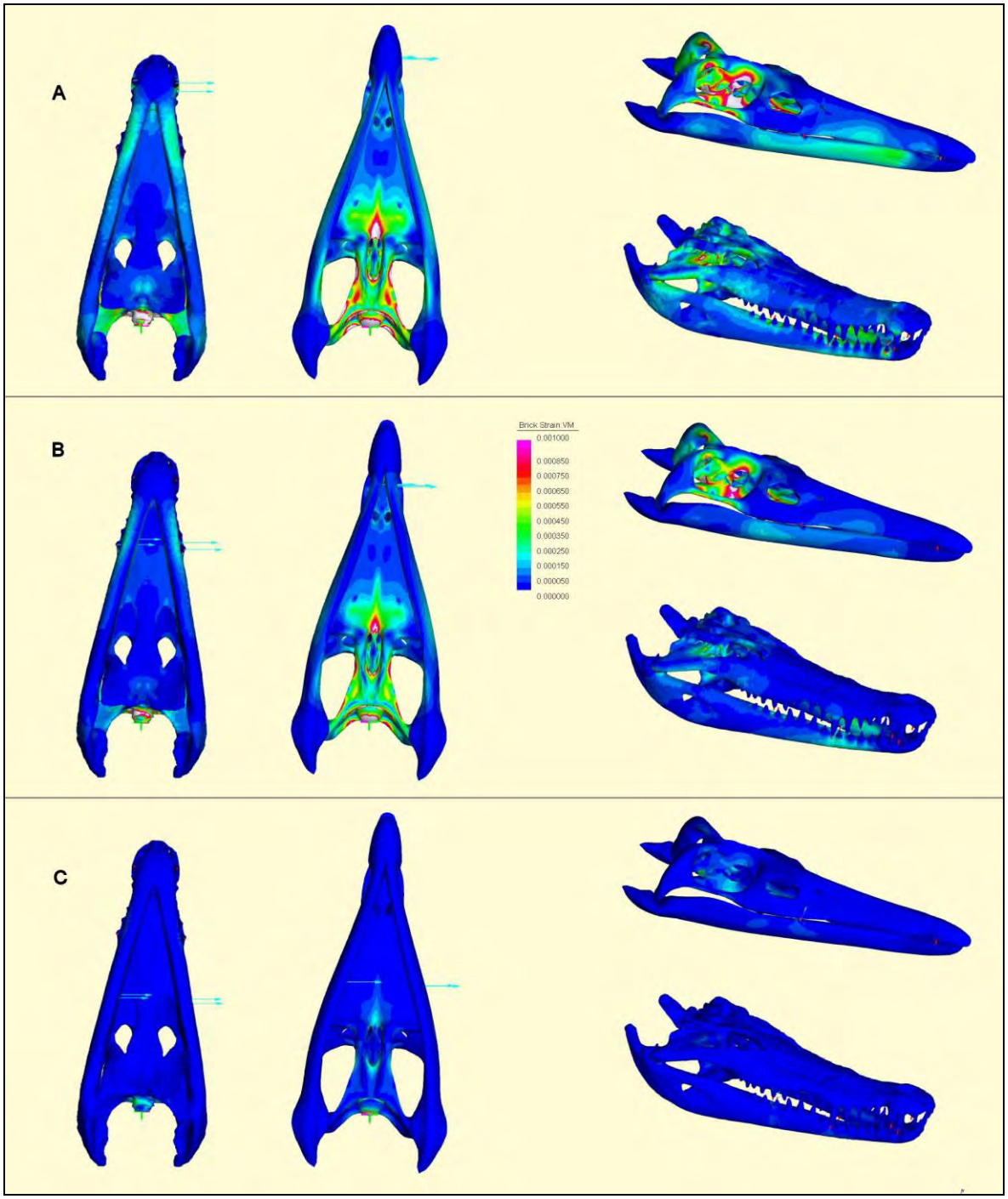

Figure 7-27: Von Mises brick strain results for the homogeneous *Crocodylus porosus* (C.p-2) and the rescaled *Kronosaurus queenslandicus* (K.q-r) models under shake loads, for front (A), mid (B), and rear (C) bite positions. In each of A, B, and C, the C.p-2 model is shown in ventral (far left) and oblique lateral (lower right), and the K.q-r model in ventral (left) and oblique lateral (upper right) views. Displacement of the models is exaggerated, and the forces applied to the respective bite positions are shown as thin blue arrows. The skulls are shown approximately to scale. For explanation of colours and legend, see Figure 7-19.

models, the levels of overall strain were highest for front bites and lowest for rear bites: strains were also higher in the *Kronosaurus* model than in the *Crocodylus* model.

In the shake load cases, the decrease in overall strain with more posterior bite positions is probably a result of the lower force applied (Table 7-13) following decreased moment. For the twist load cases, the basic tapered shape of the rostrum in each skull gives a larger second moment of inertia for the more rearward bite positions, which may allow the skull to handle the load with lower levels of strain.

Discussion

The results highlight several technical issues relating to the methodology used to model skull biomechanics. Consistent with previous studies using these methods (McHenry et al. 2007, Wroe 2007)[9], the estimate of bite force using the 3D finite element models was higher than the corresponding estimate using the 2D dry-skull approach: given that the estimates of muscle force and outlever distance are consistent between the 2D and 3D methods, this is likely to be a result of the geometry used to model the jaw muscles in the FE models increasing the lengths of the effective inlevers for the jaw muscles, as noted in Section 7.2 above.

The increase in estimated bite force was more marked for the *Kronosaurus* model, where the 3D estimate (partially fixed) was ~125% of the 2D figure, than in the *Crocodylus* model where the 3D estimate was ~110% of the 2D (Table 7-14). The technique used to model the muscles, where each beam element runs straight between its origin and insertion points, does not reflect the actual way that jaw muscles wrap around other skeletal components of the skull. This situation likely underestimated the effective inlever of the pterygoid muscle group: the direct line between the attachment points passes very close to the jaw hinge axis, whereas in reality the muscle is displaced much further away from this axis as it wraps around the underside of the mandible. Use of code, such BoneLoad (Grosse et al. 2007), that allows these types of interactions to be modelled may increase the effective inlever of the pterygoid group, and this lead to increased values of 3D bite force estimates. Since the pterygoid group is a more important component of the jaw musculature in

[9] The 3D estimate of bite force for a lion FE model was 145% of the 2D estimate (McHenry et al., 2007). Note that in that study, the 3D estimate for *Smilodon fatalis* is lower than the corresponding 2D estimate: this result is linked to the reduced coronoid process in that species.

the crocodilian than in the pliosaur (Table 7-12), this may lead to greater similarity in the ratios of 3D: 2D bite force estimates for these two groups.

The ratio of 3D to 2D bite force estimates varied with bite position, the type of restraint, and the rescaling of the *Kronosaurus* model (Table 7-15). There was no significant difference between the results of the homogeneous and heterogeneous versions of the *Crocodylus* model (Table 7-14, Table 7-15). The variation with bite position is most likely a consequence of the changing bite force vector at different bite positions (Cleuren et al. 1995), which is picked up in the 3D but not the 2D approach. The interaction between the bite force vector and the type of restraint may explain the inconsistency of the results between different models: for example, the full sized *Kronosaurus queenslandicus* model had the lowest ratio of 3D: 2D bite force for front bites when the restraints were partially fixed, but in rear bites when the restraints were fully fixed. The pattern of variation was different again with the rescaled version of the *Kronosaurus* model: the ratio of 3D: 2D estimates for rear bites were the highest with partially-fixed restraints, but the lowest when fully fixed (Table 7-15). Rounding errors resulted in some small differences in the scaling of muscle forces in the temporal and pterygoid groups between the full sized and rescaled models (Table 7-12), which may explain the qualitative difference between the full-sized and rescaled *Kronosaurus* model. These same rounding errors, together with the three dimensional interaction between the restraints and the bite force vectors, may also explain why the bite force results for the rescaled model were not exactly 6.66% of those for the full-sized model (Table 7-16).

This variation in the results emphasises the importance of restraint type in finite element modelling. The degree to which different types of restraint can affect the mechanical response of the skull can be visualised by comparing Figure 7-19D and Figure 7-19F, where the displacements of the skull have been exaggerated in the FE output. There is as yet no way of discerning which approach is more accurate, and this question will require empirical evaluation of a range of modelling techniques. However, despite the quantitative effect of restraint type upon the bite force results, the qualitative differences in von Mises strain fields between the fully- and partially-fixed *Kronosaurus* models were less marked (Figure 7-19). Whilst strain magnitude

varied between these, areas of high strain in the partially fixed model were areas of high strain in the fully-fixed model as well and the visual output is, overall, quite similar.

Likewise, the visual plots of von Mises strain are similar between the homogeneous and heterogeneous versions of the *Crocodylus* model (Figure 7-20): on the basis of these plots, strain appears to have been slightly higher in the homogeneous model but the differences are minor. This suggests that the use of homogeneous models in comparative analysis may still allow biologically relevant patterns to be identified; McHenry et al. (2007) have noted that, as long as mineralisation is consistent between specimens, results from homogeneous models are consistent with those from heterogeneous models. Whether the pattern of mineralisation in *Kronosaurus* is similar to that in *Crocodylus* is as yet an unexamined question.

The comparison between a model based upon an actual, intact specimen, and a reconstructed model, provides an opportunity to evaluate the accuracy of the reconstruction. In the case of the *Kronosaurus* model, regions that were subjected to high strain included the mandibular rami, the dorsal median ridge, the posterior palate (in front of the inter-pterygoid vacuity), the zygoma, the suspensoria, and the anterior part of the sagittal crest. Of these, the mandible, the zygoma, and the sagittal crest were noted as being based upon imperfect and ambiguous data (Chapter 4); in particular, there is plenty of scope for increasing the depth of the mandibular rami whilst remaining consistent with the data preserved in the various relevant specimens, and the depth of the rami in the present reconstruction was explicitly acknowledged as being conservative. The suspensoria was modelled without detailed 3D data, and this complex part of the skull was difficult to model in 3D using only two dimensional data. The preservation of QM F52279 suggests that the current reconstruction of the anterior parts of the pterygoids underestimates their thickness. In contrast, the dorsal median ridge is preserved in several specimens and there is little that is obviously wrong with the geometry of the model.

The opportunity to refine the *Kronosaurus* model in the light of the results from finite element modelling can lead to circular reasoning, if the model is simply altered until

all the strain hotspots are eliminated – although this approach can be useful for different types of studies, especially those concerned with optimisation. It is important to keep in mind that many of the regions showing high strain in the *Kronosaurus* model were also under high strain in the *Crocodylus* model (compare Figure 7-22 and Figure 7-23). However, if the results from this analysis are viewed as a step in identifying parts of the skull where the actually anatomy may need to be double-checked, then refinement of the model need not be circular. An example of this is the alignment of the joint reaction force vectors with the suspensoria – in the *Crocodylus* model these align closely with the suspensoria, but in the *Kronosaurus* model the vectors do not match the geometry as well (Figure 7-21). For the *Kronosaurus* model, the alignment would be better if the quadrates were positioned more posteriorly compared with the occiput, and the squamosal arch then sloped more gradually posterio-ventrally to the quadrate. Because of the problems associated with constructing a 3D model from photo-mosaics (see Chapter 4), it is entirely possible that the present model has the quadrates placed too far forward, and this detail can potentially be re-examined using 3D data acquisition techniques.

Several previous studies (Busbey 1995, Metzger et al. 2005, Thomason 1991) have considered the degree to which the mechanics of the skull can be modelled using beam theory. The pattern of principle strain in the skulls of both the *Crocodylus* and *Kronosaurus* models during intrinsic loads suggests that, to some extent, the skull does behave as beams under bending loads. During biting (i.e. intrinsic loads), beam theory suggests that the rostrum and mandible should undergo compression on their dorsal and ventral surfaces respectively, with the upper edge of the mandible and the lower (palatal) surface of the rostrum undergoing tension. The xx axes of the plates tessellated to the skull surface were aligned to the skull's longitudinal axis, and the principal strain in the plate xx axis reflects the predictions based upon beam theory in the rostrum and mandible for both models (Figure 7-24). In particular, the dorsal median ridge of the *Kronosaurus* model shows high von Mises strain, and much of this strain appears to be negative (i.e. compressive) principal strain in the longitudinal axis. This result underlies the potential importance of the complex osteology of this region described in Chapter 4: it is also of interest because traditional interpretations of the functional morphology of sutures state that, in regions dominated by

compressive forces, the sutures should be simple 'butt' joints (Hildebrand 1974), and yet the sutures between the posterior dorsal median ridge and the fronto-parietal region are highly interdigitated. More recent empirical studies have suggested that, in contrast with the traditional interpretations of sutural functional morphology, the micro-histology and location of interdigitated sutures makes them best suited for resisting tension, and that the flatter butt joints may be better suited for resisting tensional loads (Herring et al. 2005, Herring et al. 2001, Herring and Teng 2000, Rafferty and Herring 1999, Rafferty et al. 2000, Rafferty et al. 2003, Sun et al. 2004). In this context, the results of the present study are of interest.

Although bite position, as expected, has a strong effect on the strain fields in the rostrum and anterior mandible in both models, the pattern of strain in the posterior part of the skull are consistent between front, mid, and rear bites (Figure 7-22, Figure 7-23). Strain in the rear part of the skull is expected to be dominated by the jaw muscle tension acting directly on the attachment surfaces of the bone (Herring and Teng 2000), and the results from both models appear to agree with this expectation.

For mid and rear bites, the mandible is under strain in front of the bite points (Figure 7-22, Figure 7-23). This is most likely a result of medial displacement of the mandibular rami by the medial component of the jaw muscle force vectors, and points to the importance of the pterygoid flanges/ lateral buttress in resisting that medial component. For rear bites, the strain in the anterior mandible is higher in the *Kronosaurus* model than in the *Crocodylus*, despite the more medially inclined joint forces evident in the latter (Figure 7-21).

For intrinsic loads, overall strain in the *Kronosaurus* model was higher than in the *Crocodylus* model for all bite positions (Figure 7-22, Figure 7-23). Whilst this may be partly due to errors in the geometry of the *Kronosaurus* model (see above) that have underestimated the strength of its skull, this result is also consistent with the basic proportions of the skull, especially the anterior half; in the *Kronosaurus* model, the rostrum is relatively longer and, in its anterior part, narrower than in the *Crocodylus porosus* model. It appears that, for its size, the skull of *Kronosaurus* is not as strong under biting loads as the skull of *Crocodylus porosus*.

In contrast to the structural mechanics, bite force in *Kronosaurus* is predicted to be greater than in the *Crocodylus porosus* model under both 2D and 3D methods, and even if this result is exaggerated by the likely underestimation of force and effective inlever in the crocodile's pterygoid muscles, the bite force in *Kronosaurus* is nevertheless high in absolute terms. From a biological perspective, why a structure that has a lower mechanical strength than a *Crocodylus porosus* should be capable of generating similar or even greater levels of bite force is an interesting question. Given the present uncertainties in modelling bite forces in both mammals and reptiles, this issue needs to be explored further but a potential solution may lie with the hydrodynamic, as opposed the structural, issues involved with rapidly closing jaws in the aquatic medium. During jaw adduction the rostrum and mandible are subject to drag; this drag scales quadratically with jaw size (McHenry et al. 2006), and thus a skull that is absolutely much larger than the *Crocodylus porosus* specimen may require considerably more muscle force in order to close it at comparable speeds. Note that the rostrum in *Kronosaurus* is, relative to skull size, relatively long, a morphology that is associated with the capture of small, agile aquatic prey such as fish in extant crocodilians (McHenry et al. 2006), and the apparent lack of strength of the *Kronosaurus* skull relative to the *C. porosus* model may be associated with the demands of capturing small prey, rather than subduing large ones. Consistent with this interpretation, the large maxillary fangs (M1-M3) of *Kronosaurus* are much further forward in the tooth row than the functionally equivalent teeth (M5) in the *Crocodylus porosus* jaw; whilst this has the effect in the FEA of exaggerating the difference in mechanical performance between the pliosaur and the crocodile (compare Figure 7-22B with Figure 7-23B), it may also point to an emphasis on relatively smaller prey in *Kronosaurus* than in *C. porosus*.

The results from the extrinsic loads are also consistent with this interpretation. Under twist loads, the *Kronosaurus* model is subject to much higher strain for the front and mid bite positions than is the *Crocodylus porosus* model (Figure 7-26). The strain in the *Kronosaurus* model is concentrated in the anterior rostrum and the midline of the palate, both regions that are preserved in different specimens and for which the model's geometry is unlikely to be inaccurate. For twisting loads at the rear

bite position, strains are more comparable between the two models: relative to the crocodile, the rostrum is narrower at the front but wider at the rear and the results of the FEA are consistent with these basic snout proportions, as wider rostra have a larger second moment of inertia and are therefore, all else being equal, better able to resist torsional loads. Strain in the rear part of the skull is also higher in the *Kronosaurus* model for all bite positions, although no higher than under the intrinsic loads.

Under shake loads, the *Kronosaurus* skull is likewise subject to greater strain than is the *Crocodylus* model, particularly in the palate but also in the rear part of the skull around the braincase. This difference is most evident for the front and mid bite positions, although the relatively forward position of the maxillary fangs in *Kronosaurus* exaggerates the difference for the mid bites as noted above. Strains are low in both models for the shake at the rear bite position, but the forces involved are so low (Table 7-13) that the biological relevance of this load case is perhaps questionable. Interestingly, the shape of the strain hotspot in the palate of the *Kronosaurus* model, at the font of the interpterygoid vacuity, is a similar arrowhead shape to the anterior end of the parasphenoid at this exact point.

As has been noted previously (Chapter 2), the overall proportions of the skull in *Kronosaurus queenslandicus* appear to be more similar to those of the Orinoco crocodile, *Crocodylus intermedius*, than to the more robust mesorostral species such as *C. niloticus*, *C. palustris*, and *C. porosus*. However, major areas of uncertainty with the comparative approach used here concerns (1) the functional aspects of feeding behaviour in extant crocodilians such as *Crocodylus porosus* and *C. intermedius*, and (2) quantitative data on differences in feeding ecology between these species. On the first point, data on how large *Crocodylus* actually use twisting or shaking behaviours during feeding are lacking: What are the range and speed of the movements involved? Where are the prey held in the jaw during twisting or shaking? How do these change with different types and sizes of prey?

For the second point, data exists on the prey type and sizes taken by robust mesorostral forms such as *C. niloticus* over its life cycle (Cott 1961); however, little

quantitative data exists for *C. intermedius*. The Orinoco crocodile is geographically restricted to a small number of river systems in Colombia and Venezula, and following several decades of intense hunting is listed as critically endangered (IUCN 2008). Current scientific efforts are primarily concerned with conservation biology, rather than fundamental ecology. The similarity between snout proportions of large pliosaurs and *C. intermedius* is not restricted to *Kronosaurus*; it applies equally to all of the largest pliosaur taxa, including *Liopleurodon*, *Pliosaurus*, and *Brachauchenius*. Potential importance as a palaeoecological model may be esoteric, but can be added to the list of valuable features of this species, and underlines the cost of loosing biodiversity; at stake is not just our legacy for the future, but our ability to understand the past.

Conclusions

Many uncertainties remain, but on the basis of the present analysis, it appears that the skull of *Kronosaurus queenslandicus*, for its size, is not as strong as the skull of *Crocodylus porosus* under biting, twisting, or shaking loads. In as much as each of these may be functionally correlated with maximum prey size, through the mechanical demands of securing, disabling, killing, or processing large prey, it therefore seems that maximum prey size in *Crocodylus porosus*, relative to its own body size, exceeds that of *Kronosaurus queenslandicus*.

In contrast with this result, bite force in *Kronosaurus queenslandicus* was found to be higher than in *Crocodylus porosus* under 2D and 3D methods. Whilst much work remains to be done on understanding of bite force in crocodiles, taken at face value this result contradicts the patterns of structural results. This conflict may be linked with the hydrodynamics of jaw adduction in very large predators in the aquatic medium, rather than simply with the mechanics of maximum prey size as appears to be the case with terrestrial predators.

This study is the first investigation of comparative skull mechanics using 3D modelling in aquatic reptilian carnivores. Further research is needed, both on improving understanding of skull anatomy in the extinct forms, and developing a thorough understanding of the context of skull biomechanics and ecology in the living. In the absence of detailed field data on the feeding ecology of key comparative

species such as *Crocodylus intermedius*, a fruitful step may be to expand the comparative biomechanical analysis to include a broader range of living crocodilians, and even odontocetes, and use these to provide a context for an increased number of pliosaur. Integration of comparative studies of the structural mechanics with fluid dynamics of the skull in these taxa is predicted to provide insight into the upper and lower limits of prey size in pliosaurs such as *Kronosaurus queenslandicus*.

7.4 References

Binder, W. J., and B. Van Valkenburgh. 2000. Development of Bite Strength and Feeding Behaviour in Juvenile Spotted Hyenas (*Crocuta crocuta*). Journal of Zoology 252:273-283.

Blob, R. W. 2000. Interspecific scaling of the hindlimb skeleton in lizards, crocodilians, felids, and canids: does limb bone shape correlate with limb posture. Journal of Zoology, London 250:507-531.

Bourke, J., S. Wroe, K. Moreno, C. R. McHenry, and P. D. Clausen. 2008. Effects of Gape and Tooth Position on Bite Force in the Dingo (*Canis lupus dingo*) using a 3-D Finite Element Approach. PLoS ONE 3(5e2200):1-5.

Busbey, A. B. 1995. The structural consequences of skull flattening in crocodilians. Pp. 173-192. *In* J. Thomason, ed. Functional morphology in vertebrate paleontology. Cambridge University Press, Cambridge.

Christiansen, P. 2007a. Comparative bite forces and canine bending strength in feline and sabretooth felids: implications for predatory ecology. Zool. J. Linn. Soc. 151:423-437.

Christiansen, P. 2007b. Evolutionary implications of bite mechanics and feeding ecology in bears J. Zoology 272:423-443.

Christiansen, P., and S. Adolfssen. 2005. Bite forces, canine strength and skull allometry in carnivores (Mammalia, Carnivora). Journal of Zoology, London 266:133-151.

Christiansen, P., and S. Wroe. 2007. Bite forces and evolutionary adaptations to feeding ecology in carnivores. Ecology 88:347-358.

Clausen, P., S. Wroe, C. McHenry, K. Moreno, and J. Bourke. 2008. The vector of jaw muscle force as determined by computer generated three dimensional simulation: A test of Greaves' model. Journal of Biomechanics 41(15):3184-3188.

Cleuren, J., P. Aerts, and F. De Vree. 1995. Kinematics of the jaw and hyolingual apparatus during feeding in *Caiman crocodilus*. Belgian Journal of Zoology 125(79-94).

Conybeare, W. D. 1822. Additional notes on the fossil genera *Ichthyosaurus* and *Plesiosaurus*. Transactions of the Geological Society of London 2:103-123.

Corkeron, P. J., and R. C. Connor. 1999. Why do Baleen Whales Migrate? Marine Mammal Science 15(4):1228-1245.

Cott, H. B. 1961. Scientific results of an inquiry into the ecology and economic status of the Nile crocodile (*Crocodylus niloticus*) in Uganda and Northern Rhodesia. Transactions of the Zoological Society of London 29:211-357.

Ellis, J. E., J. J. Thomason, E. Kebreab, and J. France. 2008. Calibration of estimated biting forces in domestic canids: comparison of post-mortem and *in vivo* measurements. Journal of Anatomy 212:769-780.

Erickson, G. M., A. K. Lappin, and K. A. Vliet. 2003. The ontogeny of bite-force performance in American alligator (*Alligator mississippiensis*). Zool Lond 260:317–327 260:317-327.

Erickson, G. M., P. J. Makovicky, P. J. Currie, M. A. Norell, S. A. Yerby, and C. A. Brochu. 2004. Gigantism and comparative life-history parameters of tyrannosaurid dinosaurs. Nature 430:772-775.

Erickson, G. M., S. D. Van Kirk, J. Su, M. E. Levenston, W. E. Caler, and D. R. Carter. 1996. Bite force estimation for *Tyrannosaurus rex* from tooth-marked bones. Nature 382:706-708.

Farlow, J. O., G. R. Hurlburt, R. M. Elsey, A. R. C. Britton, and W. Langston. 2005. Femoral Dimensions and Body Size of *Alligator mississippiensis*: Estimating the Size of Extinct Mesoeucrocodylians. Journal of Vertebrate Paleontology 25(2):354-369.

Grosse, I., E. R. Dumont, C. Coletta, and A. Tolleson. 2007. Techniques for modeling muscle-induced forces in finite element models of skeletal structures. Anatomical Record 290(9):1069-88.

Hayward, M. W., and G. I. H. Kerley. 2005. Prey preferences of the lion (*Panthera leo*). J. Zool. lond. 267:309-322.

Herring, S. W., S. C. Pedersen, and X. Huang. 2005. Ontogeny of bone strain: the zygomatic arch. Journal of Experimental Biology 208(23):4509-4521.

Herring, S. W., K. L. Rafferty, Z. J. Liu, and C. D. Marshall. 2001. Jaw muscles and the skull in mammals: the biomechanics of mastication. Comparative Biochemistry and Physiology - Part A: Molecular & Integrative Physiology 131(1):207-219.

Herring, S. W., and S. Teng. 2000. Strain in the braincase and its sutures during function. American Journal of Physical Anthropology 112:575-593.

Hildebrand, M. 1974. Analysis of vertebrate structure. John Wiley & Sons, New York.

Holliday, C. M., and L. Witmer. 2007. Archosaur Adductor Chamber Evolution: Integration of Musculoskeletal and Topological Criteria in Jaw Muscle Homology. Journal of Morphology 288(457-484).

Hurlburt, G. R., A. B. Heckert, and J. O. Farlow. 2003. Body mass estimates of Phytosaurs (Archosauria: Parasuchidae) from the Petrified Forest Formation (Chinle Group: Revueltian) Based on Skull and Limb Bone Measurements. *In* Z. E. Ziegler, A. B. Heckert, and S. G. Lucas, eds. Paleontology and Geology of the Upper Triassic (Revueltian) Snyder Quarry, New Mexico. New Mexico Museum of Natural History and Science Bulletin 24, Albuquerque.

Ingle, J. 2007. Scaling of bite force in crocodilians using finite element analysis. University of Newcastle, Unpublished Hons. Thesis.

Iordansky, N. N. 1964. The jaw muscles of the crocodiles and some relating structures. Anat. Anz. 115:256-280.

IUCN. 2008. IUCN Red List. www.iucnredlist.org.

Jefferson, T., P. J. Stacey, and R. W. Baird. 1991. A review of Killer Whale interactions with other marine mammals: predation to co-existence. Mammal Review 21(4):151-180.

Joubert, D., and B. Joubert. 1997. Hunting With the Moon: the Lions of Savuti. National Geographic.

Keller, T. S., Z. Mao, and D. M. Spengler. 1990. Young's modulus, bending strength, and tissue physical properties of human compact bone. Journal of Orthopaedic Research 8:592-603.

Lauder, G. V. 1995. On the inference of function from structure. Pp. 1-18. *In* J. J. Thomason, ed. Functional Morphology in Vertebrate Paleontology. Cambridge University Press.

Massare, J. A. 1987. Tooth morphology and prey preference of Mesozoic marine reptiles. Journal of Vertebrate Paleontology 7:121-137.

McBrayer, L. D., and T. D. White. 2002. Bite Force, Behaviour, and Electromyogrpahy in the Teiid Lizard *Tupinambis teguixin*. Copeia 2002(1):111-119.

McHenry, C. R., P. D. Clausen, W. J. T. Daniel, M. B. Meers, and A. Pendharkar. 2006. The biomechanics of the rostrum in crocodilians: a comparative analysis using finite element modelling. Anatomical Record 288A:827-849.

McHenry, C. R., S. Wroe, P. D. Clausen, K. Moreno, and E. Cunningham. 2007. Supermodeled sabercat, predatory behavior in *Smilodon fatalis* revealed by high-resolution 3D computer simulation. Proceedings of the National Academy of Sciences 104(41):16010-16015.

McLellan, F. 2007. Density, CT attenuation, and strength in bovine bone samples. University of Newcastle, Unpublished Hons. Thesis.

Meers, M. B. 2003. Maximum Bite Force and Prey Size of *Tyrannosaurus rex* and Their Relationships to the Inference of Feeding Behavior. Historical Biology 16(1):1-12.

Metzger, K. A., W. J. T. Daniel, and C. F. Ross. 2005. Comparison of beam theory and finite element analysis with *in vivo* bone strain data from the alligator cranium. Anatomical Record 283A:331-348.

Moreno, K., S. Wroe, P. D. Clausen, C. R. McHenry, D. C. D'Amore, E. J. Rayfield, and E. Cunningham. 2008. Cranial performance in the Komodo dragon (*Varanus komodoensis*) as revealed by high-resolution 3-D finite element analysis. Journal of Anatomy 212:736-746.

Plotnick, R. E., and T. K. Baumiller. 2000. Invention by Evolution: Functional Analysis in Paleobiology. Paleobiology 26(4):305-323.

Preuschoft, H., and U. Witzel. 2005. Functional Shape of the Skull in Vertebrates: Which Forces Determine Skull Morphology in Lower Primates and Ancestral Synapsids? Anatomical Record 283A:402-413.

Rafferty, K. L., and S. W. Herring. 1999. Craniofacial sutures: Morphology, growth, and *in vivo* masticatory strains. Journal of Morphology 242(2):167-179.

Rafferty, K. L., S. W. Herring, and F. Artese. 2000. Three-dimensional loading and growth of the zygomatic arch. J Exp Biol 203(14):2093-2104.

Rafferty, K. L., S. W. Herring, and C. D. Marshall. 2003. Biomechanics of the rostrum and the role of facial sutures. Journal of Morphology 257(1):33-44.

Rayfield, E. J. 2005. Aspects of comparative cranial mechanics in the theropod dinosaurs *Coelophysis*, *Allosaurus* and *Tyrannosaurus*. Zoological Journal of the Linnean Society 144:309-316.

Rho, J. Y., M. C. Hobatho, and R. B. Ashman. 1995. Relations of mechanical properties to density and CT numbers in human bone. Medical Engineering and Physiology 17:347-355.

Ross, C. A., and S. Garnett, eds. 1989. Crocodiles and alligators. Facts on File, New York.

Schumacher, G. H. 1985. Comparative functional anatomy of jaw muscles in reptiles and mammals. Pp. 203–212. *In* Duncher, and Fleischer, eds. Proceedings of the First International Symposium on Vertebrate Morphology, Giessen, 1983. Gustav Fisher Verlag, Stuttgart.

Similä, T., J. C. Holst, and I. Christiensen. 1996. Occurence and diet of killer whales in northern Norway: seasonal patterns relative to the distribution and abundance of Norwegian spring-spawning herring. Canadian Journal of Fisheries and Aquatic Sciences 53(4):768-779.

Sinclair, A. G., and R. M. Alexander. 1987. Estimates of forces exerted by the jaw muscles of some reptiles. Journal of Zoology 213:107-115.

Sun, Z., E. Lee, and S. W. Herring. 2004. Cranial sutures and bones: Growth and fusion in relation to masticatory strain. The Anatomical Record Part A: Discoveries in Molecular, Cellular, and Evolutionary Biology 276A(2):150-161.

Taylor, M. A. 1987. How tetrapods feed in the water: a functional analysis by paradigm. Zoological Journal of the Linnean Society 91:171-195.

Taylor, M. A. 1992. Functional anatomy of the head of the large aquatic predator *Rhomaleosaurus zetlandicus* (Plesiosauria, Reptilia) from the Toarcian (Early Jurassic) of Yorkshire, England. Philosophical Transactions of the Royal Society, London B 335:247-280.

Taylor, M. A. D., and A. R. I. Cruickshank. 1993. Cranial anatomy and functional morphology of *Pliosaurus brachyspondylus* (Reptilia: Plesiosauria) from the Late Jurassic of Westbury, Wiltshire. Philosophical Transactions of the Royal Society London. B 341:399-418.

Thomason, J. J. 1991. Cranial strength in relation to estimated biting forces in some mammals. Canadian Journal of Zoology 69:2326-2333.

Thomason, J. J., A. P. Russell, and M. Morgelli. 1990. Forces of biting, body size, and masticatory muscle tension in the opossum *Didelphis virginiana*. Canadian Journal of Zoology 68:318-324.

Tucker, A. D., C. J. Limpus, H. I. McCallum, and K. R. McDonald. 1996. Ontogenetic Dietary Partitioning by *Crocodylus johnstoni* during the Dry Season. Copeia 1996(4):978-988.

Turnbull, W. D. 1970. Mammalian masticatory apparatus. Fieldiana: Geology 18:149-356.

Webb, G. J. W., and H. Messel. 1978. Morphometric Analysis of *Crocodylus porosus* from the North Coast of Arnhem Land, Northern Australia. Australian Journal of Zoology 26:1-27.

Wroe, S. 2007. High-resolution 3-D computer simulation of feeding behaviour in marsupial and placental lions. Journal of Zoology 274:332-339.

Wroe, S., P. Clausen, C. McHenry, K. Moreno, and E. Cunningham. 2007a. Computer simulation of feeding behaviour in the thylacine and dingo: a novel test for convergence and niche overlap. Proceedings of the Royal Society Series B 274:2819-2828.

Wroe, S., D. R. Huber, M. Lowry, C. McHenry, K. Moreno, P. Clausen, T. L. Ferrara, E. Cunningham, M. N. Dean, and A. P. Summers. 2008. Three-dimensional computer analysis of white shark jaw mechanics: How hard can a great white bite? J. Zoology 276(4):336-342.

Wroe, S., C. McHenry, and J. Thomason. 2005. Bite club: comparative bite force in big biting mammals and the prediction of predatory behaviour in fossil taxa. Proceedings of the Royal Society of London, Series B 272:619-625.

Wroe, S., K. Moreno, P. Clausen, C. McHenry, and D. Curnoe. 2007b. High-resolution computer simulation of hominid cranial mechanics. The Anatomical Record 290A:1248-1255.

8. Palaeoecology

Kronosaurus and Leptocleidus, by John Conway.

"The biomechanics of extinct organisms is thus one of the only areas within palaeontology amenable to direct experimental investigation (taphonomy is another)".
Plotnick & Baumiller (2000: p. 312)

"…bugger all published research exists on form and function in living animals".
Darren Naish, Tetrapod Zoology (2008)

8.1 The palaeoecology of *Kronosaurus queenslandicus* – evidence from functional morphology

The science of ecology – the attempt to describe and explain the myriad interactions between organisms and their environment – is a highly complex discipline, and a reconstruction of all of the different aspects of the palaeoecology of *Kronosaurus queenslandicus* is beyond the scope of the present work. Instead, the focus here is upon the feeding ecology of this species. Some of the other relevant palaeoecology aspects are briefly considered at the end of this chapter.

The preceding chapters of this thesis have attempted to provide a summary description of skull anatomy, body shape, and body size for *Kronosaurus queenslandicus*. Most of this information can be used to infer diet in *Kronosaurus*, especially using functional morphology based approaches. Although 'functional morphology' is a generic label applied to a variety of distinct methods, three particular methodologies are commonly used in palaeontology; morphometrics, biomechanics, and comparison with modern biological or artificial analogues. Morphometric approaches are not employed in the present analysis, although these would likely provide useful data. The following account focuses upon the two other forms of the functional morphology approach.

Biomechanics

To date, biomechanical analysis of *Kronosaurus queenslandicus* is restricted to the work presented in this thesis, i.e. (1) a 2-D estimate of bite force using a 'dry-skull' approach adapted from (Thomason 1991), in comparison with several other species of predatory reptiles, and (2) a finite element analysis, using high resolution

homogeneous models in linear static analysis, of the skull in comparison with that of a small adult saltwater crocodile *Crocodylus porosus*.

Bite force

Although large in absolute terms, bite force in *Kronosaurus* is similar, for its body size, to that of other predatory reptiles. Dry skull estimates suggest that bite force scales isometrically with skull volume within a sample of taxa that includes four specimens of crocodilian, one specimen of Komodo dragon, and a *Tyrannosaurus rex* in addition to the *Kronosaurus*, and that these reptiles have a consistent bite force per unit of skull volume. With the exception of the Komodo dragon, a similar pattern holds for the scaling of bite force with body mass. However, this method probably underestimates actual bite force, particularly for crocodilians because it may not account for the hypertrophied pterygoidus muscle in these. Comparison of predicted and measured bite force for *Alligator* (Erickson et al. 2003) indicates that the dry skull method underestimates actual bite force by approximately a factor of two.

The ecology of bite force in reptilian carnivores is largely unknown. A body mass adjusted bite force quotient (BFQ) does predict relative prey size in conical-toothed carnivorous mammals (Wroe et al. 2005): although data is limited, relatively low bite force in sabre-toothed carnivores that probably hunted relative large prey (McHenry et al. 2007) suggests that ecological inference based upon bite force holds only within ecomorphs. For reptiles, crocodilians perhaps represent the most obvious comparative group of conical toothed predators, and these are also similar to mammals in lacking cranial kinesis, but there is scant data with which to test hypotheses of bite force and feeding behaviour in this group. A complicating factor is the aquatic habitat of crocodiles: whether BFQ correlates with relative prey size in an aquatic predator is unknown but potentially information from odontocetes and pinnipeds could be used to establish broad patterns.

In the absence of comparative data, the ecological significance of the predicted bite force for *Kronosaurus* is unknown. However, the predicted force is substantially larger than that measured or modelled for any living species: the predicted bite force at the largest teeth in *Kronosaurus* is 16–23 kN (using 2D and 3D methods respectively). For fossil carnivores, this figure is exceeded only by some estimates of bite force in *Tyrannosaurus rex* (Meers 2003, Rayfield 2004) (applying the same methods used for

	BoM	Estimated BF (2D dry skull)	Predicted BF (logBF = 0.65*log BoM +1.76)	BFQ
Tyrannosaurus rex	5,654	19,169	15,814	121
Kronosaurus queenslandicus	5,781	16,401	16,044	102
Carcharodon carcharias	240	934	2,028	46
Carcharocles megalodon	47,690	29,120	63,238	46

Table 8-1: Hypothetical scaling of Bite Force (BF) and BFQ in some extinct large carnivores. Bite Force Quotient (BFQ) is based upon assumption that Bite Force scales to Body Mass (BoM) as with the data for extant reptiles generated in Chapter 7, i.e. for log-log data with a slope of 0.65 and an intercept of 1.76. 2D bite force estimate for *Carcharodon* taken from single muscle vector, anterior bite, 0° result from 3D modelling in this species (Wroe et al. 2008): estimated bite force for *C. megalodon* is scaled by mass from this amount with an exponent of 0.65. Bite force estimates for the reptiles are for 'mid' bites (Chapter 7). Forces in Newtons, masses in kg.

Kronosaurus gives an estimate of 19 kN) and for the giant lamniform shark *Carcharocles megalodon* (Wroe et al. 2008), both of which are apex carnivores believed to have been capable of taking the largest available prey. In terms of raw bite force, *Kronosaurus* therefore appears to be at least in a similar class to these, as illustrated by comparing 2D estimates of bite force in these taxa against a hypothetical scaling relationship of bite force to body mass. If, for log-log data, a slope of 0.75 and an intercept of 1.76 is used (i.e. as for the scaling of 'mid' bites in the reptile specimens analysed in Chapter 7), then *Kronosaurus* has a BFQ of 102 (i.e. 'average' for its size) whilst *Tyrannosaurus* has a BFQ of 121 (Table 8-1). With mammalian conical toothed carnivores (Wroe et al. 2005), a BFQ above 100 is a reliable indicator of the ability to feed upon prey that is larger than the predator. As with sabre-toothed mammals, the lower BFQ for *Carcharodon* and *Carcharocles* is most likely correlated with tooth shape and thus may not be a reliable guide to maximum relative prey size (Wroe et al. 2005, McHenry et al. 2007). Note, however, that these figures are illustrative and the BFQ obtained depends upon the slope and intercept of the regression for body mass and bite force; more data on the scaling on these in non-mammalian carnivores is required before BFQ can be applied rigorously to reptilian carnivores.

Skull structural mechanics

FEA of the skull in *Kronosaurus* compared with a 3.1 m TL *Crocodylus porosus*, suggests that *Kronosaurus* experienced higher strain during normal bites, particularly with front and mid bites. Note that these analyses use estimates of jaw muscle force from the

dry skull method (see above), and given the larger pterygoidus of crocodilians this might underestimate bite force in the *C. porosus* model compared to the *Kronosaurus* model. However, the result of higher strain during biting in *Kronosaurus* is also consistent with the overall proportions of the skull in *Kronosaurus*, which has a more elongate rostrum and is thus likely to be subject to higher bending stresses.

Muscle force estimates do not apply to analysis of strain under extrinsic twisting and shaking loads, and for both of these the skull of *Kronosaurus* exhibited higher strains than that of *C. porosus*. As these loads simulate behaviours that are used by crocodiles to subdue, kill, and process large prey, this result suggests that *Kronosaurus* was not as well suited to taking large as is a 3.1 m *Crocodylus porosus*.

As with bite force, attempts at extrapolating these results to interpret ecology are thwarted by lack of data. A key question is the maximum prey size of a 3.1 m *Crocodylus porosus*. Although species data for diet in *C. porosus* includes the largest available mammals such as pigs, cattle, and feral water buffalo *Bubalus*, which can exceed 500kg, these records include predation by large adult crocodiles, which can exceed 5.5 m TL and 1,000 kg. Whether a 3.1 m 105 kg *C. porosus* could take the largest available prey is unknown but is perhaps unlikely; whether it can take prey that is appreciably larger than itself has, to my knowledge, not been documented. Anecdotal evidence suggests that saltwater crocodiles of this size class include a large proportion of fish in their diet (A. Britton, pers. comm.). The morphologically similar species *Crocodylus niloticus* shares its range with even larger species of potential prey and is known to feed upon Cape Buffalo *Syncerus*, but again whether Nile crocodiles can prey upon healthy adult Buffalo, which have a maximum size of ~900kg, is unknown, and published accounts suggest that smaller or sick animals are targeted (Buchholtz 1990). *Crocodylus niloticus* is known to prey upon a range of other large mammals, such as wildebeast and zebra, and although predation upon these by crocodiles is featured in numerous television documentaries, ascertaining the body size of the predator and prey in each instance is difficult. 'Large' crocodiles tend to be 4 m (250 kg) or more, whilst adult wildebeast reach 250 kg and zebra can exceed 300 kg: it thus seems possible that Nile crocodiles do take prey of their own size or slightly larger.

By comparison, on the basis of skull biomechanics *Kronosaurus* may have had a slightly smaller maximum prey size, perhaps taking prey of up to its own size. Of course, the features of skull shape that appear to decrease its mechanical performance with respect to behaviours invoked for feeding on large prey, i.e. an elongate rostrum with a narrow anterior section, are features that have been postulated in crocodilians as adaptations for maximising foraging efficiency when hunting small, agile, aquatic prey (Busbey 1995, McHenry et al. 2006). Thus the reduced maximum prey size relative to body size for *Kronosaurus*, compared with *C. porosus*, may accompany the ability to target relatively smaller prey more efficiently. Since this aspect of feeding behaviour is likely to be limited by skull hydrodynamics, a fluid dynamics analysis of the two predators would be of interest. However, interpreting the ecological implications of any analysis will probably run into the same problem stated earlier in the case of maximum prey size; i.e. lack of data on minimum prey size for different size classes of *C. porosus*.

Whilst better refined data on prey size in relation to predator for *Crocodylus porosus* and the similar species *C. niloticus* and *C. palustris* would be useful in interpreting the results of the FEA presented above, another potentially useful strategy would be to broaden the FEA (and, potentially, fluid dynamics analysis) to include other species of crocodilians with different skull proportions. A comparison of the mechanical response of *Kronosaurus* with that of a range of crocodiles, from longirostrine species such as *Tomistoma*, *Crocodylus johnstoni*, and *C. cataphractus*, to mesorostrine species such as *C. porosus*, would likely provide insights into the nature of skull mechanics in the pliosaur. In particular, inclusion of the species that has skull proportions most like those of *Kronosaurus*, i.e. the 'intermediate' snouted Orinoco crocodile *C. intermedius*, into a broad FEA would be desirable.

Pending such an analysis, interpreting the results of the FEA in Chapter 7 in the light of the limited ecological data available suggests that *Kronosaurus* was mechanically suited for smaller maximum and minimum prey sizes, relative to its own size, than is the case for a 3.1 m *Crocodylus porosus*.

The results from the FEA do not agree completely with the estimated magnitude of bite force in *Kronosaurus*, which is comparable to that seen in a 3.1 m *C. porosus* (once

body size is accounted for). Bite force is believed to be a reliable indicator of relative prey size in conical toothed predatory mammals, but studies of bite force in reptiles are in their infancy, and much more work is need to explore this issue further. One possibility involves scaling effects; the hydrodynamics of rapid adduction of a very large jaw in water are expected to be non-linear, perhaps requiring proportionally more jaw musculature to effect the capture of small, agile prey.

Other evidence from functional morphology

Plotnick and Baumiller (2000) have contrasted biomechanical approaches to functional morphology with the 'paradigm' method of Rudwick (1964). The paradigm approach involves the interpretation of biological structures by identifying **analogous** structures for which the function is understood: the analogous structures can be biological or man-made. It is often contrasted with phylogenetic approaches, which seek to explain function by identifying **homologous** structures: phylogenetic approaches work well when the primary structure and its homologue are similar, but break down when the structures are highly derived relative to each other – for example, functional explanations of a bird wing that equated it to a primate arm would be of limited explanatory power. That the paradigm method can be applied to non-homologous objects can therefore be a strength. Although it often invokes mechanical objects as analogues, the paradigm method is not a biomechanical approach because it is phenomological and does not use the numerical techniques of mechanics and physics to evaluate hypothesised functions (Plotnick and Baumiller 2000). As such, it represents a specific approach to the problems of functional morphology[1], and in this context should not be confused with concept of scientific methodological philosophy detailed by Kuhn (1962).

Taylor used the paradigm approach to examine many of the aspects involved with feeding by aquatic tetrapods (Taylor 1987), and the reader is referred to that work for

[1] I must confess that I find the use of the word 'paradigm' in the context of functional morphology rather unfortunate and even confusing, being more used to the term in the context used by Kuhn (1962). I am not altogether sure how the 'paradigm method' as coined by Rudwick (1964) differs from the long tradition of explanation by analogy in comparative biology. He simply seems to have wished to formalise a process that anatomists had been using since at least the 1820's – see, for example, Conybeare's original account of *Plesiosaurus dolichodeirus* – but chose a word that has become more widely known in a philosophical context.

a fuller treatment of non-biomechanical aspects of functional morphology in marine reptiles. The following is an attempt to summarise miscellaneous features of *Kronosaurus* skull anatomy that may be relevant to interpretations of its functional morphology, using the 'explanation by analogy' approach which is invoked by the paradigm method.

Dentition

The teeth of *Kronosaurus* are robust, conical, and lack carinae. They are covered around their entire circumference in an ornament of longitudinal ridges which are understood to function as blood-let grooves that facilitate the withdrawal of the tooth from the tissues of soft-bodied prey. They frequently have broken tips with re-worn surfaces, similar to the wear patterns seen on macrophagous conical toothed taxa such as *Orcinus*, the large species of *Crocodylus*, and pantherine felids. The functional morphology of marine reptile teeth has been discussed elsewhere (Massare 1987, Noè 2001) and little needs to be added here; the morphology of the teeth in *Kronosaurus* is consistent with predation upon a wide range of prey including relatively large animals.

In describing the dentition of Middle Jurassic pliosaurs, Noè (2001) noted that the recurved crowns at different positions along the tooth row are aligned so as to allow passage of prey items towards the gullet. The posterior teeth of *Kronosaurus* are similar to those of Jurassic pliosaurids in being more recurved and having relatively shorter roots than the anterior caniniform teeth, but while some specimens may preserve tooth orientation to the detail discussed by Noè this has not yet been quantified for *Kronosaurus*.

As with the large Jurassic pliosaurids, the dentition of *Kronosaurus* is markedly anisodontic, but the pattern of anisodonty is different to that seen in *Liopleurodon* and *Pliosaurus*. In these Jurassic pliosaurids, the largest teeth are the 5th maxillary (M5) teeth: the maxillary teeth increase gradually in size from the comparatively small M1 teeth that lie immediately behind the short diastema at the maxillary-premaxillary suture on the jaw margin. In this respect they resemble crocodilians, where the largest teeth are the M5 (Crocodylidae) or the M4 (Alligatoridae). In contrast, the M1, M2, and M3 are the largest teeth in the jaw and are approximately the same size (in

QM F18827, 11 cm crown and 20 cm root). The anterior maxillary teeth occlude the anteriormost teeth of the mandibular rami, which are much smaller, and posterior to the M3 tooth position the maxillary teeth are gradually smaller. In front of the M1 tooth, the diastema is somewhat larger than in *Liopleurodon* and *Pliosaurus* due to the absence of a fifth premaxillary tooth: in *Kronosaurus queenslandicus* the D4 and D5 tooth positions occlude between the Pmx 4 and M1 teeth of the upper jaw, and these dentary teeth are nearly as large as the anterior maxillary teeth. In functional terms, the resulting pattern is of an array of large, caniniform teeth in the lower and upper jaws from the D4 to the M3 tooth positions, where a pair of very large dentary teeth are followed by a trio of very large maxillary teeth. In front of this, the premaxillary (Pmx1–4) and anterior dentary (D1–3) teeth are smaller and occlude in an intermeshing basket that seems to provide a more precise bite at the tip of the jaws. Posterior to the caniniform fangs, the maxillary and dentary teeth do not occlude close to the apposing teeth; for most of the tooth row posterior to M3, the lower jaw teeth lie at least 5 cm lateral to the line of the upper jaw teeth, giving *Kronosaurus* a pronounced underbite in the posterior half of the jaw. The underbite may be functionally important in processing large prey: this is explored further in Section 8.3 below.

The relatively forward position of the fangs in *Kronosaurus*, compared to Jurassic pliosaurids and extant crocodilians, may reflect an emphasis on agility of the jaws (see above). Alternatively, these deep rooted caniniforms may have represented the optimal position in the tooth row for holding prey that needed to be shaken prior to consumption; the anterior position providing increased moment and thus increased resultant force being applied to the prey.

Of the modern aquatic macrophagus predators, crocodilians display marked anisodonty, but odontocetes do not. Even with taxa such as *Orcinus* and *Pseudorca*, the teeth (bar the most anterior and posterior) are generally of the same size. Another difference is that the anisodonty of crocodilians is exaggerated by the dorso-ventrally undulating line of the jaw margin, a form that has been termed 'festooning' and which, in a large *Crocodylus*, results in the tip of the M5 tooth being much lower than would result from the crown height alone. The festooning pattern of crocodile jaws has been linked to piscivory, but this is unlikely to be the correct explanation because

the crocodiles with the least festooned jaws are the longirostine forms, which are understood to be the most piscivorous, and *Gavialis* entirely lacks festooned jaw margins. Instead, the festooning pattern may result from the need to hold deeply rooted caniniform teeth in a platyrostral skull, where the height required to house the roots is not available in the rostrum and must be completed by a downwards (in the case of the upper jaw) growth of the tooth margin. In contrast to crocodilians, odontocetes do not have festooned jaw margins and, with the exception of the expanded margin of the mid premaxillae and anterior maxillae, nor does *Kronosaurus*. This may be a result of a greater amount of 'room' for the roots of the fangs in toothed whales and *Kronosaurus*, but this idea is yet to be tested quantitatively.

Rostral morphology

The overall shape of the rostrum in *Kronosaurus* is elongate – not to the degree seen in the longirostrine crocodilians *Gavialis*, *Tomistoma*, *Crocodylus johnstoni*, and *C. cataphractus*, but more than the degree seen in the mesorostrine taxa *C. porosus* and *C. niloticus*. Of the living crocodilians, it is perhaps most comparable to the 'intermediate' proportions of the Orinoco crocodile *C. intermedius*. Perceived patterns of similarity in form can be examined quantitatively using morphometrics, but there have been few morphometric studies of extant crocodilians. Busbey (1995) devised a plot of rostral length/BSL against the ratio of snout tip width to skull width at the orbits, and included data from 115 fossil and extant species: interestingly, when added to that plot (Figure 8-1) *Kronosaurus* is placed close to the thalattosuchians *Metriorhynchus* (Figure 8-2) and *Steneosaurus*. The thalattosuchians were a Jurassic marine radiation of crocodilians which were open water predators, i.e. similar to the lifestyle assumed for pliosaurs. In Busbey's plot, the thalattosuchians occupy a part of the morphospace that no living species of crocodilian does, and it thus seems that skull shape carries a signal due to habitat. The functional reasons that might underlie this are considered in Section 8.3 below.

There are some other intriguing parallels between the skull morphology of *Kronosaurus* and that of thallatosuchians, in particular *Metriorhynchus*. Both forms have an enlarged supraorbital flange at the dorso-medial edge of the orbit, a feature shared also with at least some mosasaurs (Chapter 5). In *Metriorhynchus*, the anatomy of the pterygoid bones suggests that the pterygoidus musculature was reduced relative to

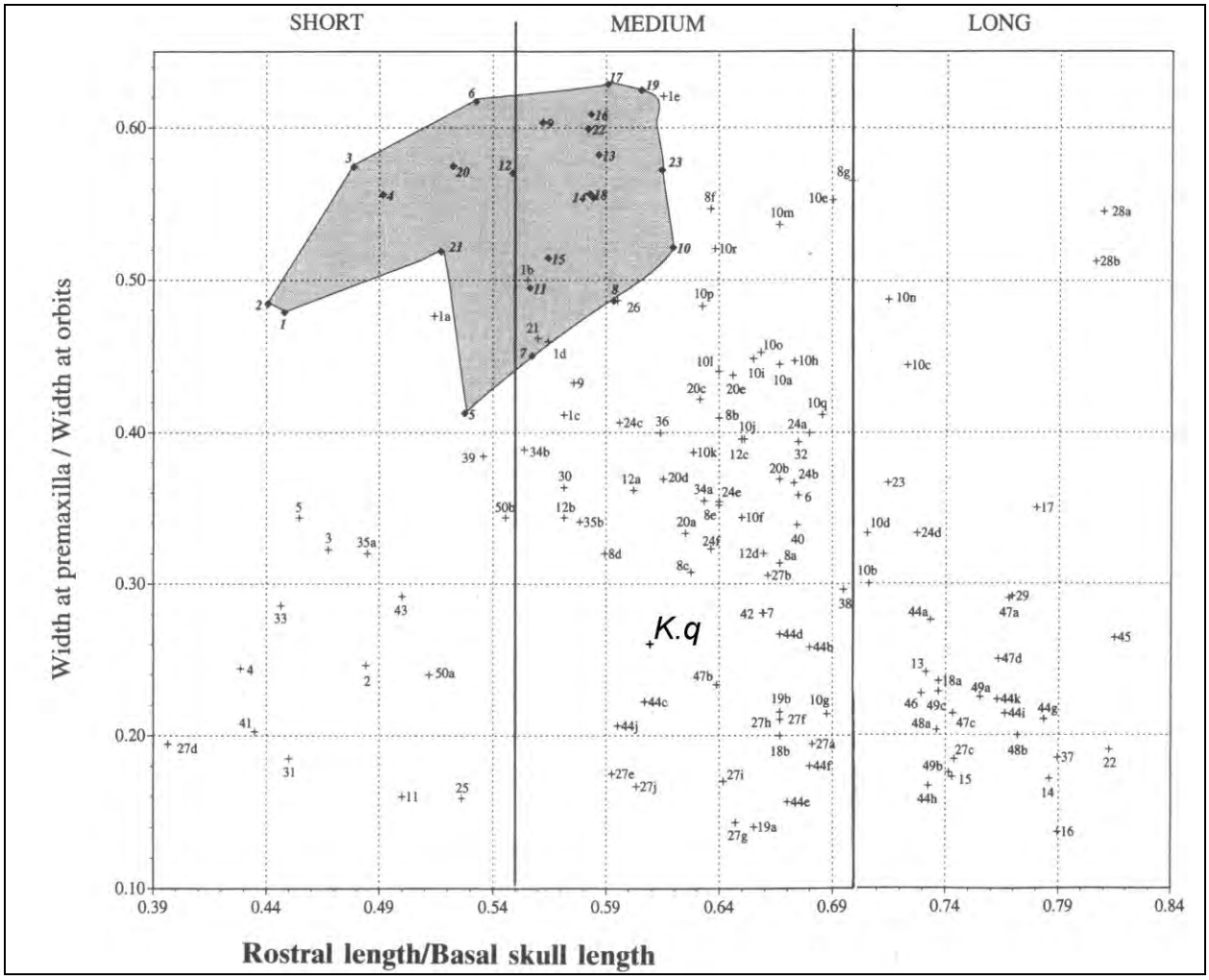

Figure 8-1: Morphometric plot of rostral proportions in crocodilians, taken from Busbey (1995: Fig. 10.2). The x axis shows the ratio of rostral length (anterior margin of orbits to anterior tip of snout) to basal skull length. The y axis shows the ratio of the maximum width across the tooth bearing parts of the premaxillae to the width of the skull at the postorbital bars. The position of *Kronosaurus queenslandicus* is indicated ('*K.q*'). Data points numbered 27 and 44 are the marine thallatosuchian taxa *Metriotrhynchus* (Figure 8-2) and *Steneosaurus* respectively; *Crocodylus* is numbered 10. The grey polygon indicates the morphospace occupied by a ontogenetic series of *Alligator mississippiensis*. For identity of other data points, see Busbey (1995).

extant crocodilians, and the enlarged temporal fenestrae (Figure 8-2) suggest a concurrent increase in the importance of the temporal musculature (in the sense used in Chapter 7). This is very similar to the situation seen in pliosaurs: indeed, *Metriorhynchus* is the only reptile that I am familiar with that has temporal fenestrae that approach those of the pliosaurids in proportions. Interestingly, the jaw musculature of living odontocetes is dominated by the temporal system, while the masseter-pterygoid (mechanically analagous to the reptilian pterygoidus – see

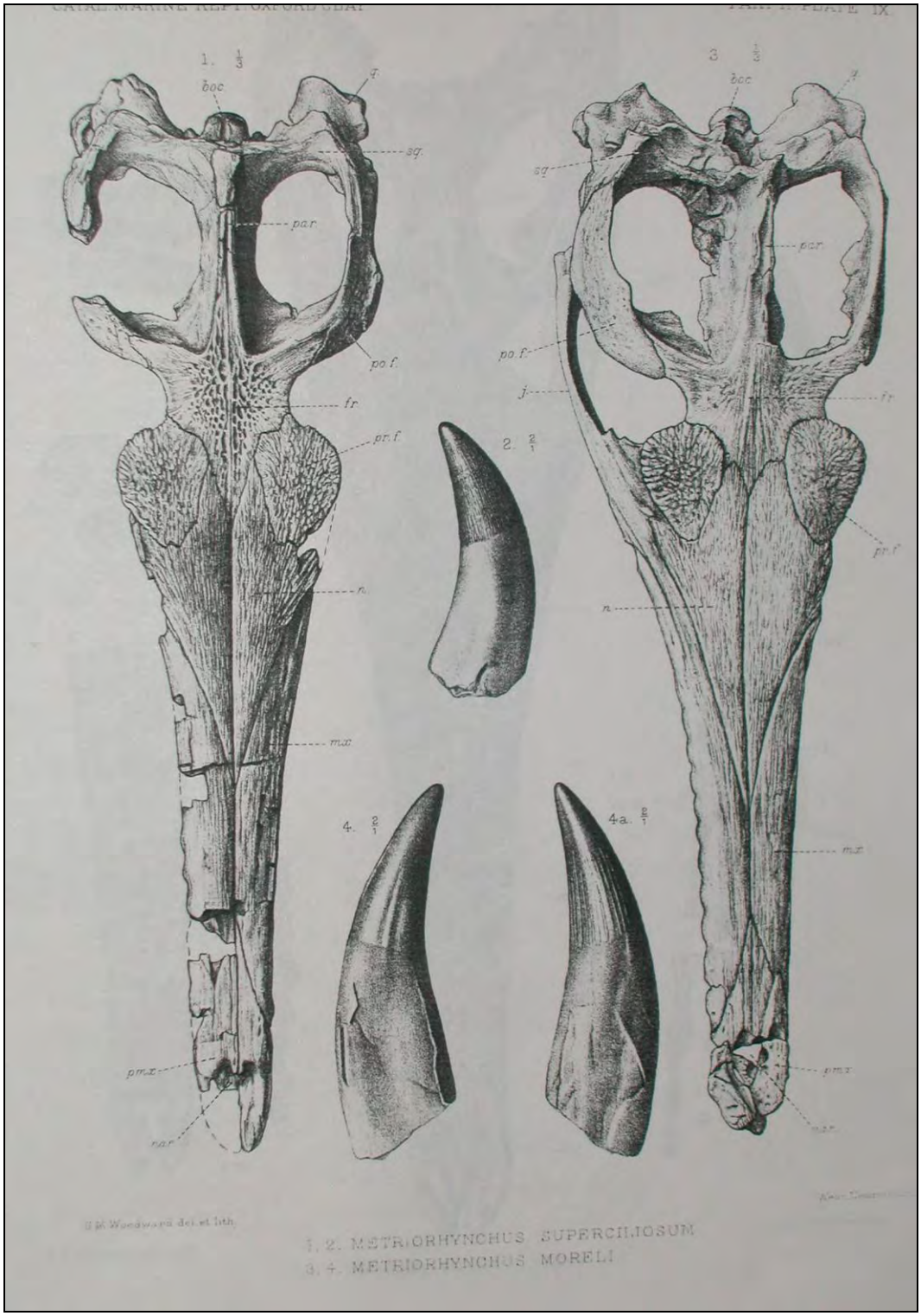

Figure 8-2: The thallatosuchian crocodile *Metriorhynchus superciliosum* from the Middle Jurassic Oxford Clay of Europe, reproduced from a plate in Andrews (1913). The overall skull proportions of this pelagic marine crocodilian were very similar to those of *Kronosaurus*. (The original plate indicates two species, *M. superciliosum* and *M. moreli*, but recent reviews suggest that these are synonymous – see Young 2007).

Chapter 7) is only weakly developed (Rauschmann et al. 2006), an unusual state for mammals (Schumacher 1985, Turnbull 1970) and perhaps indicating that, like rostral proportions, the arrangement of the jaw muscles in thallatosuchians, pliosaurs, and odontocetes may correlate with the open ocean habitat.

A unique feature of the rostrum in pliosaurs, one that is particularly well developed in pliosaurids and brachauchenіids, is the dorsal median ridge. Despite being mentioned in anatomical and phylogenetic studies of pliosaurs (Druckenmiller and Russell 2008), the functional significance of this structure has received little attention. The following scenario is provided in an attempt to simulate the generation of functional hypotheses for the pliosaur dorsal median ridge: Mechanically, it offers an important brace against the compressive loads that occur along the dorsal margin of the rostrum during biting, and may be an important component of the structural trade-off between rostral strength and snout length that pliosaurs, like crocodilians and odontocetes, appear to have faced. However, in both crocodilians and toothed whales there are constraints preventing any increase in snout height – for crocodiles, the need for streamlining during the lateral strike used to catch fish, and for odontocetes, the presence of the large acoustic organ immediately above the posterior rostum [see McHenry et al. (2006) and Section 8.3 below]. Pliosaurs did not have biosonar (Taylor 1992), and whilst the lateral sweep was undoubtedly important to them, it is likely that a greater forwards component of fluid velocity affected the hydrodynamics of their rostrum during prey capture. Thus, it seems possible that the need to minimise rostral height was not as great as it is in crocodiles or odontocetes, and so that instead of needing to increase rostral width in an attempt to brace the skull against bite forces, pliosaurs were able to use to the mechanically more effective strategy of increasing rostral height. This is why the skull of macrophagous pliosaurs is relatively narrower than the skull of both macrophagous crocodilians (e.g. *C. porosus*) and macrophagous odontocetes (e.g. *Orcinus*, *Pseudorca*); in these, the bending loads caused by bite forces are braced by increase in rostral width, which is mechanically less efficient than an increase in height but represents the only structural option available (McHenry et al. 2006).

However, because pliosaurs probably did use a component of lateral movement in prey capture, rostral height was still constrained by hydrodynamics, albeit to a lesser

extent than in crocodilians. Accordingly, the median section of the dorsal roof bones of the rostrum are increased in thickness, producing a pronounced ridge that is composed of multiple elements with a complex geometry. The presence of multiple elements – at least four pairs, two pairs of external bones, and two pairs internally – allows rapid increase in the thickness of the ridge as a consequence of bone growth at the sutural surfaces: this rapid growth phase may coincide with a dietary shift from the juvenile age class, where diet is composed entirely of small–medium sized nektonic fishes and cephalopods, to an adult diet that has a greater proportion of large prey including marine reptiles. Once this rapid growth phase is completed, most of the elements fuse, leaving on the external surface only a median suture and the lateral contact with the maxillae patent: these are sufficient for the lower rates of growth that occur during adulthood. This pattern maximises the strength of what is a relatively long rostrum, providing the animal with the ability to both efficiently catch small prey and to kill and process large prey when available: it also results in the number of elements that make up the dorsal median ridge being underestimated in descriptions based upon adult specimens.

Whilst this scenario is consistent with all of the anatomical, biomechanical, and ecological data that is presented in this thesis, it is merely a *post hoc* scenario (i.e. a 'Just So' story – see Gould and Lewontin (1979) and should be used only to generate specific functional hypotheses that can be tested rigorously. I do not propose to do that here. However, one aspect of the morphology of the dorsal median ridge in *Kronosaurus* is worth emphasising: the sutural contact between the elements of the dorsal median ridge (on the dorsal surface, principally the facial processes of the premaxillae) and the frontal-parietals that lie immediately behind them is perhaps the most complex inter-digitated suture that I have seen in any reptile. The complexity of this suture on the external surface of the skull roof in other pliosaurs has been commented upon by other authors, and from what I can make of its 3-dimensional structure it is even more complex underneath the surface of the bone (Chapter 5). Finite Element Analysis of *Kronosaurus* indicates that the concentration of compressive strain at the posterior rostrum is close to the location of this sutural contact, consistent with the functional interpretation of interdigitated sutures as a joint suited for resisting predominantly compressive loads (Popowics and Herring

2007, Sun et al. 2004) – *contra* the traditional interpretation of sutural functional morphology (Hildebrand 1974).

Mandible

The morphology of the pliosaurian mandible is rather conservative, and in the 'box-beam' section of the ramus, the robust but shallow coronoid process, deep articular cotyles, robust retroarticular processes, and strong anterior midline symphysis is very similar to that of crocodilians. In dorsal view, the rami are 'bowed' slightly outwards, exaggerating the underbite of the posterior tooth rows that is present in all pliosaurids/ brachauchenids. Indeed, apart from the dentition, the only part of gross mandibular shape that varies appreciably between different taxa is the relative length of the mandibular symphysis (another similarity to both crocodilians and odontocetes).

In crocodilians and odontocetes, the taxa that take the largest prey relative to their own size have the shortest mandibular symphyses. Conversely, species that take the largest proportion of small prey have the longest mandibular symphyses relative to total length of the jaw. *Prima facie*, this relationship seems to be so robust that it deserves more serious attention than it has apparently received in the literature. I am not aware of any studies that have attempted to quantify the relationship between symphysis length and prey size, but on a qualitative basis there seem to be few exceptions to the rule of thumb that a short symphysis predicts large maximum prey size. The functional reasons underlying this association are not well understood – they may relate to the bracing of laterally directed forces when handling larger prey, or alternatively may be linked to the developmental processes that are responsible for increasing rostral length (of course, both could be involved).

The symphysis of *Kronosaurus* is short, robust, and carries caniniform teeth – in this respect, it is similar to that of *Liopleurodon ferox* and each of these are similar to macrophagous crocodilians and odontocetes. A comprehensive study on the morphometrics and biomechanics of the mandibular symphyses is overdue.

Summary

The ability of *Kronosaurus* to take large vertebrate prey is indicated by the size, shape, and patterns of wear of the teeth, the structure of the mandible, and by its estimated bite force. However, the overall proportions and biomechanical analysis of the skull point to a maximum relative prey size that is lower than for the most macrophagous living crocodiles such as *Crocodylus porosus*, and an increased efficiency in feeding on relatively smaller prey. Several morphological features, in particular rostral proportions and the relative size of the major adductor muscle groups, suggest that the open ocean habitat of *Kronosaurus* was an important component of the factors shaping its form and should be fully considered when interpreting its functional morphology.

In their review of the importance of biomechanical approaches to palaeobiology, Plotnick and Baumiller (2000) emphasised that biomechanics offered one of the few opportunities for experimental testing of hypotheses in palaeontology (see opening quote for this chapter). However, they also noted that taphonomy provides another opportunity for testing palaeontological hypotheses. Various fossils from the Early Cretaceous of the Great Artesian Basin preserve taphonomic data that are potentially of use in this regard. In the next section, some of these fossils are evaluated to determine the extent to which they are consistent with the functional interpretation of feeding ecology in *Kronosaurus* that has been given here.

8.2 Evidence from taphonomy

Taphonomy offers a rare opportunity for palaeontologists to glimpse a narrow window in the lives of the animals they study. Whilst earlier discussion of taphonomic processes in this thesis have focussed upon the various distortions that are inflicted upon the anatomy preserved in fossils (Chapter 3), taphonomic data also includes stomach contents, coprolites, bite marks, and traces of locomotion such as footprints, burrows, and drag marks. Each of these are of great potential importance for palaeoecological reconstructions.

As mentioned in Chapter 3, the marine reptile fossils of the Great Artesian Basin are notable for the high proportion of specimens that preserve gut contents (Kear 2006a, Kear et al. 2003, McHenry et al. 2005). Two specimens of *Kronosaurus* also preserve structures in the abdominal region that are consistent with gut contents, and these are described below. I am not aware of any coprolites that can be referred to *Kronosaurus*, although an elasmosaurid coprolite/ colonite is known (McHenry et al. 2005). Some specimens of marine reptile from the GAB preserve bite marks (Thulborn and Turner 1993), and two of these that may be linked to behaviour by *Kronosaurus* are also discussed. Lastly, the curious association between a small *Kronosaurus* and a large shark (Chapter 4) is revisited for the possibility that it may represent a circum-mortem rather than a post-mortem event.

Although evidence from stomach contents, bite marks, etc. offer a unique insight into the lives of animals that cannot be observed directly, taphonomic data is just as vulnerable to narrow interpretation as is functional morphology. For example, a narrow functional interpretation of the teeth of elasmosaurids from the GAB would indicate a diet of fish and cephalopods, whilst a narrow view based upon gut contents would emphasise benthic invertebrates (McHenry et al. 2005). Probably, elasmosaurs fed on both types of prey. Stomach contents are a single data point in the life history of one individual, and whilst they do not necessarily indicate typical behaviour they can serve as a powerful complement to functional morphology.

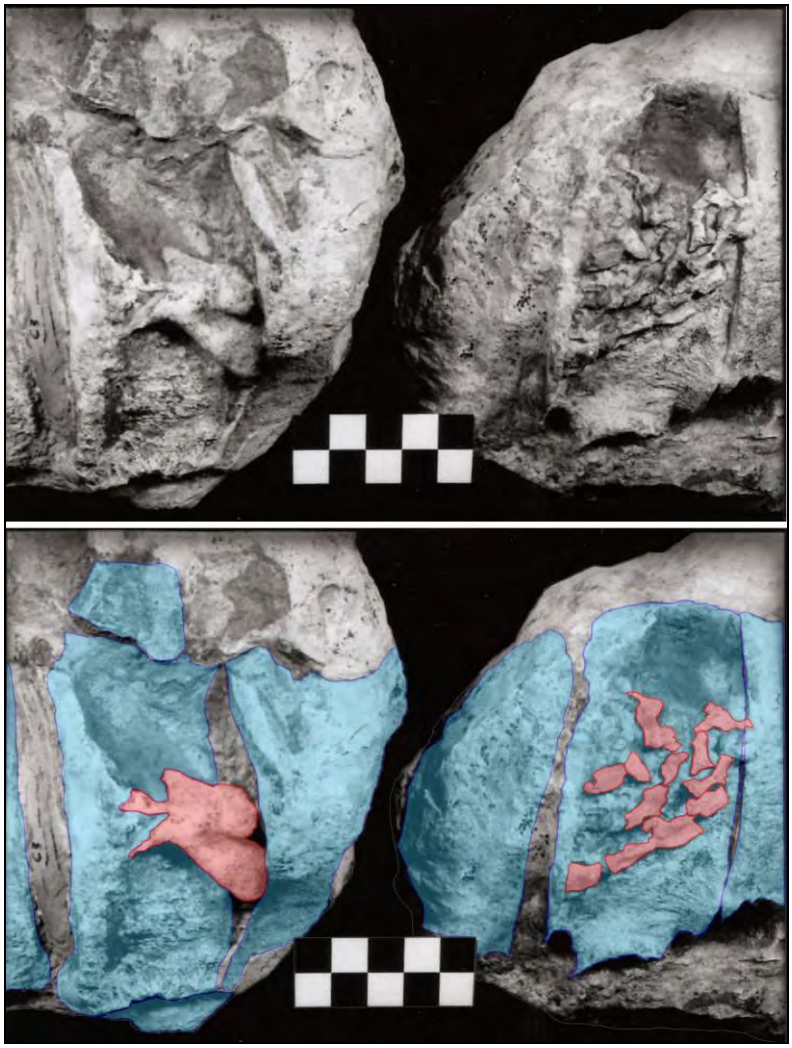

Figure 8-3: Posterior neck region of QMF10113 in ventral view (top), with interpretation (below). Five of the pliosaur's cervical vertebrae (c8–c12: blue shading) are contained in two nodules: anterior is to the left. A partial propodial head and vertebrae from a turtle (red shading) lie on the ventral surfaces of the 9th and 11th cervical vertebrae respectively. Scale bar is 5 x 2 cm.

QMF10113 – turtle

QM F10113 comprises a partial skeleton from the Late Albian Toolebuc Formation that includes an articulated series of cervical, dorsal and sacral vertebrae in addition to a large amount of cranial material (Chapter 6). Estimated total length is 8.6 m and mass *c.* 5,700 kg (Chapter 6). A summary description of QM F10113 is provided in Chapter 4.

On the ventral surfaces of the pliosaur's 9th and 11th cervical vertebrae lie the proximal part of a broken humerus, together with several articulated vertebrae from a small turtle (Figure 8-3). In the abdominal section of the pliosaur, just forward of the

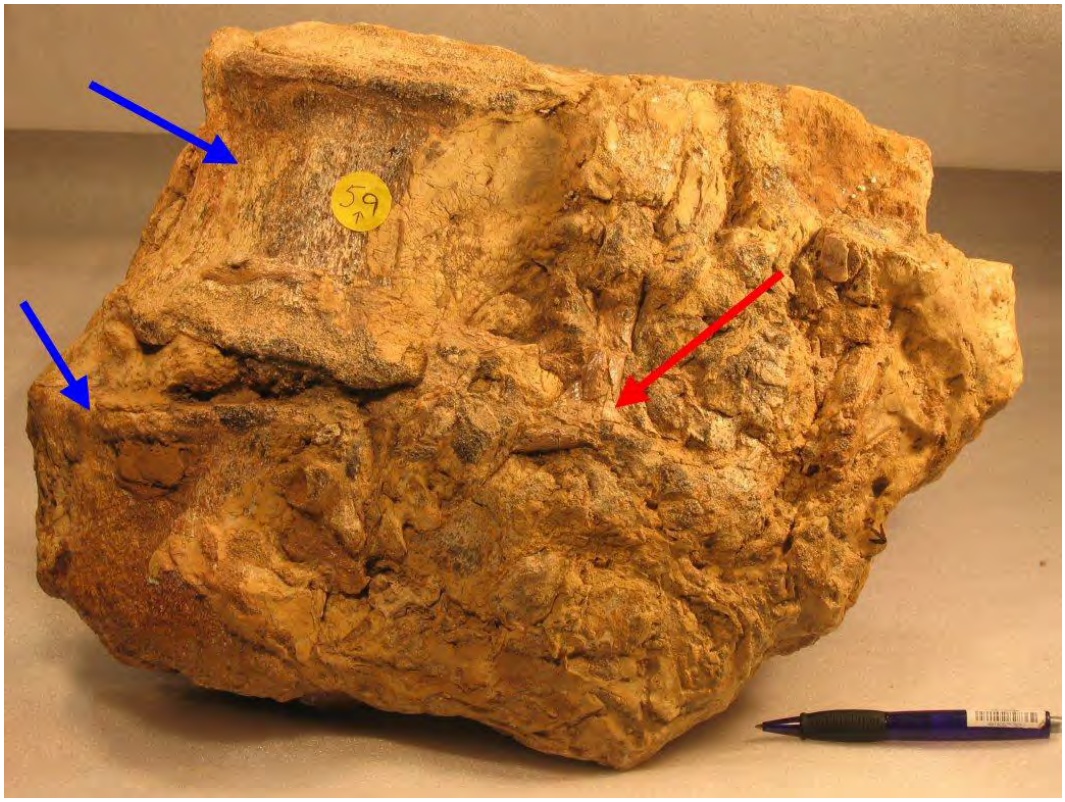

Figure 8-4: Stomach contents of QM F10113: surface of block from trunk region showing vertebrae 29-30 of the pliosaur (blue arrows) with associated turtle pectoral girdle elements (red arrow).

anterior edge of the pubis and alongside a lumbar vertebra, the limestone matrix contains a large amount of small, broken bony material. Some of this material has a small, flat surface consistent with the broken turtle carapace, and a fused scapula-coracoid that is characteristic of Chelonia (Figure 8-4). The scapula-coracoid is of a similar size class to the remains lying on the ventral surface of the pliosaur.

Estimates of body size: turtle remains

Based upon comparison of the scapula, coracoid, and proximal humerus, estimated linear dimensions of the turtle within QM F10113 are 42% of those of a leatherback turtle *Dermochelys coriacea* (QM J81592) which had a curved carapace length (CCL) of 164 cm; CCL of the fossil turtle is therefore estimated at 69 cm. Extrapolation from CCL and body mass from a large leatherback turtle (Price et al. 2004) gives an estimate of 20 kg for the turtle preserved with QM F10113.

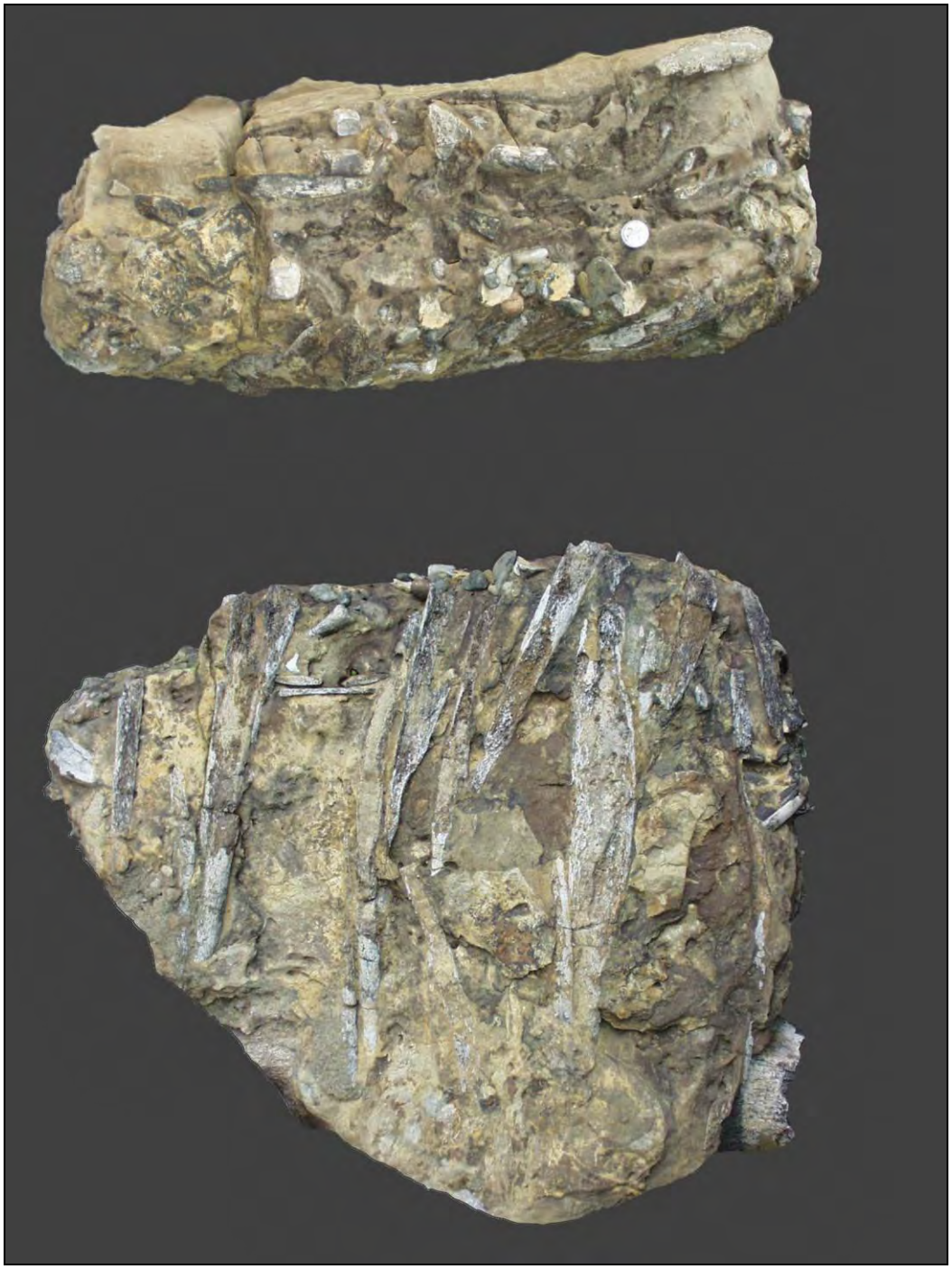

Figure 8-5: QMF33574, limestone nodule containing lumbar/abdominal region of QMF33754 in lateral (top) and ventral (bottom) views. Scale bar = 5 x 2 cm. For interpretation see Figure 8-6.

The remains are too fragmentary for identification of species, but a CCL of ~70 cms may be close to maximum recorded size for *Notochelone*, the most common and the smallest of the three species of chelonian recorded from the GAB (Kear 2003, 2006b, Kear and Lee 2006, Molnar 1991).

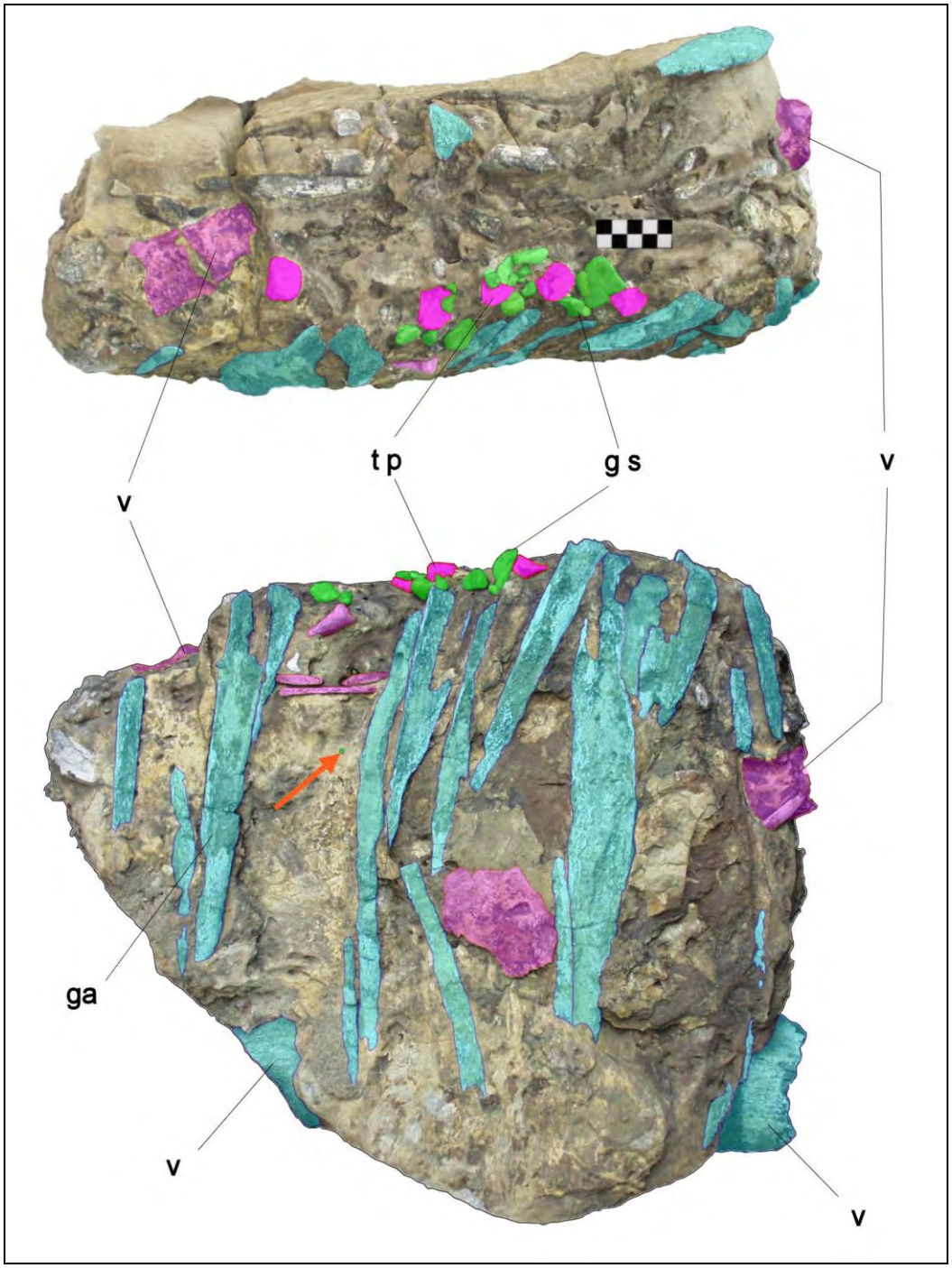

Figure 8-6: Interpretive diagram of QMF33754 shown in Figure 8-5, in lateral (top) and ventral (bottom) views. *Kronosaurus* bones shaded blue, bones of prey (QMF33575) shaded pink, gastroliths shaded green, position of isolated fish vertebra indicated by orange arrow (see Figure 8-7); ga, gastralia; g s, gastrolith; t p, transverse process; v, vertebra. The anterior face of the block is to the left of the image as shown. Scale bar = 5 cm.

Interpretation

Some of the turtle remains are pulverised, while the humerus has been cracked across the mid-shaft. Several factors argue against the association of the turtle and pliosaur

remains being a result of post-mortem association; a heavily dismembered carcass is unlikely to be transported as a unit, and the matrix of QM F10113 indicates a low energy depositional environment, as for most of the Toolebuc Formation (Chapter 4). Further, the turtle remains are located in regions that match the location of the alimentary canal of the pliosaur: the stomach / intestine in the abdominal region, and the oesophagus ventral to the cervical vertebrae. Indeed, the position of the turtle's propodial and vertebrae at the cervical vertebrae of QM F10113 raise the possibility that the pliosaur choked on its last meal, although it is also possible that the turtle remains were forced into the oesophagus from the stomach by the gases of decomposition.

QM F10113 and the turtle remains preserved with it are therefore interpreted as evidence of predation by a ~5 tonne *Kronosaurus* on a small (20 kg) turtle.

QM F33574 – elasmosaurid

An articulated series of vertebrae and associated elements was recovered[2] from the Doncaster Formation of Grampian Station (Richmond area) in 1995 and accessioned as QM F33574. The vertebrae are large, plesiosaurian, and lack sub-central foramena: they are thus referred to the Brachaucheniidae and to the only taxon of brachaucheniid known from the GAB, *Kronosaurus*. The morphology of the vertebrae indicates that they are dorsals and that the specimen represents a partial torso of a large pliosaur.

The specimen was preserved within a series of four large limestone blocks, each approximately 100 kg, aligned along the axial column of the pliosaur. One block preserves a partial but articulated set of gastralia from the pliosaur (Figure 8-5, Figure 8-6) and thus represents the abdominal cavity. Amongst the bones that definitely belong to the pliosaur are a series of seven vertebrae that are much smaller than the pliosaur's own and appear to be articulated within the block: a loose vertebra found immediately anterior to the block (Figure 8-7A, B) evidently articulated with these and this vertebra (QM F33575) preserves the overall shape and the sub-central

[2] With the assistance of L. Beirne, H. Dick, M. Dick, E. McKenzie, M. Wade, and R. Wilson, and the support of Landrover Australia

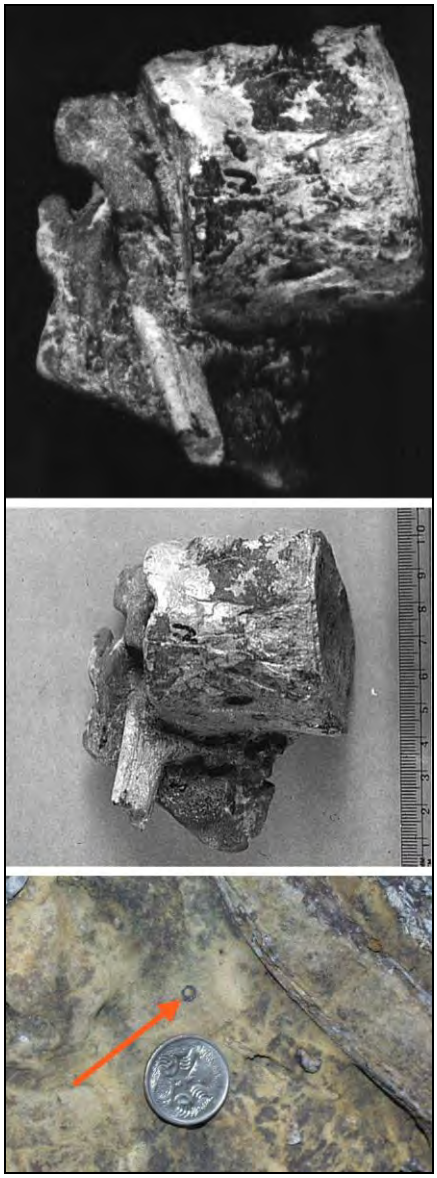

Figure 8-7: Close ups of stomach contents associated with QM F33574. Top and centre, vertebra of QMF3375 associated with QM F33574, collected immediately anterior to nodule in Figure 8-5 shown in oblique ventral views. Bottom, close-up of teleost vertebra in nodule shown in Figure 8-5 (orange arrow). Rule in centre image in cm; diameter of coin at bottom = 10mm.

foramina characteristic of a dorsal vertebra from a small elasmosaurid. Within the same block can be seen 17 small, rounded pebbles (Figure 8-5, Figure 8-6) that are of exotic lithology, and which are similar to gastroliths commonly found in association with elasmosaurid specimens in the Great Artesian Basin and worldwide (Cicimurri and Everhart 2001, McHenry et al. 2005), together with a small isolated vertebra from a bony fish (Figure 8-7C).

Estimates of body size

Centrum length for a mid-dorsal vertebra of the *Kronosaurus* specimen is 145 mm, which is almost identical with the maximum length of a dorsal vertebra from MCZ 1285 and suggests an animal of similar size, i.e. a total length of ~10.5 m and a mass of ~11,000 kg (Chapter 6).

Comparative data for length and mass estimates of fragmentary elasmosaurid material was collated from published accounts of three specimens which include articulated series of dorsal vertebrae; these specimens were DMNH 1588 (*Thalassomedon haningtoni*) and UCMP 33912 (*Hydrotherosaurus alexandrae*) (Welles 1943), and QM F6890 (holotype of *Woolungasaurus glendowerensis*) (Persson 1960). For each of these, measurements of the length, width, and height of vertebral centra were used to provide a basis for estimating body size in less complete elasmosaurid specimens.

	av. dorsal length	**head**	**neck**	**torso**	**tail**	**TL**	**volume**
BMNH model ('Plesiosaur')		16	134	80	90	305	0.11
DMNH 1588 *(Thalassomedon)*	107	470	6,618	2,924	1,356	11,368	5,372
UCMP 33912 *(Hydrotherosaurus)*	87	330	4,626	1,884	1,205	8,045	1,436
QM F6890 *(Woolungasaurus)*	68			1,214			385
	extrapolating body size by comparison with						
	av. dorsal length	**DMNH 1588**		**UCMP 33912**		**QM F6890**	
		torso	**volume**	**torso**	**volume**	**torso**	**volume**
QM F33575	47	1,287	458	1,017	226	844	268
QM F420	86	2,353	2,798	1,859	1,381	1,543	489

Table 8-2: Body size estimates for elasmosaurids. Segment lengths are derived from summing vertebral lengths for relatively complete specimens (see text). Volume is derived by comparing torso length with the equivalent measurement of the BMNH model, and scaling the measured volume accordingly. Estimates of body size in fragmentary Australian elasmosaurid specimens (QM F33575, QM F420) are based upon comparison of short lengths of vertebrae with equivalent parts (Figure 8-8, Figure 8-9) of the more complete specimens listed above (DMNH 1588, UCMP 33912, QM F6890): this produces a range of size estimates for each specimen. QM F33575 was recovered from the abdominal cavity of a *Kronosaurus* specimen; QM F420 is a Late Aptian specimen that represents one of the larger elasmosaurids known from the Australian Cretaceous to date. Lengths in mm, volume in litres.

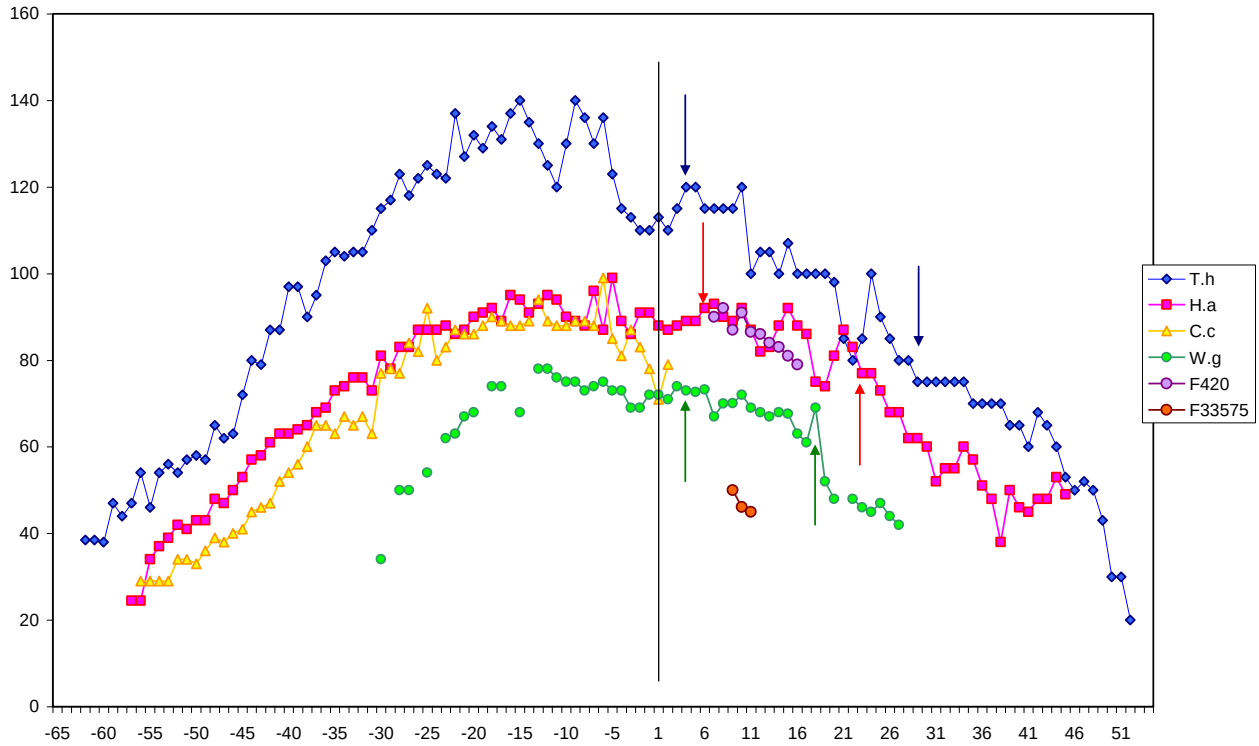

Figure 8-8: Elasmosaurid vertebral lengths, taken from published and direct measurements. 'T.h', *Thalassomedon haningtoni* DMNH 1588 (Welles 1943); 'H.a', *Hydrotherosaurus alexandrae* UCMP 33912 (Welles 1943); 'C.c', *Callawayasaurus colombiensis* (Welles 1962); 'W.g', *Woolungasaurus glendowerensis* (Persson 1960); 'F420', QM F420 (Table 8-2); 'F33575', QM F33575 (Table 8-2, Figure 8-4 – Figure 8-7). Numbers on the x axis show the axial position of vertebrae, with the first pectoral vertebrae assigned the number 1 (marked with vertical black line), and neck vertebrae assigned negative numbers. Measurements on the y axis are centrum length in mm. For each of the *Thalassomedon* (blue), *Hydrotherosaurus* (pink), and *Woolungasaurus* (green) series, the position of the anterior-most (left) and posterior-most (right) dorsal vertebrae is indicated by arrows of respective colour. Note that QMF 420 appears to indicate a similarly sized animal as UCMP 33912, but that QM F33575 is much smaller than any of the other specimens listed.

Summing centrum length (Figure 8-8), allowing 5% of total vertebral length for intervertebral joints, provided estimates of total length and body segment length (Table 8-2). The ratio of centrum length to average diameter has been used as a vertebral length index (VLI) to analyse morphology variation within the vertebral column of plesiosaurs (Brown 1981), and can be used to refine diagnosis of anatomical position of individual vertebrae.

The only one of the elasmosaurid vertebra (Figure 8-7) from which the length, height, and width can be measured has a VLI of 0.87 and, by comparison with the more complete specimens, appears to be a thoracic (i.e. anterior dorsal – see Chapter 6) vertebra (Figure 8-9). The mean length of this vertebra, and two others from

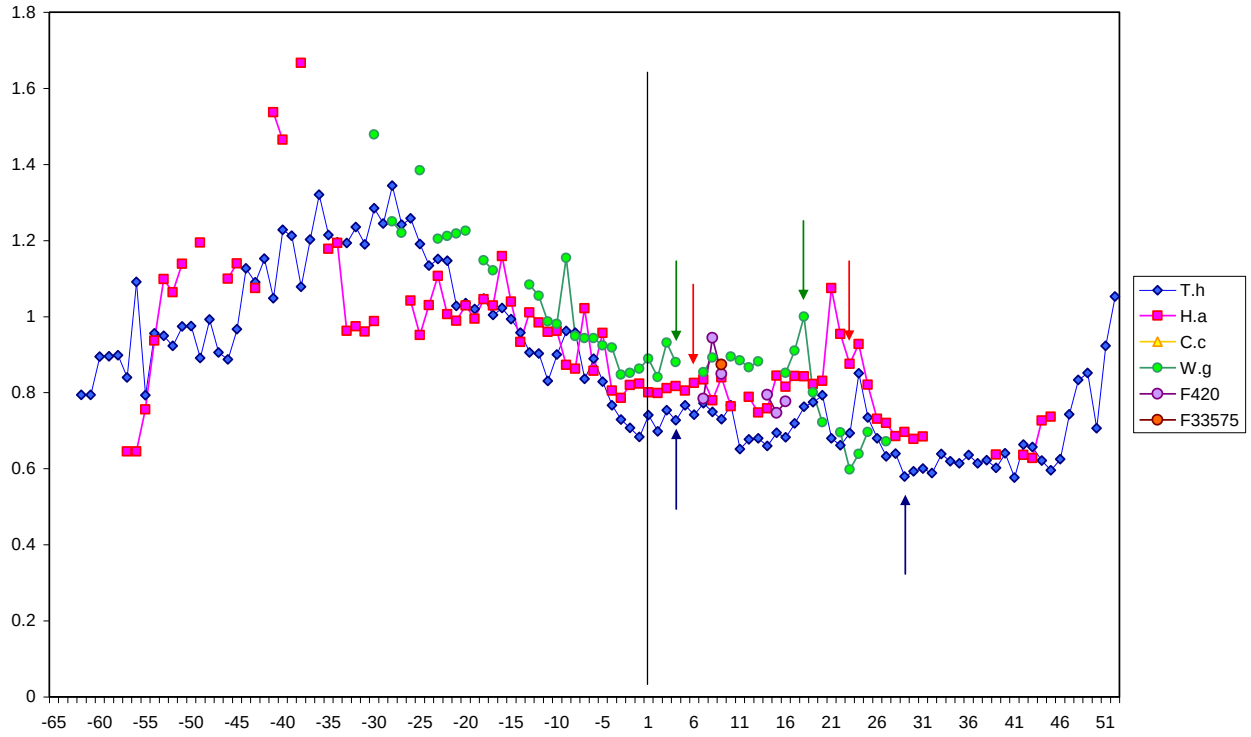

Figure 8-9: Vertebral Length Index (VLI: centrum length divided by average diameter of centrum - (Brown 1981)) for the elasmosaur specimens shown in Figure 8-8. Legend and colours as for Figure 8-9. VLI for 'dorsal' vertebrae lie within a consistent range, even for specimens of different taxa and body size.

which only centrum length can be measured, is 47mm; comparing this with the average centrum length of the thoracic vertebrae in DMNH 1588, UCMP 33912, and QM F6890 provides estimates of torso length (defined as mid-pectoral to mid-sacral inclusive – see Chapter 6) for QM F33575 of between 844 and 1287 cm (Table 8-2). These estimates of torso suggest an animal with a total length between 3.3 and 5 metres.

Body mass was estimated using a similar approach to that employed for mass estimates of *Kronosaurus* (Chapter 6); the volume of a scale model of *Elasmosaurus* (Invicta Plastics)[3] was measured and, scaled by the ratio of the estimated torso lengths, this allowed an estimate of body mass in the comparative specimens and QM F33575 (Table 8-2). Torso length was used as a scalar because neck lengths within the Elasmosauridae vary greatly and are a major component of snout-vent and total length but not body mass. Note that the volume of the model was measured

[3] Labeled 'Plesiosaur', but from the overall proportions and the cited length (14 m) the model is most likely based upon *Elasmosaurus*. See www.rubberdinosaurs.com/invicta-reptiles.htm#plesio for details of the 'BMNH' Invicta range.

using Archimedes' Principle (Alexander 1989), as 3D scan data was not available. This method provided three estimates of body mass for QM F33575, ranging from 226–458 kg: the mean of these was 317 kg. Both this estimate, and a simple comparison of centrum length with other elasmosaurid specimens (Figure 8-8) indicates that QM F33575 was a small individual.

Interpretation

QM F33574 is preserved in a micritic grey limestone that preserves no sign of appreciable energy in the depositional environment; this, together with the location of the elasmosaurid vertebrae within the abdominal region of the *Kronosaurus*, suggests that the elasmosaurid remains were ingested by the pliosaur.

Gastroliths are frequently associated with elasmosaurid specimens with the GAB (see Chapter 3), but of the *Kronosaurus* material previously described (Chapter 4) only QM F18154 is preserved with two gastrolith-like pebbles. The gastroliths and fish vertebra are associated not only with the stomach region of the pliosaur, but the torso of the elasmosaurid and it appears that the elasmosaurid's own stomach contents were ingested by the pliosaur as part of its meal.

That the elasmosaurid vertebrae are articulated with the pliosaur's stomach region suggests this ~60 cm long segment was removed from the carcass and swallowed whole. If the gastroliths and fish vertebra do represent the elasmosaurid's stomach contents, as argued above, then the presence of the ingested elasmosaurid's own stomach contents strongly suggests that this animal was consumed before decomposition of its carcass had progressed to an advanced stage.

Like all pliosaurs, *Kronosaurus* lacked the flexible kinetic skull possessed by other predatory marine reptile such as mosasaurs (Everhart 2004), preventing it from swallowing anything wider than the internal distance between the quadrates. For QM F33574, this distance is estimated as 50–60 cms. There is little information on the girth of elasmosaurids; data from Welles (1943) indicates that the combined span of the pubes in both *Thalassomedon* and *Hydrotherosaurus* is approximately 35% of the torso lengths calculated for these specimens in Table 8-2. Applied to QM F33575, this equates to a span of 30–45 cms, although the maximum torso width was at the

thorax and pubes-span is likely to be a substantial underestimate of girth. On balance, the elasmosaurid, although small, was probably too large to be swallowed whole; furthermore, the presence of the elasmosaurid's own gut contents strongly suggests that this animal was intact immediately prior to being consumed, and that the *Kronosaurus* could not have ingested it without somehow processing it into swallowable chunks.

Eromangasaurus – *bite marks*

The only complete elasmosaurid skull from the Great Artesian Basin is QM F11050, which was originally referred to *Woolungasaurus* (Persson 1960) but has recently been used to erect the genus *Eromangaurus* (Kear 2005, 2007). Although complete, the skull is heavily distorted and a pair of large, widely spaced depression fractures along the mandible have been interpreted as bite marks from a large predator with robust non-ziphondont dentition, most likely *Kronosaurus* (Thulborn and Turner 1993). The bones of the cranium show extensive breakage (Figure 8-10) and the skull has been compressed obliquely from upper left to lower right, a mode of preservation that is very unusual for marine reptile fossils in the Toolebuc Formation (Chapter 3) and which suggests that the skull was subjected to a large force prior to burial.

Only the skull and an articulated set of five anterior cervical vertebrae are known from the specimen. Thulborn and Turner (1993) interpreted the isolation of the specimen from the rest of the post-cranium, combined with the trauma inflicted upon the skull, as evidence for an attack strategy whereby the head of the elasmosaurid was targeted by the predator, as part of a powerful killing strike which decapitated the prey.

The body proportions of Australian elasmosaurids are, on the basis of described material, largely unknown, and no skull has been found in association with postcranial remains. Dorsal cranial length of QM F11050 is 331 mm (Kear 2005). The skull of *Callawayasaurus colombiensis* from the Aptian of South America is marginally longer (340 mm) (Welles 1962) and is articulated with a 3.7 metre long complete cervical series: comparison with more complete elasmosaurid specimens (see above) suggests an overall length of ~7 m and a mass of 1–2 tonnes for *Callawayasaurus*, and QM F11050 was most likely slightly smaller. The body size of

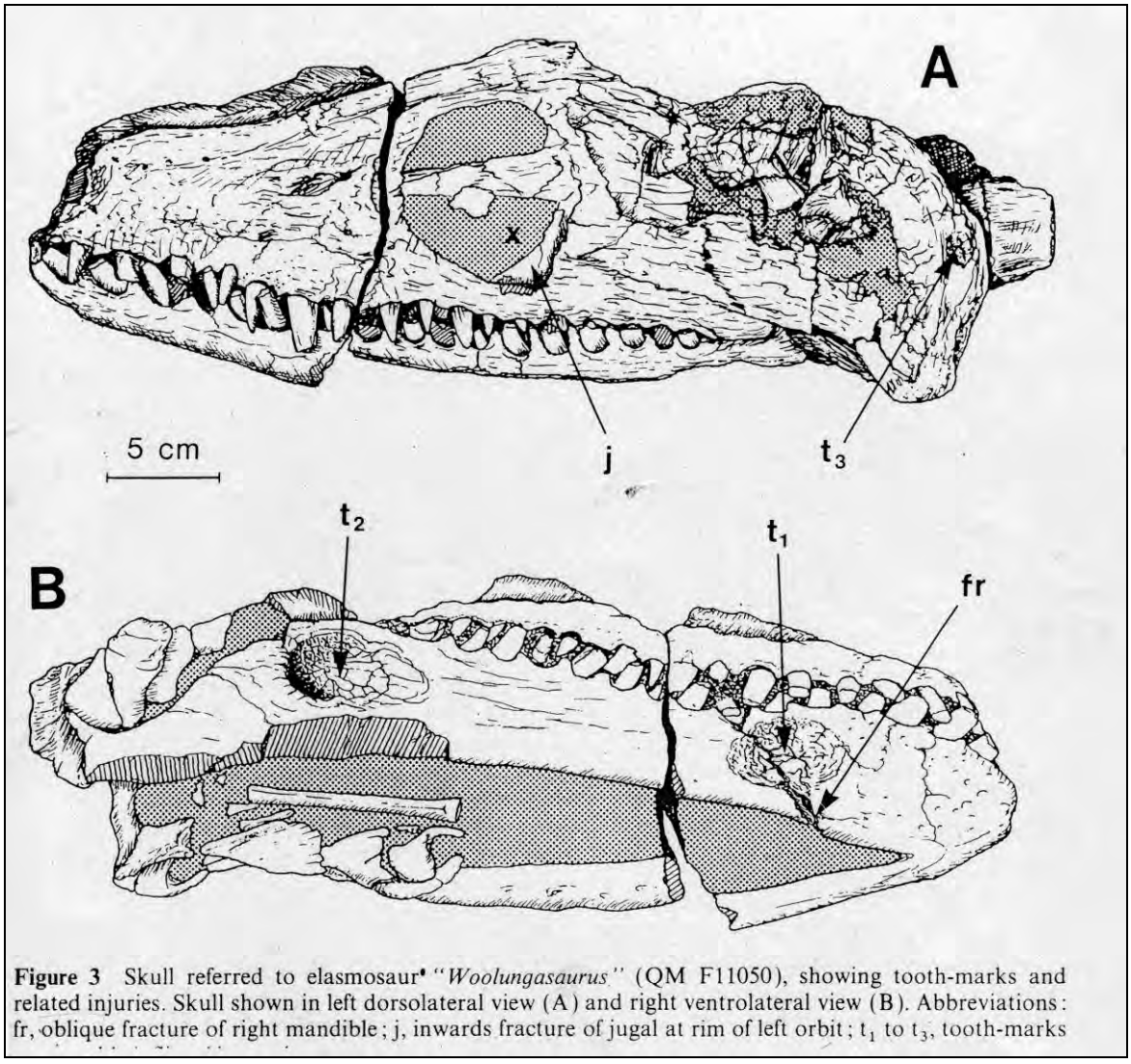

Figure 3 Skull referred to elasmosaur "*Woolungasaurus*" (QM F11050), showing tooth-marks and related injuries. Skull shown in left dorsolateral view (A) and right ventrolateral view (B). Abbreviations: fr, oblique fracture of right mandible; j, inwards fracture of jugal at rim of left orbit; t_1 to t_3, tooth-marks

Figure 8-10: QM F11050, an elamsosaurid skull, reproduced from Thulborn and Turner (1993). The caption from the original figure details their interpretation of bite marks to the specimen (see text). © Tony Thulborn, used with permission.

the putative predator cannot be determined, but the morphology of the compression fractures, and the absence of the 'cutting' bite marks typical of large sharks (Shimada and Everhart 2004) suggests that the predator was most likely a large pliosaur.

QM F51291 – bite marks

As described in Chapter 4, QM F51291 is a partial skull from a small *Kronosaurus* that displays no signs of sedimentary compaction, but which has three regions of broken bone in the inter-orbital region Figure 8-11. The morphology of these breaks is

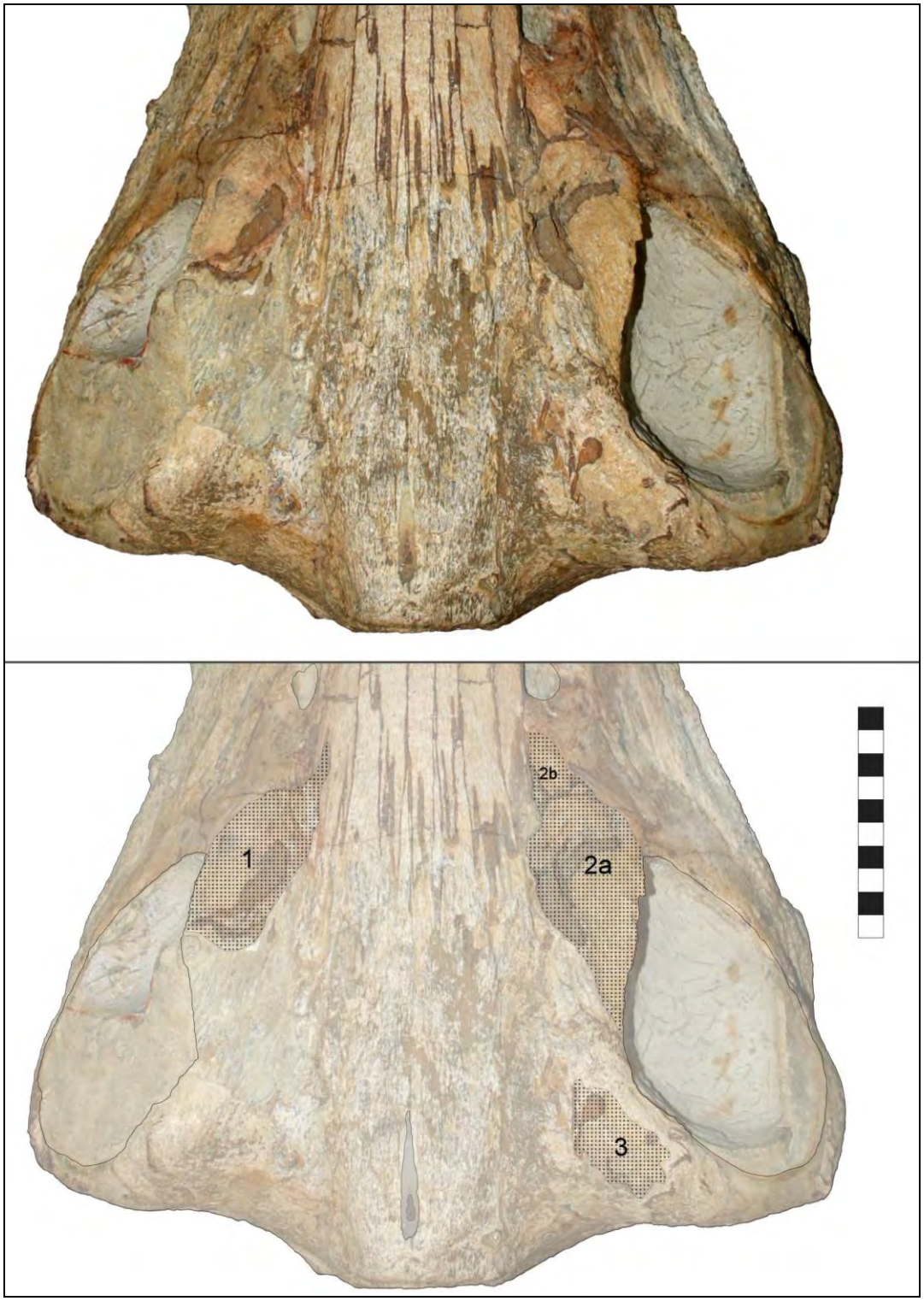

Figure 8-11: Compression fractures (numbered 1 to 3) in Kronosaurus queenslandicus QM F51291. The extent of the fractures is indicated by stippled regions in the interpretative figure a bottom. The fractures are interpreted as bite marks (see text); the regions marked '2a' and '2b' may represent the marks caused by adjacent teeth of the attack penetrating to different depths. Scale bar in cm.

consistent with a compression fracture from a blunt object, such as a pliosaur tooth; the possibility of a shark bite is argued against because of the lack of cut marks as discussed above. There is no evidence of healing.

The remarkable preservation of QM F51291 has been noted earlier, but warrants emphasis here: based upon direct observation of the preserved bone and CT scan data of the whole fossil, this specimen appears to have the least amount of post-depositional taphonomic distortion of any of the *Kronosaurus* specimens considered in the present work. Surface bone is eroded in places but, where it had been covered by matrix prior to preparation, is preserved in excellent condition. In contrast, the surface bone within the depressions is crushed into small fragments that give a texture like a broken eggshell: the presence of the localised depressions, and the broken 'eggshell' texture of the surface bone within them, differ markedly with the preservation of the rest of the specimen and is difficult to explain in terms of post burial taphonomic processes. The depressions cannot be explained as the result of erosional processes, as the two largest depression ('1' and '2' of Figure 8-11) contain cortical bone, albeit broken. Interpretation as depression fractures resulting from trauma seems to be the only plausible explanation.

QM F51291 is the smallest *Kronosaurus* specimen known from the GAB, and is estimated to have had a total length of ~5.4 m and a body mass of approximately 1.4 tonnes (Chapter 6). Given that maximum size of *Kronosaurus* is around 10.5 metres and 11 tonnes, and that of the 12 specimens described in this thesis[4] only 3 are from animals smaller than 7 metres TL, QM F51291 appears to have been a juvenile. The only blunt-toothed predator from the GAB large enough to have inflicted a potentially fatal trauma is an adult *Kronosaurus*, indicating the potential for intra-specific aggression and/or cannibalism, although it is also possible that the bites were inflicted shortly after death by other causes. Intra-specific aggression between adults and juveniles is common amongst crocodilians (Ross and Garnett 1989) and may have been exhibited within species of large pliosaurs such as *Kronosaurus*.

[4] Body size estimates for 11 of these are given in Chapter 6; the twelfth specimen is QM F33574, described above. In addition, QM F188726 and QM F2137, which have not been described in this thesis, both indicate 'adult' animals with a Total Length greater than 7 metres (pers. obs.).

QM F52279 – shark

As described in Chapter 4, QM F52279 is a partial skull from a small *Kronosaurus* from the Late Albian Toolebuc Formation which has been fossilised in association with at least seven or eight vertebrae from a shark (Figure 8-12). The vertebrae are similar in morphology to a set of articulated vertebrae (Figure 8-13) described by Blanco-Piñón et al. (2005) from the Late Cretaceous (Turonian) of Mexico; these were identified as lamniform based upon the presence of 'well-calcified radiated lamellae'. Blanco-Piñón et al. further noted the resemblance of the Mexican vertebrae to fossils of cretoxyrhinid sharks from North America, comparing them in particular to *Cretalamna appendiculata* and *Cretoxyrhina mantelli*. Both of these taxa are thought to be present in the Late Albian fauna of the Great Artesian Basin (Kemp 1991 – see Chapter 3). The vertebrae associated with QM F52279 are larger and appear to be

Figure 8-12: Shark vertebrae associated with QM F52279. Diameter of coin is 28 mm. See text for discussion.

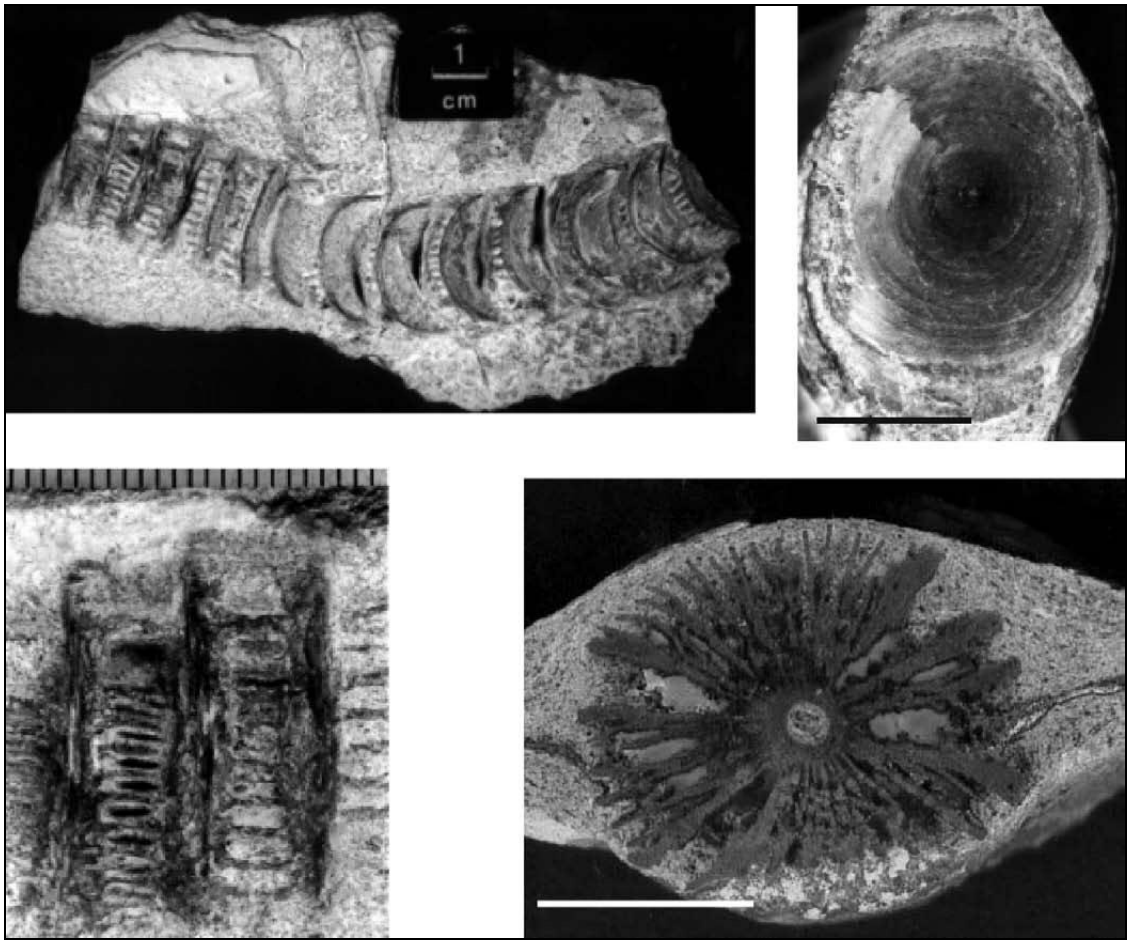

Figure 8-13: Articulated vertebrae from a Late Cretaceous (Turonian) lamniform shark cf Cretoxyrhinidae. Reproduced from Blanco-Piñón et al. (2005). See text for discussion.

relatively shorter for their diameter, but are otherwise remarkably similar to the vertebrae figured by Blanco-Piñón et al (2005).

Body size

The lamniform vertebrae associated with QM F52279 are mostly obscured by matrix, and the transverse face is only visible on one vertebra; this has a maximum diameter of 69 mm, and although it is broken along one edge: the radius, measured normal to the maximum diameter, is 31 mm. Assuming that the larger diameter is height, this gives a height to width ratio of 1.11. Blanco-Piñón et al. compared the diameter of the Mexican vertebrae with vertebral dimensions described for complete specimens of *Cretoxyrhino mantelli*, wherein trunk vertebra (FHSM VP2184) had a height to width

		Height	Width	ratio	ID	TL	BoM
FHSM VP-2187	v-185	33	31	1.06	caudal	500	1,294
FHSM VP-2187	v-40*		87		trunk	500	1,294
CMN 40906	v23	74	68	1.09	post trunk?	670	3,222
CMN 40906	v25*	76				670	3,222
Qld (with QM F52279)		69	62	1.11			
comparing Qld vertebra (c.f. QM F52279) with;							
CMN 40906	v25				post trunk	608	2,385
FHSM VP-2187	v-40				trunk	397	627

Table 8-3: Vertebral measurements and estimated body mass for lamniform cf Cretoxyrhinidae vertebrae. Comparison of the diameter of the Queensland vertebra (associated with QM F52279) with different parts of more complete Cretoxyrhina specimens provides a range for the possible size of that specimen (see text for explanation). TL, total length; BoM, body mass. Lengths in mm, mass in kg.

ratio of 0.99, whilst a caudal vertebra (FHSM VP2187, "v-185") had a height to width ratio of 1.06. The proportions of the QM vertebra appear to be most similar to a posterior trunk vertebrae ('v23') from a large specimen of *Cretoxyrhina mantelli*, CMN 40906, which has a height to width ratio of 1.09 (Shimada et al. 2006). The total length of CMN 40906 was estimated at between 6.4 and 7.0 metres; assuming a median value of 6.7 m, and comparing the dimensions of the Queensland vertebra with this provides an estimate for total length (TL) of 6.08 m for the QM F52279 shark (Table 8-3). Alternatively, if the measured vertebrae is assumed to represent the largest vertebra in the axial column (i.e., an anterior trunk vertebra, then comparison with FHSM VP-2187 (Shimada 1997b, 2008, Shimada et al. 2006) yields an estimate of TL for the QM F52279 shark of 3.97 metres. These probably represent upper and lower estimates for the body size of the Queensland shark, although the laterally compressed shape of the vertebra argue against them being from the anterior trunk and the actual size may be closer to the maximal figure.

Even a minimum size of 4 metres is a large shark, and may justify referral of these vertebra to *Cretoxyrhina* as this is the largest cretoxyrhinid shark known from the mid-Cretaceous. On the basis of articulated specimens from the Niobrarra Chalk, Shimada has suggested that *Cretoxyrhina* had a body shape most like the white shark

Carcharodon (Shimada 1997a, b, Shimada et al. 2006). Length-weight data from large *Carcharodon* (Kohler et al. 1996) indicates that a 3.97 m individual is predicted to have a mass of 627 kg: although a >6 metre animal is slightly larger than the largest animal measured by Kohler et al. (~5.1 m), the predicted mass of a 6.08 m white shark is 2,385 kg (Table 8-3).

QM F52279 itself represents a small *Kronosaurus*, with a calculated total length of 5.9 metres and an estimated mass of 1.9 tonnes (Chapter 6). As argued for QM F51291, it is substantially smaller than 7 metres and appears to represent a juvenile or sub-adult animal.

Interpretation

A key question to the interpretation of this fossil is whether the association between the pliosaur and the shark is a result of feeding behaviour or post-mortem taphonomic processes. As outlined in the earlier description of QM F52279 (Chapter 4), some aspects of this specimen suggest that the depositional environment had slightly higher energies than are typical for the Toolebuc Formation: grain size of the matrix is large, and on the ventral surface includes fragments of inoceramid shells that do not appear to be in situ, and a bone that may be the atlas-axis is preserved in the right temporal fenestra. This, together with the fact that none of the shark vertebrae that can be seen at the surface of the fossil are lying within the jaws of the pliosaur, was interpreted as arguing against this association being the result of feeding behaviour – at least, of the pliosaur feeding on the shark – and more likely the result of post-mortem association.

However, these results must be considered to be preliminary, as the sedimentological context of the specimen has yet to be examined in detail. It is also possible that more vertebrae from the shark lie within the mouth of the pliosaur, and CT scanning of the specimen may reveal additional data. Whilst QM F52279 cannot at this time be considered strong evidence of trophic interactions between a small pliosaur and a large shark, it is also true that post-mortem association of large vertebrates in the Toolebuc Formation appear to be rare – I am not aware of any documented instances beyond the possibility of QM F55279. For the present discussion, the

specimen is interpreted as a possible record of feeding behaviour, although who may have been feeding on whom is not immediately clear.

Discussion

The five specimens described above suggest a broad dietary range for *Kronosaurus* which included turtles, elasmosaurids, possibly sharks, and perhaps even smaller members of its own kind. Prey appears to have included the largest available, including an elasmosaurid that may have been 1 – 2 tonnes, and perhaps a shark of similar size, but also smaller animals including a 300 kg elasmosaurid and a 20 kg turtle. Of the five specimens that are potential records of feeding behaviour, only one, QM F52279, suggests an individual *Kronosaurus* that may have attacked an animal as large or larger than itself, and this fossil constitutes an uncertain record of feeding behaviour.

Even for the specimen that preserves the smallest prey relative to the predator, QM F10113, it is perhaps questionable whether even a 8.5 m pliosaur would attempt to swallow a 60 cm long turtle whole. The highly fragmented preservation of the carapace within the pliosaur's abdominal region suggests that the turtle was subjected to crushing bites before being swallowed; given the damage evident upon the turtle it is certainly possible that the prey was processed into smaller pieces before ingestion. As a tactic for processing prey, twist-feeding requires that the prey is large enough, relative to the predator, to have sufficient inertia so that the predator can 'twist-off' bite sized portions; the turtle was probably too small for twist feeding, but may have been processed through shaking or simple biting.

Whether the 300 kg elasmosaurid was large enough for twist-feeding to be viable, or whether it was small enough to be shaken or simply 'bitten in two', is unknown: but it is considered unlikely that a 3.3–5 metre plesiosauroid was swallowed whole, even though the predator in this case appears to have been a very large *Kronosaurus*. However, the apparent articulation of a 70 cm long segment of the elasmosaurid's vertebral column, tightly associated with its presumed gut contents, does indicate the potential size of the portions that *Kronosaurus* was able to swallow. Further study of

the limestone block containing the pliosaur's stomach contents may provide additional information.

Although the shark associated with QM F52279 is potentially larger than the individual pliosaur, that this fossil represents attempted hunting behaviour on the part of the *Kronosaurus* is equivocal, although it is certainly of interest and this fossil clearly deserves further examination, particularly with regard to its taphonomy. Pending this, the fossil that provides the best evidence for predation by *Kronosaurus* upon larger animals is QM F11050, the holotype specimen of *Eromangasaurus*. Although the identity of the animal that attacked this individual is unknown, the tooth marks are inconsistent with those of a shark and suggest that the predator possessed large, robust, conical teeth; the only species known from the relevant fauna that can be a possible candidate is *Kronosaurus queenslandicus*. The size of the attacker is unknown, but since the majority of specimens of *Kronosaurus* known thus far exceed 7 m TL and 3,500 kg mass (Chapter 6) it is perhaps reasonable to suppose that it was at least of this size. The Australian Early Cretaceous elasmosaurids, although abundant, are poorly understood because of the highly fragmentary nature of most specimens, and given that the only specimen thus far referred to *Eromangasaurus* is QM F11050, consisting of a bitten skull and five anterior cervical vertebrae, its size can only be guessed at. Even for the North American Late Cretaceous elasmosaruids, generally known from better material than the Australian forms, body size is poorly understood, and species such as *Thalassomedon* and *Hydrotherosaurus* can be expected to be somewhat derived compared with the Early Cretaceous species. The South American Aptian species *Callawayasarus* is at least comparable to *Eromangasaurus* on the basis of age and region, but the body proportions of this species are also poorly known. At present, the best guess for the size of QM F11050, based upon comparison of skull length with *Callawayasaurus*, is 1–2 tonnes – a large animal, but unlikely to have been larger than its attacker.

If the taphonomic features of QM F51291 that are identified above as compression fractures have been correctly interpreted as bite marks, this fossil is of interest because it may indicate inter-specific aggression between individual *Kronosaurus*. As for QM F11050, the shape of the fractures suggest a conical-toothed rather than blade-toothed attacker, leaving another *Kronosaurus* as the only potential candidate.

Using modern species of large predatory reptile as a guide, the motivation for the attack may have been territorial rather than feeding, although straightforward cannibalism is well documented in crocodilians and varanids (Auffenberg 1981, Ross and Garnett 1989), especially between animals of different size classes, and given that QM F51291 is the smallest individual of *Kronosaurus queenslandicus* found so far predation by a large adult is certainly a possibility. Alternatively, QM F51291 may represent a size at which sub-adult animals sought to establish territories.

Taphonomic evidence of diet is an important line of evidence for reconstructing feeding ecology in extinct species, and it is usually the only direct evidence of diet available. As such, it complements reconstructions based upon evidence of functional morphology, and can be used to test functional hypotheses of diet. In some instances, the taphonomic data serves as a reminder to avoid overly deterministic interpretations of morphology: an example from Australian plesiosaurs is the gut contents of elasmosaurids – from morphology reconstructed as predators of nektonic fish and cephalopods – that indicate a diet including a large proportion of benthic molluscs and crustaceans (McHenry et al. 2005). If the five instances described above are all accepted as evidence of predation by *Kronosaurus* on various types of prey, then the taphonomic data broadly agrees with the argument made from functional morphology; all of the prey are nektonic vertebrates, and with one possible exception are smaller than the predator. This broadly agrees with taphonomic data of diet from other species of large pliosaurid; stomach content data suggests a diet of relatively smaller prey, especially nektonic cephalopods (Martill 1992), but with some evidence for scavenging upon large vertebrates (Taylor et al. 1993), while bite marks on the bones of plesiosauroids suggest feeding upon some species that are large in absolute terms but still smaller than the presumed pliosaurian predator (Clarke and Etches 1991).

However, caution is also required when interpreting taphonomic data. Bite marks constitute good evidence of feeding behaviour, but even if the identity of the attacker can be ascertained (often, on the basis of a very short list of potential candidates), the size of the predator is usually unknowable. Stomach content preserves better information of the identity and size of predator and prey, but represents only a snapshot of feeding behaviour and should not be interpreted in a restrictive sense.

The other observation to be made about fossilised stomach contents is the obvious one: whatever feeding behaviour they seem to indicate, the predator invariably died soon after, and whether that behaviour was typical or even viable for that predator is thus open to question.

8.3 A reconstruction of feeding ecology in *Kronosaurus queenslandicus*

Kronosaurus as a crocodile

The similarity between the skulls of pliosaurs and crocodiles has been remarked upon ever since modern science started to study the two groups. Both groups have robust crania that are of limited height and are sub-triangular in dorsal view: the mandibles are joined in a strong anterior symphysis, have deep sockets for the articulation of the quadrates, and a strong retroarticular process for attachment of the jaw muscles. The teeth are conical and also robust. Both groups include taxa with long, relatively narrow (longirostrine) jaws and sharp, needle-like teeth; species with medium (mesorostrine) length jaws that are broader and have more robust teeth; and even species with relatively short (brevirostrine) snouts. Even the etymology of the name 'pliosaur' ("nearer reptile") originates from Richard Owen's observation that these animals resembled crocodiles even more strongly than did their plesiosauroid relatives.

The crocodiles that take the largest prey are the mesorostral taxa; *Crocodylus porosus*, *C. niloticus*, *C. palustris*, *C. acutus*, and *Melanosuchus niger*. These are all large species, with maximum body lengths exceeding 4 and even 5 metres, but even relative prey size is impressive and it is likely that all of these species are capable of taking terrestrial mammals that are larger than themselves (Ross and Garnett 1989). In terms of their overall skull proportions, these species of crocodiles are cited as the closest analogues to species of large pliosaur such as *Pliosaurus*, *Liopleurodon*, and *Kronosaurus* (Ellis 2003).

The skull of these mesorostrine crocodiles is widely viewed as the acme of jaw power in modern reptiles, and yet from biomechanical principles the lower height and elongated snout is quite different to the morphology that is predicted to maximise resistance to the bending loads incurred by biting (Busbey 1995). For that, a shorter, higher vaulted skull is predicted, i.e. more like that of *Tyrannosaurus rex*. These predictions, based upon classical beam theory, are supported by low resolution finite

element modelling (McHenry et al. 2006). Similarly, suggestions that the flattened 'platyrostral' condition in mesorostrine crocodilians is a response to the torsional loads incurred during twist feeding is contradicted by results from beam theory and finite element analysis (Busbey 1995, McHenry et al. 2006). An alternative explanation for the platyrostry is that it reduces drag during the rapid, laterally directed strike ('lateral sweep') of the jaws used by many species of crocodilians to catch fish and other small, agile aquatic prey, and that rather than being optimised solely for the structural loads incurred in feeding on very large animals, crocodilian skull morphology is thus constrained by the hydrodynamics of feeding on small prey (Busbey 1995, McHenry et al. 2006).

The generally low profile of the skull in large pliosaurs suggests that similar selective forces may have applied to them. However, they may also have been some important differences. Modern crocodilians are generally characterised as ambush predators, and when hunting fish they attack from a 'standing start', i.e. with low overall body speed, even though the sideways acceleration of the head and jaws can be rapid. This contrasts with the 'pursuit' predation used by many oceanic odontocetes, in which a large component of forward motion is coupled to any yaw or pitching of the jaws required to catch the prey. In terms of the hydrodynamics involved, this means that the drag forces involved are likely to be quite different; mesorostrine odontocetes generally have narrower jaws than mesorostrine crocodilians, and the increased forwards directed vector of movement may be related to this. The different types of movement during hunting are likely to be linked with habitat; crocodilians inhabit restricted waterways, often with low visibility, that have limited opportunities for pursuit, whilst odonocetes typically hunt in open water habitats. In this regard, pliosaurs are likely to have been more similar to odontocetes and thallatosuchian crocodilians (Section 8.1), and the relatively narrower (compared with a mesorostrine crocodilian) anterior rostrum of *Kronosaurus* is similar to the proportions of a mesorostrine odontocete (see below). At the same time, the anterior snout of *Kronosaurus* is relatively taller than that of a mesorostrine crocodilian or odontocete. If pliosaurs were pursuit predators, as suggested by their overall body shape (Massare 1988), then the narrower, taller snout may represent an adaption to increase the resistance of the rostrum against bite forces that does not compromise the hydrodynamic performance of the snout during feeding. The interactions of

forwards motion, sideways motion, speed, and the absolute size of the jaws is likely to be complex and further work on this aspect of skull hydrodynamics is required. Skull hydrodynamics are undoubtedly an important part of the selective pressures affecting skull shape, but unfortunately lie beyond the scope of the present work. The biomechanical analysis presented in this thesis concerns the structural mechanics involved with feeding on large prey, using the behaviour of modern crocodilians as a guide. In particular, crocodilians employ a unique behaviour, twist feeding, which is used to subdue and process large prey, and previous work on pliosaur functional morphology has speculated upon whether pliosaurs may have been capable of similar behaviour (Taylor 1992, Taylor and Cruickshank 1993). In particular, the enlarged pterygoid flanges of crocodiles, which tightly abutt the medial surface of the mandibles and are covered with hyaline cartilage, have been interpreted as reinforcing buttresses that resist the torsional forces imposed upon the mandibles during twist feeding (Taylor 1992, Taylor and Cruickshank 1993). Pliosaurs do have pterygoid flanges (Taylor 1992, Taylor and Cruickshank 1993, Chapter 4), but in the large mesorostrine taxa they are smaller than in crocodilians and this has been interpreted an indication of reduced capacity to resist torsional loads (Taylor and Cruickshank 1993). However, the pterygoid flanges have alternatively been explained as a brace against the significant medial component of the jaw adductor forces that result from the low profile of the skull (Busbey 1995), an explanation supported by finite element analysis (Ingle 2007), and given the relatively lesser medial component of jaw reaction forces in *Kronosaurus* (Chapter 7) the smaller pterygoid flange may simply correlate with the increased height of the temporal region. Finite element analysis does suggest that the skull of *Kronosaurus* has a lower resistance to twisting loads (Chapter 7), but given that the contact between mandible and pterygoid flange was fixed identically in the *Kronosaurus* and *Crocodylus porosus* models this cannot be a result of the morphology of the pterygoid flanges, and is due to other aspects of skull shape.

Although much attention has been focused upon the performance of the skull in pliosaurs and crocodiles under torsional loads, twist feeding involves the whole of the skeleton and thus postcranial anatomy is also important. The neck of crocodiles offers flexibility in the lateral direction, allowing the neck and head to be flexed to the side, but the morphology of the cervical ribs and zygapophyses prevents rotation

of the cervical vertebra around the long axis: the head can only be twisted by rotation at the occipital-cervical joint, which is well braced by the neck muscles. Axial rotation of the neck is potentially dangerous because of the potential for damage to the spinal chord, and the bracing of the neck in crocodilians reflects the need to prevent vertebral rotation when the head is subjected to high torsional loads during twist feeding. In *Kronosaurus*, the cervical ribs are not as elongate as those of crocodilians, but the zygapophyses of the cervical vertebrae are robust and aligned in the frontal plane, which is expected to allow considerable sideways bending of the neck but prevent rotation of the neck about the vertebral axis. Rotation is possible at the occipital-cervical joint, but as with crocodilians this joint was probably well braced by the neck musculature. Even for brachauchenіids, which have the shortest neck of any pliosaur, the neck is longer than that of crocodilians and it is uncertain how neck length affects bracing against torsional loads; conceivably, the shorted neck and elongate cervical ribs of crocodiles may be involved with supporting the weight of the head out of water (Salisbury and Frey 2001), which is presumably something pliosaurs did not have to do.

The neck of a crocodile is important during twist feeding because it must carry the torsional moment from the rest of the body forwards to the skull. An important point is that moments required to impose torsional forces upon the prey are not generated at any of the cervical joints, but rather from whole-body movements whereby the axial column, especially the trunk and the tail, uses a coordinated series of undulations to spin the whole animal about its long axis whilst holding the prey securely in the jaws. In this, the elongate body form of the crocodile, which is relatively narrow width for its length, in undoubtedly an important factor. The importance of the long, powerful tail in swimming may be a preadaptation that allows powerful movements of the tail to drive the whole-body twisting movement; during twist feeding, the legs are tucked against the side of the torso, minimising drag, and the small second moment of inertia in transverse axis is probably important in allowing the crocodile to accelerate quickly to high rotational velocities. Because twist feeding works by applying torsional loads to an animal or carcass with high interia, the speed with which the torsional moment is generated and applied is critical to its effectiveness – when both predator and prey are floating in water, a twist applied at a slow rate of turn will simply result in both animals rolling around.

This in mind, it is questionable whether pliosaurs had a body shape that was at all suited to the use of twist feeding. Unlike crocodiles, the large pliosaurid and brachaucheniid pliosaurs – *Pliosaurus*, *Liopleurodon*, and *Kronosaurus* – had a compact body form, with a short, barrel-like torso. In particular the tail was very short: in pliosaurs, locomotion was powered by the limbs and morphology of the four large, paddle shaped limbs reflect that role. In a large *Kronosaurus*, the span of the hind limbs probably exceeded 5 m, and the morphology of the shoulder and hip joints do not suggest that the limbs could have been adducted against the body. In addition, the enlarged ventral girdle elements and robust array of gastralia in plesiosaurs are generally considered to have prevented extreme flexion of the torso; combined with the large size and interia of a 10.5 m, 11,000 kg *Kronosaurus*, it is hard to see any way that the large pliosaur could have accelerated rapidly about its long axis whilst holding onto a large prey item. Large dolphins can spin rapidly about their long axis, but only during rapid forwards motion and the spinning is a result of differential lift across the pectoral limbs, analogous to a rolling manoeuvre by a fixed wing aircraft: because the lift is generated by the forward movement of the foil through the fluid it is impossible to generate this movement when 'hove to' next to a floating carcass. Pinnipeds are capable of some whole body twisting without necessarily moving forwards, but these rotations are slower than those accompanied by forward motion and pinnipeds are in any case anatomically far more flexible than any pliosaur. In this context, it is difficult to see what relevance twist feeding may have had for *Kronosaurus*. There have been some suggestions by Taylor and Cruickshank, based upon interpretation of skull functional morphology, that the *Rhomaleosaurus* was better suited to using twist feeding than was *Pliosaurus* (Taylor 1992, Taylor and Cruickshank 1993): although these arguments based upon skull morphology are inconsistent with the results of the FEA discussed above, it may be that their conclusion remains valid as a result of the smaller skull, longer neck, longer tail, and smaller body size of rhomaleosaurids giving them the capacity to generate higher twisting moments than was possible for pliosaurids and brachaucheniids.

The fact that crocodiles are able to access terrestrial prey raises two further points. Firstly, the largest terrestrial prey are relatively larger than the crocodile, a situation that is, historically, rare for fully marine carnivores. Thus, not only are crocodiles

capable of twist-feeding, they need to in order to exploit prey larger than themselves. Conversely, the skull of *Kronosaurus* was not as suited to resisting torsional loads, and could probably not generate them to the same degree in any case, but *Kronosaurus* did not have access to prey larger than itself and thus may not have needed to use twist feeding. Shaking is best suited to prey that is too large to be swallowed whole but which is still relatively much smaller than the predator: crocodiles use it on prey that is too small for twist feeding, and leopard seals use it when feeding on penguins. For prey that is too large for shaking – in the case of *Kronosaurus*, likely to have been the larger elasmosaurs and perhaps ichthyosaurs and turtles, it is possible that the pronounced underbite at the rear of the tooth row was of functional significance. Combined with a high bite force, the underbite would have caused high shear loads on a food item held in the back of the jaws and it is possible that *Kronosaurus* may have been able to use these to simply bite its prey 'in half'. A similar scenario has been proposed for *Tyrannosaurus rex*, which has a pronounced over bite along its entire jaw line (Meers 2003). It is interesting that the underbite described here for *Kronosaurus* is also present in the other large pliosaurs *Liopleurodon* and *Pliosaurus* (Noè 2001, Taylor and Cruickshank 1993), and if validated by further study this strategy may have represented a 'pliosaurian' approach to rending large prey into swallowable pieces.

The second point that is linked to the terrestrial nature of crocodiles' largest prey is that this very fact is exploited by crocodiles when killing large mammals; a favoured tactic is to drown the prey. In this case, the importance of bite force and skull strength is unclear: the crocodile's skull and jaw muscles simply need to be strong enough to hold the prey firmly for long enough to drown. Although crocodiles can undoubtedly inflict severe trauma upon a range of animals, it is also true that the drowning tactic does not require trauma to be inflicted for a successful kill to be made. Although it is unclear how this observation might affect reconstructions of killing behaviour for *Kronosaurus*, this tactic actually work on any air-breathing animals, as killer whales appear to use drowning as one way of killing large whales (Jefferson et al. 1991).

One final aspect of crocodilian skull mechanics deserves mention. As described in Chapter 6, the skulls of the largest species of crocodilian appear to undergo extreme

allometric increase in skull width, height and mass in very large individuals, a trait seen in some other species of reptile and which has been termed macrocephaly (Cann 1998, Georges et al. 2002, Legler 1981). The ecological consequences of macrocephaly in crocodilians are unclear, but they may allow predation upon significantly larger prey than is possible for non-macrocephalic adults, a feature which could potentially allow the exploitation of a qualitatively different niche, especially in longirostine taxa such as *Tomistoma*. However, even if macrocephalic skulls are of use in feeding on large prey, this does necessarily mean that this is the explanation, in evolutionary terms, for the origination of that pattern of growth. The need to consider that the selective forces that maintain current form may be different from the forces responsible for the origination of that form is an important aspect of evolutionary biology (Dwyer 1988). In the case of macrocephalic crocodiles, as the largest individuals of their respective species these animals are presumably all males. Male-male combat is well documented in crocodilians, particularly in saltwater crocodiles, and are violent enough to cause death; in addition, many of the largest skulls in museum collections show signs of healed but extensive damage to the anterior rostrum, in some cases involving the anterior half of the premaxillae (pers. obs.), and this seems likely to have resulted from intraspecific aggression. Even if large males do attack buffalo as prey, it seems likely that the most dangerous animal for any crocodile is another crocodile and the fact that it is the largest males, usually the dominant animals in their territories, that exhibit macrocephalic growth of the skull may be linked to the pressures of sexual selection rather than feeding behaviour. There are as yet no clear instances of macrocephaly in pliosaurs, although one specimen from the Oxford Clay potentially represents a macrocephalic adult (Chapter 6): the taphonomic evidence discussed above seems to indicate *Kronosaurus* engaged in intra-specific aggression. The implications of behaviours other than feeding upon skull biomechanics and allometry in pliosaurs certainly merit further attention.

Kronosaurus *as an odontocete*

Pliosaurs are known almost exclusively from marine settings and in this regard living crocodilians make poor analogues. The range of habitats from which pliosaurs are known, from freshwater lakes and rivers to estuaries, and predominantly coastal and open marine environments, is similar to that of odontocetes, the toothed whales.

With the possible exception of the sperm whale (depending on the size of the largest pliosaurs – see Chapter 6), odontocetes also match the range of body sizes likely for pliosaurs. When considering potential ecological analogues for various pliosaurs, it is therefore tempting to compare small estuarine species such as *Leptocleidus* with species of small river dolphins such as *Pontoporia*, whilst the large pliosaurids such as *Pliosaurus*, *Liopleurodon*, and *Kronosaurus* have been compared with the top predator of modern oceans, the killer whale *Orcinus*.

Functional morphology and ecology of toothed whales

Structurally, odontocetes have an aberrant skull morphology, even by mammalian standards. The presence of a large acoustic organ (the melon) above the facial region, and the posterior location of the nares, have had major consequences on the overall appearance of the skull: in particular, the rostrum always has a low profile, whether it is broad or narrow, a condition that is termed platyrostry in crocodilians but which has presumably evolved for different reasons (i.e. accommodation of the acoustic organ) in odontocetes. The cranial cavity is also enlarged, commensurate with the high intelligence reported for many species.

Despite their anatomical oddities, odontocetes do share some morphological features with pliosaurs. The dentition is always conical, although generally isodontic, and the jaw margin always lacks festooning. The temporal group is the dominant component of the jaw musculature. In addition, there are operational similarities; odontocetes are generally denizens of open water and therefore actively pursue their prey, rather than ambushing it from a static position in restricted waterways as do crocodiles. Consequently, when an odontocete catches smaller, agile prey such as fish, there is usually a significant forwards component to the movement of the jaws through the water in addition to any sideways movement that might be necessary to complete the catch. In contrast, the movement of a crocodiles jaws in water when catching fish is believed to be almost entirely sideways. In this regard, as predominantly open water predators pliosaurs are expected to have resembled odontocetes more than crocodiles.

There are more than 70 living species of toothed whale, and whilst the ecology of some – notably, the enigmatic ziphiid beaked whales – remains a mystery, a number of species are familiar to mariners, whalers, and marine biologists and good data on

diet is available for these. Odontocetes can thereby offer an insight into the range of possible niches that are viable for a group of air-breathing marine predators, and this information is important for attempts to reconstruct the ecology of extinct analogues such as pliosaurs.

To illustrate the relationships of prey size with body size and gross skull morphology, data on diet from 12 species was compiled from various sources [(Culik 2003, Froese and Pauly 2007, Gaskin 1982) and references therein, and the cetacean species entries from the American Society of Mammologists Cumulative Index of Mammalian Species (Hayssen 2008)] and used to generate plots of prey size. Data was restricted to recorded instances of feeding upon fishes, both osteichthyan and chondrichthyan. Accounts of diet in particular odontocete species typically identify species or higher taxa taken but do not necessarily indicate the proportion of each type of prey taken, nor the size of the predator and the size of the prey in each instance. To examine the quantitative patterns of prey size in each odontocete species, the following assumptions were made: (1) prey taxa were taken in equal proportions, (2) individuals of each species of odontocete were of a 'standard' adult size, and (3) prey were of the mean length specified for respective taxa by the online database FishBase (Froese and Pauly 2007).

For each species of odontocete, records of prey taxa were converted to prey size data on the basis of body mass, applying the fisheries Length-Weight equation

$$W\,(g) = \mathbf{a} \,.\, L^{b}\,(cm)$$

using taxon specific values for **a** and **b** provided by FishBase. Ideally, data on feeding ecology should identify prey taxa to species but in many accounts only the genus, family, or even order of the prey is listed; whilst this data creates problems, omitting it can lead to bias and so mean sizes for supraspecific taxa were calculated by averaging lengths and weights for component species. In total, length and weight data was generated for approximately 2,600 species of fish and the resulting patterns of prey size were generated from these.

Odontocete species were chosen on the basis of adequate dietary data and to cover the range of body sizes in extant toothed whales. Length and size data for each odontocete species were taken from 'typical' (i.e. not maximal) values given by

Species	Family	BoM	size category	TL	rank	
					kg	relative
Orcinus orca	Delphinidae	8,000	4	9.0	1	1
Pseudorca crassidens	Delphinidae	1,500	3	5.5	2	5
Delphinapterus leucas	Monodontidae	1,100	3	5.0	5	10
Tursiops truncatus	Delphinidae	400	2.5	2.9	4	6
Sousa chinensis	Delphinidae	250	2.5	2.8	7	8
Kogia simus	Kogiidae	200	2.5	2.5	10	11
Orcaella brevirostris	Delphinidae	150	2	2.5	6	4
Delphinus delphis	Delphinidae	100	2	2.4	11	9
Lissodelphis borealis	Delphinidae	100	2	2.8	9	7
Stenella longirostris	Delphinidae	70	2	2.2	12	12
Phocoena phocoena	Phocoenidae	60	2	1.8	3	2
Pontoporia blainvillei	Pontoporiidae	30	1.5	1.7	8	3

Table 8-4: Body size and prey size rankings for selected Recent odontocetes for which prey size data is presented in Figure 8-14 and Figure 8-15. Species listed in order of body mass; 'rank' shows rankings based upon an index of prey size, for absolute (kg) and relative prey size, with '1' indicating the largest prey and '12' the smallest. Size category is based upon the log of body mass (BoM), rounded to the nearest 0.5. TL, total length. Lengths in m, mass in kg.

(Jefferson et al. 1993). Delphinids (oceanic dolphins) were emphasised (8 species – see Table 8-4) as their range of jaw and dental morphologies is superficially closest to the range seen in pliosaurs. Ziphiids and physeterids were not included as their morphology is highly derived and as deep diving, offshore bathypelagic predators their ecology is very specialised. The data on prey size was collated for each species and used to generate two plots, one showing absolute prey size (Figure 8-14) and the other showing prey size relative to the predator's (Figure 8-15). Size data was presented as mass (in kg) and grouped into size categories on a logarithmic scale (x axis); the y axis shows the number of prey taxa in each prey size category as a proportion of the total number of fish taxa in the diet.

Figure 8-14 shows the results for absolute prey size, with the odontocete species ranked according to an index of prey size taken. The range of prey taken by each species is predominantly smaller than the predator's own body size: only the killer whale *Orcinus* takes relatively larger prey and only two other species (the harbour propose *Phocoena* and the Franciscana river dolphin *Pontoporia*) take prey of their own size class. The size range of prey taken is broad for all species; the minimal difference

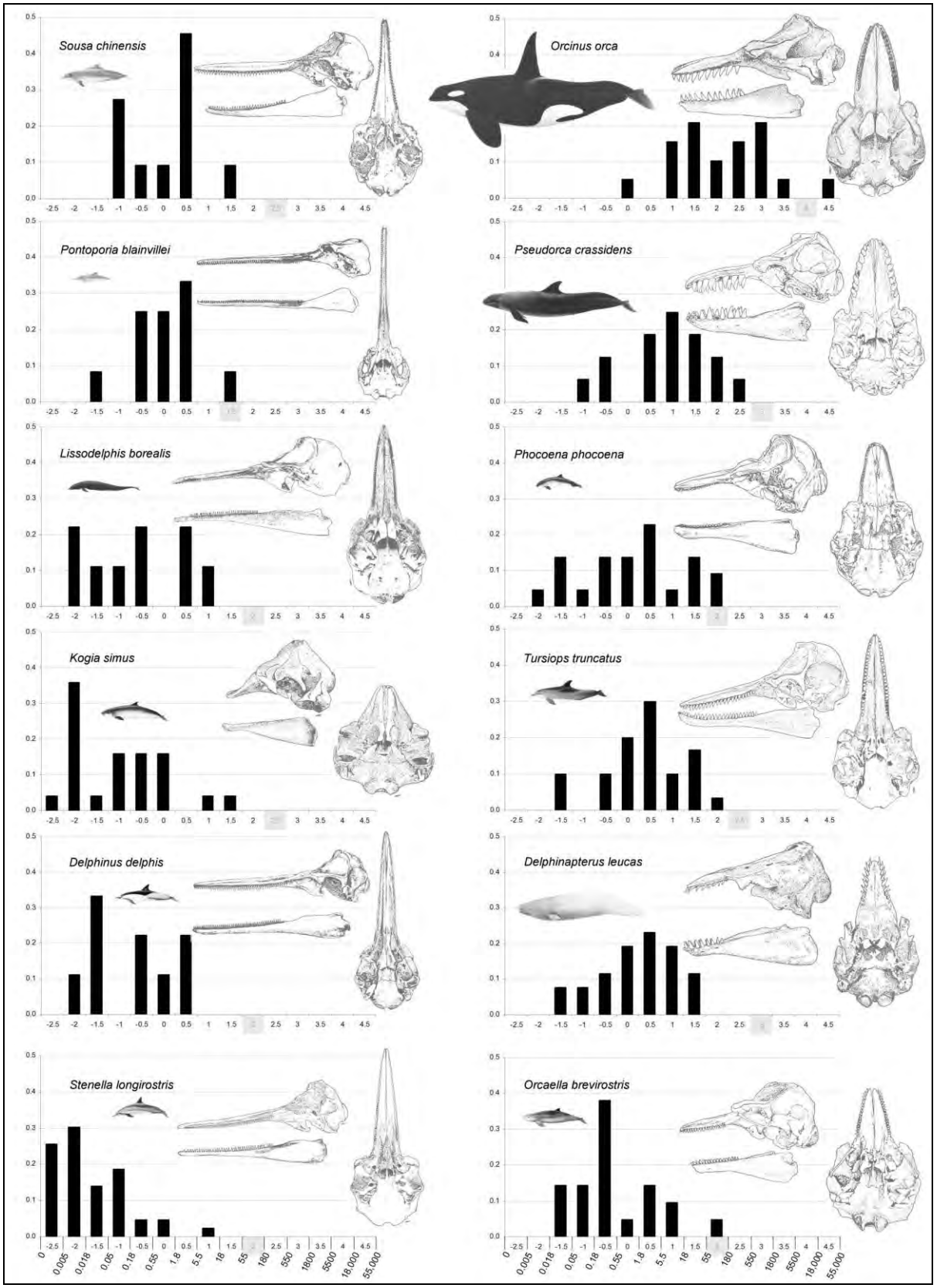
Sousa chinensis
Orcinus orca
Pontoporia blainvillei
Pseudorca crassidens
Lissodelphis borealis
Phocoena phocoena
Kogia simus
Tursiops truncatus
Delphinus delphis
Delphinapterus leucas
Stenella longirostris
Orcaella brevirostris

Figure 8-14 (facing page): Absolute prey size in selected species of Recent odontocetes (listed in Table 8-4). The charts are arranged in ascending order (bottom to top, left to right) of a simple prey size index. For each chart, the y axis shows the proportion of prey taxa in each size class (represented by one black bar) out of the total number of prey taxa taken by that species of odontocete. For all charts, the numbers on the x axis indicate the size category (based upon log prey mass in kg) of the prey taxa. Greyed rectangles on the x axis of each chart indicate the body size category of the respective odontocete. The values given at the bottom of the figure, underneath the x axis for *Stenella* and *Orcaella*, indicate the boundary values for adjacent categories, in kg of prey mass. Body profile of each odontocete species are to scale (using the values for total length listed in Table 8-4). Lateral and dorsal views of the skull are not to scale: both body profiles and skull drawings taken from Jefferson et al. (1993). See text for data sources and discussion.

between the largest and smallest prey size is 2½ orders of magnitude (e.g. log prey mass = 0.5 to log prey mass = -2), for the common dolphin *Delphinus* and the humpback-dolphin *Sousa*, whilst the range exceeds 3 orders of magnitude for most other species and is 4½ for *Orcinus* (i.e. the smallest prey of killer whales is 1/30,000th the size of the largest). The rank for each species tends to match body size, i.e. larger odontocetes take larger prey, but there are some notable exceptions; the white whale *Delphinapterus* is the third largest species but ranks fifth according to prey size taken; *Pontoporia* and *Phocoena* are the two smallest species but rank 8th and 3rd respectively; the dwarf sperm whale *Kogia simus* is the sixth largest species but ranks tenth. Interestingly, these exceptions involve all of the non delphinid species, and ranks within the delphinds follow body size very closely, with only the Irrawaddy dolphin *Orcaella* ranking above a larger delphinid (*Sousa*): this suggests that phylogenetic history is an important component of the ecological signal.

In the plot showing relative prey size (Figure 8-15) the very smallest prey have been merged into a single category, '10', which indicates prey less than 0.0005 the size of the predator. Prey of the predator's own size class is shown as category '3'. Rankings according to an index of relative prey size show similarities to the ranking based upon absolute prey size; *Orcinus* takes the largest prey and the spinner dolphin *Stenella longirostris* the smallest. However, there are some differences between the two sets of rankings; *Phocoena* and *Pontoporia* are the highest ranking species behind *Orcinus*, whilst *Kogia* and *Delphinapterus* are the lowest ranking behind *Stenella*. Within the

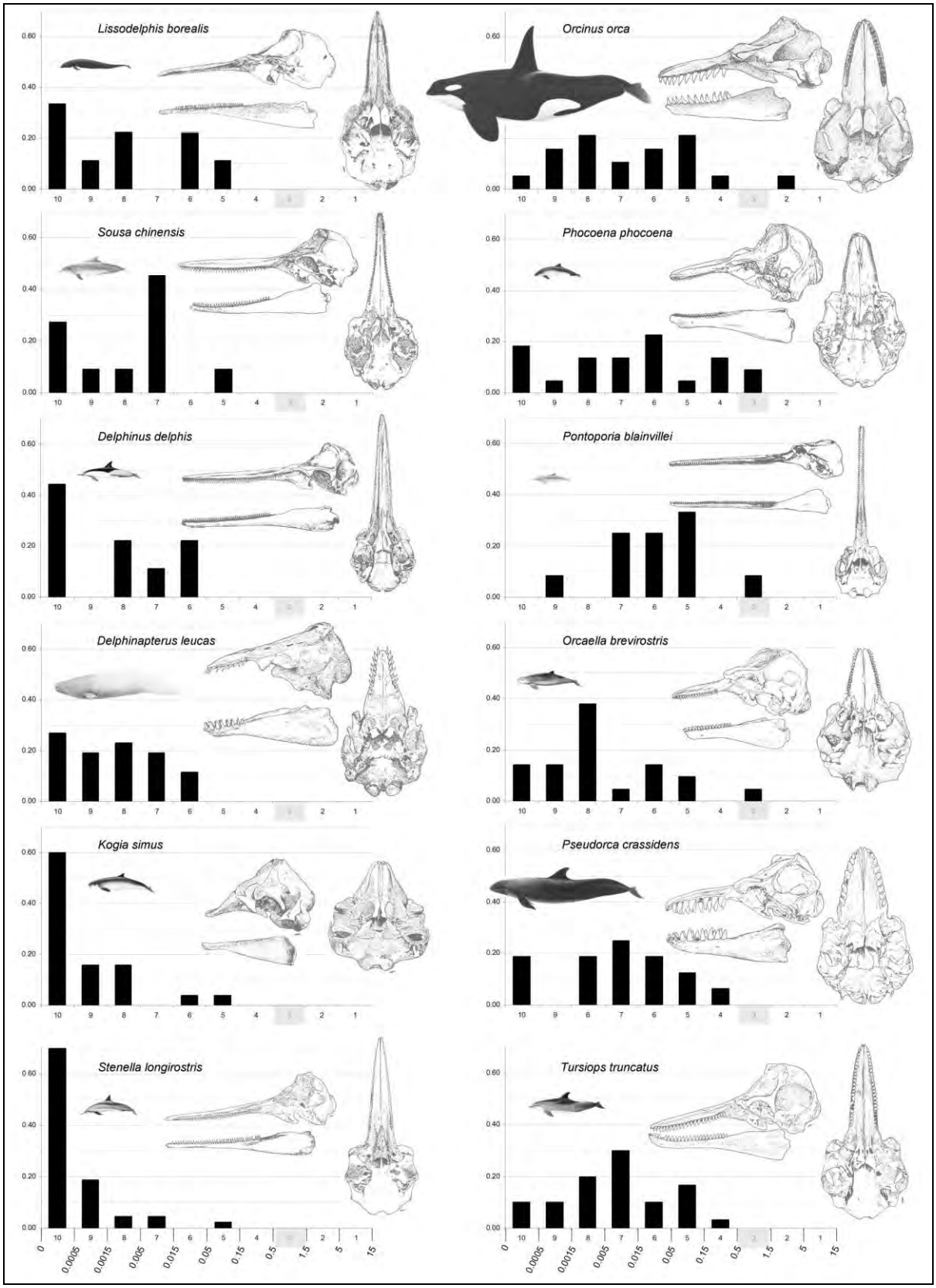
Lissodelphis borealis
Orcinus orca
Sousa chinensis
Phocoena phocoena
Delphinus delphis
Pontoporia blainvillei
Delphinapterus leucas
Orcaella brevirostris
Kogia simus
Pseudorca crassidens
Stenella longirostris
Tursiops truncatus
0.60
0.40
0.20
0.00
10 9 8 7 6 5 4 3 2 1
0 0.0005 0.0015 0.005 0.015 0.05 0.15 0.5 1.5 5 15

Figure 8-15 (facing page): Relative prey size for the toothed whales shown in Figure 8-14. The charts are arranged in ascending order (bottom to top, left to right) of a simple index of **relative** prey size (compare with Figure 8-14 – rankings also listed in Table 8-4). For each chart, the y axis shows proportions of prey taxa in each size class taken out of the total number of prey taxa taken by that species of odontocete. For all charts, the numbers on the x axis indicate the **relative** size category, based upon the difference between the log body mass of the predator and the log body mass of the prey, in kg. Greyed rectangles on the x axis of each chart indicate the body size category of the respective odontocete (arbitrarily set to 3). The values given at the bottom of the figure, underneath the x axis for *Stenella* and *Tursiops*, indicate the boundary values for adjacent categories, as proportions of predator body mass. Body profile of each odontocete species are to scale (using the values for total length listed in Table 8-4). Lateral and dorsal views of the skull are not to scale: both body profiles and skull drawings taken from Jefferson et al. (1993). See text for data sources and discussion.

Delphinidae, the false killer whale *Pseudorca* ranks behind *Orcaella* and *Sousa* drops a place behind *Lissodelphis*.

Of particular interest from a functional perspective, the overall proportions of the snout appear to correlate with relative prey size. Killer whales have robust jaws and large teeth and take the largest prey relative to their own size; spinner dolphins have elongate, narrow jaws with large numbers of small teeth and take a very high proportion of small prey. Functional relationships between snout shape, dentition, and prey size have been suggested for crocodilians, odontocetes, and various extinct groups (Berta et al. 2006, Busbey 1995, Ellis 2003, Massare 1987, McGowan 1991, McHenry et al. 2006, Taylor 1987) but are rarely examined qualitatively. Within the delphinids, the correlation between relative prey size ranking and rostral morphology is striking; only *Pseudorca* and *Delphinus* appear to be slightly out of sequence. The skull used to illustrate *Delphinus* is the long snouted form *Delphinus capensis*, whilst the dietry data includes data from all three of the variants of *Delphinus* that are currently recognised as separate species. For *Pseudorca*, although false-killer whales take a large proportion of large pelagic fishes, particularly scrombroids and dolphinfish (Stacey et al. 1994), this species does hunt marine mammals, mainly smaller delphinids (Culik 2003) but with one recorded instance of an attack on a humpback whale (Jefferson et al. 1993). As with *Orcinus*, data based upon predation on fishes underestimates the proportion of relatively larger prey taken, and it is therefore quite possible that the fit between relative prey size ranking and overall snout shape is better than indicated by the data presented here.

For functional hypotheses of fits between snout shape and relative prey size, the non-delphinid species are illuminating. *Phocoena* takes relatively large prey, but it is itself a small animal and in terms of absolute size the prey base is very similar to that of the much larger (and sympatric) bottlenose dolphin *Tursiops* [this is of interest given documented instances of aggression by bottlenose dolphins against harbour porpoises which do not appear to represent feeding behaviour and may thus represent competition for a similar set of resources (Patterson et al. 1998, Ross and Wilson 1996)]. For both species, the largest fish taken is the North Atlantic cod *Gadus morhua*, which can reach 2 m TL, but whether a 2 m harbour porpoises take 2 m long cod is questionable and this example reveals the limitations of using average and discontinuous data to analyse patterns of prey size. Nevertheless, prey of a given size is relatively larger for a harbour porpoise than for a bottlenose dolphin, and the shorter, broader snout of the former is consistent with a functional link between snout morphology and relative prey size.

For their size, both white whales *Dephinapterus* and dwarf sperm whales *Kogia simus* take relatively small prey and yet have relatively short, broad snouts. *K. simus* feeds on small bathypelagic fishes and cephalopods associated with continental slopes; lanternfish (Myctophidae) are an important part of the diet (Nagorsen 1985). Relative to skull size, the rostrum of *Kogia* is the shortest of any odontocete and rostral morphology is correlated with the 'suction' mode of feeding used to catch prey (Bloodworth and Marshall 2005). *Delphinapterus* takes a large variety of pelagic fish but also takes a large proportion of benthic invertebrates: the large size of *Delphinapterus* may allow it to exploit polar habitats that are not available to species such as *Phocoena* that take a range of similarly sized prey (Stewart and Stewart 1989). *Delphinapterus* also uses suction feeding (Bloodworth and Marshall 2005). As emphasised earlier, functional explanations of skull morphology are valid only for species with similar feeding strategies, and the hypothesised association of prey size with rostral shape is based upon predators that use 'ram feeding' (i.e. the prey is captured as a consequence of rapid movement of the jaws, rather than use of suction feeding) of agile aquatic prey (McHenry et al. 2006). Predators that use suction feeding, or that feed upon less agile prey such as benthic crustaceans (or, as in the case of *Delphinapterus*, both) would therefore not be expected to show the same

relationships of snout shape to relative prey size that are evident in the ram feeding oceanic delphinids.

The idea that rostral morphology correlates with prey size, at least in ram feeding piscivores, is at odds with the ranking of *Pontoporia* as a predator of relatively large prey. *Pontoporia* has the most elongate, narrow rostrum of any odontocete, and whilst the size range of its prey is very similar to that of *Phocoena* (Figure 8-15), there is a notable contrast in the morphology of their skulls. Like *Phocoena*, *Pontoporia* is a small animal, and the data presented here might be biased by the inclusion of Atlantic cutlassfish *Trichiurus lepturus* in the diet; although *T. lepturus* can reach lengths of 2 m, it has an eel-like body form and does not apparently exceed 5 kg body mass; however the equations used in this analysis produced an estimate of 20 kg. Compounding this, maximum reported size of *T. lepturus* eaten by *Pontoporia* is 80 cm, i.e. 390 grams (Bassoi 2005). After *Trichiurus*, the next size class indicated for *Pontoporia* from the data presented in Figure 8-14 and Figure 8-1 is 1.8–5.5 kg, which stills exceeds the maximum reported size of prey reported from analysis of stomach contents (Bassoi 2005).

These types of error illustrate the problems with attempting to analyse quantitative patterns in diet using qualitative and poorly resolved data, and for this reason the data presented here can only be considered a preliminary analysis. However, the present purpose is to provide a broad illustration of extant odontocete ecologies in order to frame a reconstruction of ecology in an extinct marine reptile, and given that there have been very few attempts to examine form-function relationships in odontocetes, the data presented here will have to suffice for now. In spite of the problems with the data, *Pontoporia* nevertheless offers some intriguing insights into the functional morphology of longirostrine marine predators. Phylogenetically, *Pontoporia* is basal to the Delphinoidea and lies within a paraphyletic grouping of odontocetes that almost exclusively inhabit large river systems and are thus known as river dolphins (May-Collado and Agnarsson 2006). *Pontoporia* is atypical for this group in that it is more common in shallow coastal and estuarine waters, although it does spend some time in freshwater (Culik 2003, Jefferson et al. 1993). One of the remarkable features of river dolphins is that they all have very long rostra, much longer than those of delphinids. This morphology does not result from a decreased

emphasis on biosonar, as the echolocation of river dolphins is regarded as highly advanced. Rather, it may correlate with habitat and locomotary mode. Rivers are more restricted habitats than oceans, and river dolphins tend to be slower swimmers that oceanic dolphins (Fish and Hui 1991). Visibility is often poor in rivers, and it is possible that this leads to river dolphins relying on a form of ram feeding (the possibility of suction feeding is precluded by the length of the jaws) that involves less of a forwards vector in the motion of the jaws, and proportionally more of a sideways vector, in a manner similar to that used by crocodilians (see above). Indeed, the jaws of river dolphins do tend to resemble those of piscivorous, longirostrine crocodilians. *Pontoporia* is generally a costal marine species, feeding in waters of less than 20 metres (Bassoi 2005), but it is does appear to spend time around estuaries where water is turbid and visibility is low (Cremer and Simões-Lopes 2005, Moreno et al. 2003); although it is also characterised as a slow mover (Cremer and Simões-Lopes 2005, Crespo and De Cidre 2005), and the functional arguments concerning the predominance of lateral vectors of movement during feeding for crocodilians and other river dolphins may also apply to this species. In this context, kinematic data on feeding for *Pontoporia* would be interesting.

Attempts to apply functional arguments to morphology should be made with caution, however (Gould and Lewontin 1979, Lauder 1995, Plotnick and Baumiller 2000), and whilst there does seem to be some correlation between rostral shape and relative prey size in the twelve species of odontocete discussed here – particularly in the delphinids – there is also a strong correlation between rostral shape and body size. This suggests that the interaction between feeding ecology, skull morphology, and size are complex and that rostral shape may be affected by non-linear processes that scale allometrically with body size. A fuller analysis, using quantitaive approaches to examine the role of scaling relationships, morphometrics, and phylogenetics is certainly warranted, and should make use of more finely resolved dietry data than has been possible here, but this is a long way beyond the scope of the present thesis. For now, we must be satisfied with a 'rough' initial summary, and use it with caution to provide insight into the possible ecology of *Kronosaurus*.

A dolphin's-eye view of the palaeoecology of Kronosaurus

The data presented above on odontocete ecology suggest the following broad patterns;

- few species of marine predators take prey of their own body size or larger.
- large marine predators (i.e. >100 kg) tend to take a broad range of prey sizes.
- smaller, longirostrine species take relatively smaller prey than do larger, shorter snouted species.

In the absence of biomechanical or morphometric analyses, comparing *Kronosaurus* to odontocetes is subjective but in terms of overall snout proportions the bottlenose dolphin *Tursiops* appears to be similar. *Tursiops* is much smaller than *Kronosaurus* and, depending upon just how important scaling is in making these sorts of comparisons, may not be an appropriate analogue, but almost nothing is known about larger longirostrine species such as *Tasmacetus* and so *Tursiops* must serve as a potential analogue for now. The data presented in Figure 8-15 suggest that *Tursiops* is a generalist that takes prey over a size range of 4 orders of magnitude, with the largest size class of prey less than half of its own body mass. The dentition of *Tursiops* is robust but does not include caniniform teeth: on that criterion, *Kronosaurus* is perhaps more comparable to *Pseudorca*. Like *Tursiops*, *Pseudorca* takes a broad range of prey, but the data shown here underestimates its maximum prey size because instances of feeding upon marine mammals are not included, and although *Pseudorca* does not exploit marine mammals to the degree seen in *Orcinus*, it is known to prey upon smaller delphinids and even baleen whales.

The killer whale *Orcinus* has been cited as an analogue for large pliosaurs such as *Pliosaurus*, *Liopleurodon*, and *Kronosaurus*. *Orcinus* is of a similar body size to *Kronosaurus* and has robust, conical, caniniform teeth, but the rostrum is shorter and broader. The extent to which rostral shape in *Orcinus*, or indeed any odontocete, is constrained by the soft-tissues involved with its biosonar has not been quantified, but given the location of the acoustic organ (above the posterior rostrum) there is presumably

some trade-off between rostral height and space for the acoustic organ. On mechanical grounds, a taller rostrum is expected to provide better resistance to the increased bending loads that are associated with feeding upon large animals. It has been suggested that the broad snout of *Alligator* confers increased resistance to bending in the face of constraints (hydrodynamic, in the case of the alligator) upon rostral height (Busbey 1995, McHenry et al. 2006), and a similar scenario is possible for *Orcinus*, but unfortunately very little is known about the biomechanics of feeding in killer whales. Instances of predation upon marine mammals, including large whales, are well documented for *Orcinus* (Jefferson et al. 1991); however, the extent to which predation upon much larger prey is enabled by the pack hunting strategies used by killer whales is also unknown. What is clear is that killer whales take a very wide range of prey, most of which appears to be smaller than itself. On balance, it seems that the same was likely true of *Kronosaurus*.

A reconstruction of feeding ecology in Kronosaurus

In seeking to understand the biology of extinct animals, we are dependent upon living species for information. Whilst limitations are usually the result of an imperfect understanding of living animals, this approach can lead to misleading conclusions if the fossil ecosystem is qualitatively different from the modern analogue. One such example involves Cretaceous and Paleogene marine tetrapod communities; Neogene marine tetrapod (mammal) communities are unusual in that the largest members are not carnivores, but plankonivores (and one teuthivore). In contrast, for the majority of time since the Early Triassic, the largest marine animals have also been the apex carnivores (see Chapter 6). This feature of Cretaceous marine systems provides limited opportunity for predation upon larger species.

Previous accounts of large pliosaurs have emphasised the more superlative aspects of pliosaur anatomy, in particular, the impressive size and apparent power of the skull and dentition. Explanations of the assumed ecology of species such as *Pliosaurus*, *Liopleurodon*, and *Kronosaurus* have made explicit comparisons with the most aggressive modern species of aquatic carnivore, such as saltwater crocodiles and killer whales. Although both saltwater crocodiles and killer whales have the ability to take prey that is larger than themselves, it is important to remember that they inhabit systems where larger prey is available to them. As far as we know, *Kronosaurus* did not.

That *Kronosaurus* was the top predator of its ecosystem is not in question. Rather, what is missing from the more superficial accounts is any consideration of what this might mean in the context of mid-Cretaceous marine ecosystems. Apart from *Kronosaurus*, the largest animals in the inland sea of Early Cretaceous Australia were a 1–2 tonne elasmosaur, an ichthyosaur that may have reached a similar size, as well as a gigantic protostegid turtle and a cretoxyrhinid shark that may have been slightly larger (perhaps up to 3 tonnes). Taphonomic evidence suggests that *Kronosaurus* did feed upon the elasmosaur, and perhaps may have had some interesting interactions of an as yet unknown nature with the shark. With their small head a top an incredibly long neck, elasmosaurs must have been a relatively simple prey to kill if they could be surprised, and the bitten skull of *Eromangasaurus* suggests that *Kronosaurus* did indeed employ the obvious strategy of simply biting off its head. Whether the more compact body-form of 2 tonne ichthyosaurs and sharks was as vulnerable seems open to question, and although *Kronosaurus* undoubtedly fed on smaller turtles, a 2–3 tonne *Cratochelone* may have been a different proposition. Letpocleidoid plesiosaurs ranged in size from 2 to 5 m and were likely to be potential prey.

Whilst prey of that general size class is, as far as we can tell with the limited comparative data available, consistent with the biomechanical and functional morphology aspects of the skull and dentition, both the elongated rostrum and comparison with living odontocetes strongly suggests that even smaller prey were most likely an important part of the diet of *Kronosaurus*. If the size range of prey taken, relative to body size, was similar to that seen in *Orcinus*, *Pseudorca*, or *Tursiops* – species which appear to be the most likely functional analogues for *Kronosaurus* – then prey as small as 1 kg (i.e. 1/10,000 its own size) probably formed part of the diet. From the data presented in the previous section, fish that are less than 1/50 of the size of the predator constitute more than half of the diet of all three of those toothed whales.

In the context of the Australian Early Cretaceous, the likely prey for *Kronosaurus* possibly included a large range of nektonic and demersal species. Large squid (> 1 m mantle length) were likely prey, but smaller squid, belemnites, and perhaps even ammonites were also probably taken. Small shoaling clupeiforms ('baitfish') are fed

on by predators of all sizes in modern oceans and were a potential food source for *Kronosaurus*. Larger teleosts of up to 3 m were also present. Perhaps the most abundant potential prey, however, particularly in the Late Albian Sea, were sharks: although one species may have rivalled *Kronosaurus* as a top predator, most species were much smaller, 3 m or less, and these may have constituted a very important component of diet for *Kronosaurus*.

Benthic invertebrates represent a potential food source that is exploited by many modern marine amniotes. Several species of odontocete, pinniped, and chelonian include a large portion of epibenthic and infaunal invertebrates in their diet, and some species have specialised on hard shelled taxa such as pteriomorph bivalves, developing specialised jaws and duraphagous dentition (e.g. the walrus *Odobenus*). There is no indication of such specialisation in *Kronosaurus*: however, many species of odontocetes and pinnipeds are known to take benthic prey, especially crustaceans and in particular larger species of decapod (Culik 2003), and *Kronosaurus* may have been similar in this respect.

Whether the elongate rostrum of a 10 tonne pliosaur is analogous in any way to the elongate rostrum of a 500 kg delphinid (*Tursiops*) or a 1000 kg crocodilian (*Crocodylus intermedius*) is a question that can potentially be addressed by analysis of feeding kinematics and hydrodynamics. For present purposes, however, these species suggest that relatively small prey were mechanically available to *Kronosaurus*. It is unlikely to be a coincidence that this is more or less the size range of prey that coexisted with *Kronosaurus*.

There is no mechanical evidence that *Kronosaurus* was a large prey specialist, and there was in any case no ecological opportunity for it to have been so. Despite its size and apparent ferocity, attempts to reconstruct its palaeoecology with reference to species such as *Allosaurus*, *Carcharocles*, and *Smilodon* – all of which are likely to have been regular hunters of much larger animals – are of questionable relevance. Even comparisons with *Orcinus* may be misleading, for while killer whales have an illuminatingly broad range of prey, their ability to feed upon larger prey is rare in the context of the marine ecosystems over the last 250 million years. It is salutary to consider than the African lion is capable of taking larger prey than *Kronosaurus* ever

encountered. Although the skull of *Kronosaurus* is an impressive structure, we should appreciate it for what it was; a feeding apparatus that, whilst capable of taking the largest prey available, was of sufficient mechanical flexibility to allow its owner to feed upon a very large part of the ecosystem in which it lived. Large pliosaurids and brachaucheniids were the apex carnivores in marine ecosystems from the Callovian to the Turonian – a period of some 70 million years, and perhaps the longest amount of time that a single group of closely related species have occupied that role. The interpretation of the skull of *Kronosaurus* as a generalist feeding organ is consistent with that remarkable history.

Other aspects of palaeoecology

The reconstructions of feeding ecology provided in this chapter are merely one component – albeit an important one – of the palaeoecology of *Kronosaurus queenslandicus*. The ecological role reconstructed here, i.e. of an apex carnivore within its ecosystem, is a function of both the capacity of its feeding apparatus and its large body size, but body size has many other ecological consequences for a marine predator.

Some of these are discussed in Chapter 6, including the observation from living taxa that large air-breathing predators are capable of deeper dives and thus foraging at greater depths than smaller-bodied species (Schreer and Kovacs 1997). A similar capacity might thus be reasonably supposed for *Kronosaurus*, although how relevant this would have been for individuals inhabiting the Great Artesian Basin is uncertain, given that the maximum depth of the seaway was perhaps 120 m (Chapter 3), which is considered shallow in the context of deep-water foraging. Not all large marine animals are necessarily deep divers, however – the largest modern marine mammals, the balaenid and balaenopterid whales, are relatively shallow divers (Acevedo-Gutiérrez et al. 2002, Croll et al. 2001) and this is linked with the depths of their preferred food (in particular, euphausiid shrimps) (Brodie 1993). Perhaps *Kronosaurus* similarly concentrated on prey inhabiting shallower waters. Alternatively, if capable of foraging in deeper waters, it may have done so in other parts of its range where the water was deeper than in the Great Artesian Basin.

The likely presence of *Kronosaurus* outside of the GAB – after all, modern apex carnivores such as *Orcinus*, *Pseudorca*, *Carcharodon* are cosmopolitan in distribution – itself has important ecological implications. Were the individuals living in the GAB resident in territories throughout the year, or did the high palaeolatitudes of the seaway (particularly in the Aptian) require a seasonal migration within the seaway, or even to oceanic waters further away? The large body size of *Kronosaurus* is potentially important to this question also – large bodied species may be capable of travelling great distances, as demonstrated by the migrations of modern balaenopterid whales between summer feeding and winter calving grounds (Ellis 1982, Sigurjónsson 1995). Body size can also influence the timing of any long-distance travel – the largest balaenopterid, the blue whale *Balaenoptera musculus*, arrives in polar waters several weeks before any of its potential competitors for the summer krill bloom and its large body size is considered to be an important factor in this ability, as the large size allows it to thermoregulate in water temperatures that are too cold for smaller species (Gaskin 1982). Indeed, the interplay between feeding, migration, and thermoregulation may be the key factor in the evolution of such large body sizes in baleen whales. How such an interplay might have applied to *Kronosaurus* is unknown: several authors have noted the distribution of plesiosaurian fossils at high palaeolatitudes (Chatterjee and Small 1989, Cruickshank et al. 1999, Kear 2003) and have suggested that, as a group, plesiosaurs may have been capable of exploiting waters too cold for other groups of Mesozoic marine reptile, and it has even been postulated that the Southern coast of the GAB may have been a calving ground for some species (Kear 2006c), although there is as yet no evidence of these grounds including juvenile *Kronosaurus*.

The relationship between body size and reproduction is also one of potential interest for air-breathing marine mammals and reptiles. Whether reproduction involves egg-laying or live birth, for amniotes the marine environment presents a significant challenge to what is a straightforward process for non-amniotes. Egg-layers must lay the eggs out of water, requiring the gravid female to come onto land (e.g. crocodilians, turtles, penguins). Live-bearers can give birth on land (seals, sea-lions) or in water (whales, sirenians), but only the latter strategy frees the species completely from the need to be able to move out of water. The constraint of terrestrial locomotion, required for reproduction, has probably had a significant effect on the

evolutionary pathways of all of the groups that reproduce on land – similarly, freedom from this constraint has likely been a major factor in groups such as cetaceans and ichthyosaurs being able to achieve highly specialised body-forms (which are incapable of terrestrial locomotion but which are highly capable in the aquatic medium) and large body size. The question of whether plesiosaurs used terrestrial or aquatic modes of reproduction has been debated for years: plesiosaurs have a paraxial gait, and amongst marine extant amniotes there is a notable correlation between paraxial gait and terrestrial reproduction (*viz*, turtles, pinnipeds, penguins); conversely, plesiosaurs such as *Kronosaurus* far exceeded the body size of any modern marine amniote that is capable of reproducing on the land. Recent finds suggest that Triassic sauropterygians were capable of live birth (Cheng et al. 2004), suggesting that viviparity may have been primitive for plesiosaurians; it seems that a 10 tonne *Kronosaurus* would not have needed to haul itself out of water in order to breed.

Very small individuals of *Kronosaurus* are unknown, despite the high frequency of smaller marine reptiles such as the protostegid turtle *Notochelone* in the Toolebuc Formation of the Great Artesian Basin, and it is possible that juvenile size classes of *Kronosaurus* did not co-occur with the adults in this fauna. This might represent migration by newborns away from the environments frequented by the adults (as with turtles), or instead may indicate that the calving environments are not preserved in the Toolebuc and may have been situated outside of the GAB. As discussed above, the size distribution of *Kronosaurus* specimens described in this thesis suggests these were mostly adults, and that adult size may have been reached at around seven metres Total Length; the three specimens that are smaller than this size may indicate sub-adults. If the patterns of intra-specific interactions were similar to modern species such as saltwater crocodiles, then those sub-adults may have been at risk of aggression from large adults. The interpretation of the depression fractures on one such sub-adult, QM F51291, as bite marks from a larger *Kronosaurus* is consistent with this scenario but does not in itself constitute strong support for it; such a refined understanding of ecology in *Kronosaurus* will require much more data and study.

Of course, all of these aspects of the ecology of *Kronosaurus* interact with each other – that is, after all, the nature of ecology. Studies that attempt to synthesise

understanding of all the different facets of ecology for one species constitute a significant amount of work, and are rare even for living species of marine mammals and reptiles. I am not aware of any such study being applied to pliosaurs. Although there have been some informal treatments[5], even general accounts of the factors involved with the ecology and evolution of pliosaurs are lacking. However, new insights from biology and palaeontology have the potential to make an impact in this area, which promises to be a fruitful area of research for future workers.

[5] See, for example, an essay on the evolutionary and ecological pattern of large body size in marine animals; http://dml.cmnh.org/2002Jun/msg00105.html

8.4 Summary

Based upon the analysis in this thesis, the fossilised remains of large pliosaurs from the Early Cretaceous marine sequence of the Great Artesian Basin represent a single genus of brachauchenid pliosaur, *Kronosaurus*. Specimens from the Doncaster Formation and the Toolebuc Formation indicate the presence of this taxon in the Late Aptian and Late Albian epeiric seas respectively: some isolated teeth from the Griman Creek Formation may be referable to *Kronosaurus* and thus record its presence in the Early Albian Sea. Available evidence is consistent with the presence of a single species in the Late Albian, *Kronosaurus queenslandicus* Longman, 1924. The Late Aptian material is consistent with *Kronosaurus queenslandicus*, pending further study of the Colombian species *Kronosaurus boyacensis* Hampe 1992.

Analysis of 11 specimens from the Late Aptian and Late Albian of Queensland indicates a size range from 4 to 10 metres in Total Length, and 1–10 tonnes in body mass. By the criterion of the degree of fusion of cranial elements in the rostrum and circum-orbital region, smaller individuals are interpreted as immature sub-adult animals.

The reconstructed cranial morphology indicates an elongate, long-mesorostrine to longirostrine skull. The anterior rostrum is relatively narrow, but in the context of aquatic predators is not notably platyrostral and the anterior rostrum is approximately as tall as wide. The dentition is markedly anisodont, with the largest teeth in the anterior part of the tooth row. The teeth are conical, ornamented with strong longitudinal ridges, and vary in size, curvature, crown-root ratio, and ornament along the tooth row. Maximum basal skull length is 2.2 m, with a mandible length of 2.7 m. The mandibular symphysis is short, encompassing the anterior 6-7 dentary tooth positions, and of these the forward-most five pairs are caniniform and held in a spatulate anterior expansion of the dentary. Of large pliosaur taxa described to date, only *Kronosaurus queenslandicus* has four pairs of premaxillary teeth.

The post-cranial skeleton is of a compact, fusiform body shape with a short (but flexible) neck and a short tail. Presacral vertebral count is 35, including 13 cervicals

and 3 pectorals. The centra of the posterior pectorals/ anterior dorsal vertebrae have the largest diameter, with height exceeding width. Transverse processes are robust, suggesting robust ribs in the thoracic region. The femuri are longer and more robust than the humeri, and the pectoral limbs appear to have been of a lesser diameter than the pelvic. The distal limbs are hydrofoils with a high aspect ratio. Maximum total length is 10.5 metres, with a hind limb span of 5 metres and a body mass of ~11,000 kg.

Comparative biomechanical analysis suggests that bite force was large: 15–22 kN for an anterior bite, and 27–38 kN for a posterior bite, depending on the modelling approach used. For its skull volume and its body size, bite force magnitude is comparable to that of modern crocodilians. Finite element analysis indicates that, compared with a 3.1 m small adult saltwater crocodile *Crocodylus porosus*, the rostrum of *Kronosaurus* was subject to higher strains during normal bites. Similarly, when subjected to torsional and laterally directed loads that simulate the twisting and shaking behaviours used by large extant *Crocodylus* to kill and process large prey, the skull of *Kronosaurus* carried more strain than that of *C. porosus*. Based on this result, maximum prey size, relative to body size, is considered to have been smaller in *Kronosaurus* than for a 3.1 m *C. porosus*, although the actual magnitude of this limit is unknown due to insufficient data on diet in *C. porosus*. The apparent discrepancy between the bite force result, which suggest comparable sized prey, and the finite element analysis may be due to hydrodyamic factors involved with rapid adduction of a >2 m mandible.

Data from stomach contents confirms that *Kronosaurus* fed upon other reptiles and was able to process large animals into smaller pieces suitable for swallowing. Confirmed prey includes a small turtle, a small elasmosaur, a large elasmosaur, with a possible instance of a large shark. Biomechanical and functional considerations suggest that twist feeding may not have been employed to process large prey, but that the pronounced underbite in the rear half of the tooth row, coupled with large bite forces, may have allowed *Kronosaurus* to process prey through straightforward biting. There is also evidence of intra-specific aggression directed at a sub-adult, possibly by a larger animal.

Non-biomechanical comparison with the functional morphology of various species of crocodilian and odontocete suggests that the elongate rostrum and flexible neck might have allowed *Kronosaurus* to take relatively smaller prey than can *Crocodylus porosus*. General patterns in the ecology of large marine amniotes suggest that a broad prey base was likely, perhaps ranging from a lower limit of 1 kg an upper limit of 3,000 kg. Potential prey were probably nektonic and demersal, and may have included teleosts, cephalopods, sharks, and reptiles. Ontogenetic shifts in diet most likely involved an increasing proportion in relatively large prey with age. *Kronosaurus* is therefore characterised as a dietary generalist, capable of taking large reptilian prey due to its own large size and robust dentition, but with much smaller reptiles, sharks, teleosts and cephalopods comprising most of its diet.

A broad overview of the functional morphology of aquatic marine predators suggests that they operate under a pair of conflicting constraints of (1) selection for a skull morphology that allows efficient capture of small agile prey, which is predicted to be a longirostrine form, and (2) selection for a skull shape that resists the bending loads caused by biting large prey, which is predicted to be a high vaulted, brevirostral shape. A skull morphology that lies close to either one of these opposing ends of this morphological spectrum is interpreted as specialisation on small and large prey respectively. The playtrostral, mesorostral skull of extant carnivorous odontocetes and crocodilians is interpreted as a biological trade-off between these conflicting requirements. In *Kronosaurus*, a different pattern of trade-off is achieved involving (1) an elongate mesorostral to longirostral skull, (2) an array of caniniform teeth placed relatively far forward in the jaw, (3) a robust dorsal median ridge on the rostrum that acts as a dorsal compression member, and (4) a high bite force. This functional complex requires complex patterns of growth in the orbital and rostral regions of the skull that result in an osteology exhibiting pronounced ontogenetic variation.

Maximum body size of *Kronosaurus* is estimated at 10.5 metres total length and approximately 11,000 kg mass. This size class is consistent with the maximum size of apex marine predators in neritic environments from the Middle Triassic to the Recent. Estimates of body size that are significantly greater than this class may indicate a qualitatively different niche, as with modern mysticete whales and the sperm whale *Physeter*.

8.5 Concluding remarks

Dinosaurs and other extinct reptiles excite a sense of wonder and curiosity that seems almost universal. This thesis is an attempt to give a scientific context to the question asked by five-years olds all over the world when faced with images of prehistoric monsters: what did they eat? In this respect, some progress has been made, but many more questions raised – this is the nature of science (Pirsig 1974).

It also represents a personal journey that, whilst perhaps unconventional in some respects, has provided me with the opportunity to indulge my curiosity for the rich diversity of biology. For as long as I can remember, I have been fascinated by the sea and the organisms that inhabit it – a trait I seem to have inherited from my father. As a student, the first glimpse I got into the excitement and creativity of doing science was with evolutionary biology, and this too has remained with me. Although fascination with Darwin's legacy is hardly unique, in my case I became particularly interested at an early stage in one of the fundament questions of biology, the relationship between structure and function. If nothing else, this thesis has provided the opportunity to explore all of these interests.

Kronosaurus is itself, of course, an amazing animal that has for a long time been the subject of a lot of talk and not much actual study. When I started my initial graduate studies, in 1994, I had high hopes of redressing that sate and of providing a comprehensive – indeed, the definitive – account of the anatomy of this species. Unfortunately, along the way I have been forced to relinquish this goal: I found the material too logistically challenging, and there is so much of it, that all I have been able to do in the present work is provide a summary and review of the most important specimens. In this thesis I have almost completely ignored the osteology, and although I have of necessity collated some information on this aspect, there is not space here to do it justice and in any case there are still a great many questions about particular details. I regret to say that the descriptive anatomy of *Kronosaurus* remains as urgent a task now as it was when I first set eyes on the material, and I can only hope that the information contained in this thesis will help to provide some sort of context for that work.

The reconstruction of the skull geometry of *Kronosaurus* provided in this thesis is inevitably wrong – some of the inaccuracies are listed in Chapter 5, and there are certainly more that I am not currently aware of – but it is a first attempt and hopefully it is close enough to the actual shape to be useful. However, I believe that it is less wrong than previous reconstructions and is therefore a step in the right direction; I hope that this reconstruction will be refined as part of future work, as anything else can be taken as an indicator of stagnation in this field.

The biomechanical approach used in this study is part of a growing body of work that is using this method in palaeontology, and quite simply it is very exciting to be involved with that work. In particular, the opportunity to be involved with developing some of the techniques along with my colleagues in the Computational Biomechanics Research Group (CBRG) has been a privilege. I think that it is clear to anyone that has experience of the biomechanical approaches used by the CBRG and other groups around the world that these tools offer a truly exciting potential for the science of palaeontology and our understanding of the lifestyle of animals that we can never see for ourselves. However, whilst enthusiasm for these techniques is certainly warranted, it would be unfortunate if a new, powerful, computer based tool achieved a hegemony within its broader discipline. As a cautionary tale, I offer the example of the advent of cladistic tools within the field of phylogenetics over the last two or three decades. My own view is that cladistic approaches encompass some useful ideas but are also subject to some fundamental problems; however, the near complete dominance of cladistics within the discipline of phylogenetics appears to have stifled debate and critical review of the strengths and weaknesses of the method. Of course, science is like any activity conducted by humans and quality varies enormously, and whilst there are certainly some studies that use cladistics in an intelligent and sensible manner (fortunately, some of these even involve plesiosaurs), there seem to be a great number that apply the method more-or-less robotically, apparently with suspension of all critical faculties. I cannot believe that the overwhelming focus on one particular approach to phylogenetics has not contributed to this state. Consequently, I would urge anyone and everyone involved with functional morphology and particularly biomechanics to be watchful against the apparent dominance of any one method, and I worry that, if applied uncritically,

finite element analysis may fall into the same trap that I think cladistics did. For biologists and palaeontologists, FEA is a genuinely exciting tool that offers enormous potential for the understanding of the complexity of biological structures, and I would certainly not want to undersell its value. But it has limitations and problems – some of them potentially very profound – and we must always be mindful of these. My hope is that functional morphologists continue to use the whole range of methods that have been brought to bear on the question of biological form and function, and that FEA simply becomes another tool in the kitbag, albeit a particularly useful one. Indeed, that is the approach that I have attempted to use in this chapter.

In my experience functional morphologists are all splendid, intelligent people who enjoy pluralistic approaches, and with luck these concerns will prove unfounded. These leaves one further issue, which I am more certain will have to be faced. It is clear to me that, no matter how complex and apparently intractable the biological structure at the heart of a functional morphological analysis may seem, the techniques available have now advanced to such a degree that the limiting factor will inevitably be the biological knowledge required to interpret the results. For just about every group of living animals, the crucial aspects of anatomy, physiology, behaviour, and ecology, all required to provide a proper framework for palaeobiological analyses, are limited or non-existent. This means a couple of things; firstly, palaeobiologists have always had to be familiar with living groups, even to the extent of conducting the primary experimental or observational studies upon them, and this will only continue. However, the breadth and detail of information required to properly interpret palaeobiomechanics is such that palaeobiologists will also need to develop effective working relationships with other disciplines, especially neontologists, medical scientists, and engineers. Of course, this has always been the case to some degree – expect to see more of it.

As an activity, science is poorly understood and often caricatured, and in some cases it is too complicit in this. Although most people who are involved in scientific research fully appreciate the creativity that is involved and required, we often fail to communicate this aspect to people in other spheres of life. Instead, we allow our work to be presented as a simple application of the 'observe-hypothesise-experiment-

test' formula. My own experience is that science does not work like this, and it would be disingenuous to create the impression that, in starting this thesis, I set out to test a particular hypothesis of ecology in *Kronosaurus*. Rather, I had a more foggy idea of exploring the information provided by the fossils and seeing what patterns might arise. As such, I'm not really sure of whether I've tested any theories or rejected any hypotheses – being able to write a report that makes it look like you did does not mean that you actually did it that way – but I think I've got a better idea of what *Kronosaurus* might have been doing, and I've certainly got a pile of questions about cetaceans, seals, and crocodiles that I would like to explore. In particular, I'm now extremely curious about the natural history of the Orinoco crocodile. Also, I'm starting to wonder if the majority of the attention given to post-Neocomian marine ecosystems isn't really a footnote to the evolution of clupeomorph teleosts and lamniform sharks. Ultimately, I can only hope that others find some value in this work. If nothing else, it has certainly heightened my appreciation and enjoyment of the richness and complexity of living ecosystems and the history of life on Earth.

8.6 References

Acevedo-Gutiérrez, A., D. A. Croll, and B. R. Tershy. 2002. High feeding costs limit dive time in the largest whales. Journal of Experimental Biology 205:1747-1753.

Alexander, R. M. 1989. Dynamics of Dinosaurs and Other Extinct Giants. Colombia University Press, New York.

Andrews, C. W. 1913. A descriptive catalogue of the Marine Reptiles of the Oxford Clay, Part II. BM(NH), London.

Auffenberg, W. 1981. The behavioural ecology of the Komodo monitor. University Presses of Florida.

Bassoi, M. 2005. Feeding ecology of franciscana dolphin, *Pontoporia blainvillei* (Cetacea: Pontoporiidae), and oceanographic processes on the Southern Brazillian coast. University of Southampton, Ph.D. Thesis.

Berta, A., J. L. Sumich, and K. M. Kovacs. 2006. Marine Mammals: Evolutionary Biology. Academic Press, Burlington.

Blanco-Piñón, A., K. Shimada, and G. González-Barba. 2005. Lamnoid vertebrae from the Agua Nueva Formation (Upper Cretaceous: lower Turonian, northeastern Mexico. Revista Mexicana de Ciencias Geológicas 22(1):19-23.

Bloodworth, B., and C. D. Marshall. 2005. Feeding kinematics of *Kogia* and *Tursiops* (Odontoceti: Cetacea): characterisation of suction and ram feeding. Journal of Experimental Biology 208:3721-3730.

Brodie, P. F. 1993. Noise generated by the jaw actions of feeding fin whales. Canadian Journal of Zoology 71:2546-2550.

Brown, D. S. 1981. The English Upper Jurassic Plesiosauroidea (Reptilia) and a review of the phylogeny and classification of the Plesiosauria. Bulletin of the British Museum (Natural History), Geology series 35(4):253-347.

Buchholtz, C. 1990. Cattle. *In* S. P. Parker, ed. Grzimek's Encyclopedia of Mammals (vol. 5). McGraw-Hill, New York.

Busbey, A. B. 1995. The structural consequences of skull flattening in crocodilians. Pp. 173-192. *In* J. Thomason, ed. Functional morphology in vertebrate paleontology. Cambridge University Press, Cambridge.

Cann, J. 1998. Australian Freshwater turtles. Beaumont Publishing, Singapore.

Chatterjee, S., and B. J. Small. 1989. New plesiosaurs from the Upper Cretaceous of Antarctica. Origins and Evolution of the Antarctic Biota. Geological Society Special Pub. 47:197-215.

Cheng, Y., X. Wu, and Q. Ji. 2004. Triassic marine reptiles gave birth to live young. Nature 432:383-386.

Cicimurri, D. J., and M. J. Everhart. 2001. An elasmosaur with Stomach Contents and Gastroliths from the Pierre Shale (Late Cretaceous) of Kansas. Transactions of the Kansas Academy of Science 104(3-4):129-143.

Clarke, J. B., and S. Etches. 1991. Predation amongst Jurassic marine reptiles. Proceedings of the Dorset Natural History and Archaeology Society 113:202-205.

Cremer, M. J., and P. C. Simões-Lopes. 2005. The occurence of Pontoporia blainvillei (Gervais & d;Orbigny) (Cetacea, Pontoporiidae) in an estuarine area in southern Brazil. Revista Brasileria de Zoologia 22(3):717-723.

Crespo, F. A., and L. L. De Cidre. 2005. Functional significance of bronchial sphincters in two Southwestern Atlantic Dolphins: *Pontoporia blainvillei* and *Lagenorhynchus obscurus*: a comparative approach. Mammalia 69(2):233-238.

Croll, D. A., A. Acevedo-Gutiérrez, B. R. Tershy, and J. Urbán-Ramírez. 2001. The diving behavior of blue and fin whales: is dive duration shorter than expected based on oxygen stores? Comparative Biochemistry and Physiology - Part A: Molecular & Integrative Physiology 129A:797-809.

Cruickshank, A. R. I., E. Fordyce, and J. Long. 1999. Recent developments in Australian Sauropterygian palaeontology. Records of the Western Australian Museum (Supplement) 57:23-36.

Culik, B. 2003. Review on Small Cetaceans: Distribution, Behaviour, Migration and Threats. Convention on Migratory Species, United Nations Environment Program, www.cms.int/reports/small_cetaceans/

Druckenmiller, P. S., and A. P. Russell. 2008. A phylogeny of Plesiosauria (Sauropterygia) and its bearing on the systematic status of *Leptocleidus* Andrews, 1922. Zootaxa 1863:1-120.

Dwyer, P. D. 1988. The perception and reconstruction of the apt-organism. Journal of Social and Biological Structures 11:221-233.

Ellis, R. 1982. The Book of Whales. Alfred Knopf, New York.

Ellis, R. 2003. Sea Dragons: predators of the prehistoric oceans. Kansas University Press.

Erickson, G. M., A. K. Lappin, and K. A. Vliet. 2003. The ontogeny of bite-force performance in American alligator (*Alligator mississippiensis*). Zool Lond 260:317–327 260:317-327.

Everhart, M. J. 2004. Plesiosaurs as the food of mosasaurs; new data on the stomach contents of a *Tylosaurus proriger* (Squamata; Mosasauridae) from the Niobrara Formation of western Kansas. The Mosasaur 7:41-46.

Fish, F. E., and C. A. Hui. 1991. Dolphin swimming-a review. Mammal Review 21(4):181-195.

Froese, R., and D. Pauly. 2007. FishBase. www.fishbase.org.

Gaskin, D. E. 1982. The Ecology of Whales and Dolphins. Heinemann, London.

Georges, A., M. Adams, and W. McCord. 2002. Electrophoretic delineation of species boundaries within the genus *Chelodina* (Testudines: Chelidae) of Australia, New Guinea, and Indonesia. Zoological Journal of the Linnean Society 134:401-421.

Gould, S. J., and R. C. Lewontin. 1979. The spandrels of San Marco and the Panglossian paradigm: a critique of the adaptionist programme. Proceedings of the Royal Society Series B 205:581-598.

Hayssen, V. 2008. Cumulative Index of Mammalian Species. American Society of Mammalogists. http://www.science.smith.edu/departments/Biology/VHAYSSEN/msi/.

Hildebrand, M. 1974. Analysis of vertebrate structure. John Wiley & Sons, New York.

Ingle, J. 2007. Scaling of bite force in crocodilians using finite element analysis. University of Newcastle, Unpublished Hons. Thesis.

Jefferson, T., S. Leatherwood, and M. A. Webber. 1993. FAO species identification guide. Marine mammals of the world. FAO, Rome.

Jefferson, T., P. J. Stacey, and R. W. Baird. 1991. A review of Killer Whale interactions with other marine mammals: predation to co-existence. Mammal Review 21(4):151-180.

Kear, B. P. 2003. Cretaceous marine reptiles of Australia: a review of taxonomy and distribution. Cretaceous Research 24:277-303.

Kear, B. P. 2005. A new elasmosaurid plesiosaur from the Lower Cretaceous of Queensland, Australia. Journal of Vertebrate Paleontology 25(4):792-805.

Kear, B. P. 2006a. First gut contents in a Cretaceous sea turtle. Biology Letters 2(1):113-115.

Kear, B. P. 2006b. Reassessment of *Cratochelone berneyi* Longman, 1915, A giant sea turtle from the Early Cretaceous of Australia. Journal of Vertebrate Paleontology 26(3):779-783.

Kear, B. P. 2006c. Marine reptiles from the Lower Cretaceous of South Australia: elements of a high-latitude cold water assemblage. Palaeontology 49(4):837-856.

Kear, B. P. 2007. Taxonomic clarification of the Australian elasmosaurid genus *Eromangasaurus*, with reference to other Austral elasmosaur taxa. Journal of Vertebrate Paleontology 27(1):241-246.

Kear, B. P., W. E. Boles, and E. T. Smith. 2003. Unusual gut contents in a Cretaceous ichthyosaur. Proceedings of the Royal Society Series B 270(Suppl. 2):S206-S208.

Kear, B. P., and M. S. Y. Lee. 2006. A primitive protostegid from Australia and early sea turtle evolution. Biology Letters 2(1):116-119.

Kemp, N. R. 1991. Chondrichthyans in the Cretaceous and Tertiary of Australia. Pp. 497-568. *In* P. Vickers-Rich, J. M. Monaghan, R. F. Baird, and T. H. Rich, eds. Vertebrate Palaeontology of Australasia.

Kohler, N. E., J. G. Casey, and P. A. Turner. 1996. Length-Length and Length-Weight Relationships for 13 Shark Species from the Western North Atlantic. NOAA Technical Memorandum NMFS-NE-110.

Kuhn, T. S. 1962. The Structure of Scientific Revolutions. University of Chicago Press, Chicago.

Lauder, G. V. 1995. On the inference of function from structure. Pp. 1-18. *In* J. J. Thomason, ed. Functional Morphology in Vertebrate Paleontology. Cambridge University Press.

Legler, J. M. 1981. The taxonomy, distribution, and ecology of Australian freshwater turtles (Testudines: Pleurodira: Chelidae). National Geographic Society Research Reports 13:391-404.

Martill, D. 1992. Pliosaur stomach contents from the Oxford Clay. Mercian Geologists 13(1):37-42.

Massare, J. A. 1987. Tooth morphology and prey preference of Mesozoic marine reptiles. Journal of Vertebrate Paleontology 7:121-137.

Massare, J. A. 1988. Swimming capabilities of Mesozoic marine reptiles: implications for methods of predation. Paleobiology 14(2):187-205.

May-Collado, L., and I. Agnarsson. 2006. Cytochrome *b* and Bayesian inference of whale phylogeny. Molecular Phylogenetics and Evolution 38:344-354.

McGowan, C. 1991. Dinosaurs, Spitfires and Sea Dragons. Harvard University Press.

McHenry, C. R., P. D. Clausen, W. J. T. Daniel, M. B. Meers, and A. Pendharkar. 2006. The biomechanics of the rostrum in crocodilians: a comparative analysis using finite element modelling. Anatomical Record 288A:827-849.

McHenry, C. R., A. G. Cook, and S. Wroe. 2005. Bottom-Feeding Plesiosaurs. Science 310:75.

McHenry, C. R., S. Wroe, P. D. Clausen, K. Moreno, and E. Cunningham. 2007. Supermodeled sabercat, predatory behavior in *Smilodon fatalis* revealed by high-resolution 3D computer simulation. Proceedings of the National Academy of Sciences 104(41):16010-16015.

Meers, M. B. 2003. Maximum Bite Force and Prey Size of *Tyrannosaurus rex* and Their Relationships to the Inference of Feeding Behavior. Historical Biology 16(1):1-12.

Molnar, R. E. 1991. Fossil Reptiles of Australia. Pp. 605-701. *In* P. Vickers-Rich, J. M. Monaghan, R. F. Baird, and T. H. Rich, eds. Vertebrate Palaeontology of Australasia.

Moreno, I. B., C. C. A. Martins, A. Andriolo, and M. H. Engel. 2003. Sightings of Franciscana Dolphins (*Pontoporia blainvillei*) off Espirito Santo, Brazil. Latin American Journal of Aquatic Mammals 2(2):131-132.

Nagorsen, D. 1985. *Kogia simus*. Mammalian Species 239:1-6.

Naish, D. 2008. Terrestrial stalking azhdarchids, the paper. Tetrapod Zoology (http://scienceblogs.com/tetrapodzoology)

Noè, L. F. 2001. A Taxonomic and Functional Study of the Callovian (Middle Jurassic) Pliosauroidea (Reptilia, Sauropterygia). Unpublished PhD Thesis. University of Derby.

Patterson, I. A. P., R. J. Reid, B. Wilson, K. Grellier, H. M. Ross, and P. M. Thompson. 1998. Evidence for infanticide in bottlenose dolphins: an explanation for violent interactions with harbour porpoises? Proceedings of the Royal Society Series B 265:1167-1170.

Persson, P. O. 1960. Lower Cretaceous plesiosaurs (Reptilia) from Australia.

Pirsig, R. M. 1974. Zen and the Art of Motorcycle Maintenance. William Morrow & Co.

Plotnick, R. E., and T. K. Baumiller. 2000. Invention by Evolution: Functional Analysis in Paleobiology. Paleobiology 26(4):305-323.

Popowics, T. E., and S. W. Herring. 2007. Load transmission in the nasofrontal suture of the pig, *Sus scrofa*. Journal of Biomechanics 40(4):837-844.

Price, E. R., B. P. Wallace, R. D. Reina, J. R. Spotila, F. V. Paladino, R. Piedra, and E. Vélez. 2004. Size, growth, and reproductive output of adult female leatherback turtles *Dermochelys coriacea*. Endangered Species Research 5:1-8.

Rauschmann, M. A., S. Huggenbebrger, L. S. Kossatz, and H. H. A. Oelschläger. 2006. Head Morphology in Perinatal Dolphins: A Window Into Phylogeny and Ontogeny. Journal of Morphology 267(1295-1315).

Rayfield, E. J. 2004. Cranial mechanics and feeding in *Tyrannosaurus rex*. Proceedings of the Royal Society Series B 271:1451-1459.

Ross, C. A., and S. Garnett, eds. 1989. Crocodiles and alligators. Facts on File, New York.

Ross, H. M., and B. Wilson. 1996. Violent interactions between bottlenose dolphins and harbour porpoises. Proceedings of the Royal Society Series B 263:283-286.

Rudwick, M. J. 1964. The inference of function from structure in fossils. British Journal for the Philosophy of Science 15(27-40).

Salisbury, S. W., and E. Frey. 2001. A biomechanical transformation model for the evolution of semi-spheroidal articulations between adjoining vertebral bodies in crocodilians. Pp. 85-134. *In* G. C. Grigg, C. E. Franklin, and F. Seebacher, eds. Crocodilian Biology and Evolution. Surrey Beatty & Sons, Chipping Norton.

Schreer, J. F., and K. M. Kovacs. 1997. Allometry of diving capacity in air-breathing vertebrates. Canadian Journal of Zoology 75(3):339-358.

Schumacher, G. H. 1985. Comparative functional anatomy of jaw muscles in reptiles and mammals. Pp. 203–212. *In* Duncher, and Fleischer, eds.

Proceedings of the First International Symposium on Vertebrate Morphology, Giessen, 1983. Gustav Fisher Verlag, Stuttgart.

Shimada, K. 1997a. Paleoecological relationships of the Late Cretaceous Lamniform Shark, *Cretoxyrhina mantelli* (Agassiz). Journal of Paleontology 7(5):926-933.

Shimada, K. 1997b. Skeletal anatomy of the Late Cretaceous lamniform shark, *Cretoxyrhina mantelli*, from the Niobrarra Chalk in Kansas. Journal of Vertebrate Paleontology 17(4):642-652.

Shimada, K. 2008. Ontogenetic parameters and life history strategies of the Late Cretaceous lamniform shark, *Cretoxyrhina mantelli*, based on vertebral growth increments. Journal of Vertebrate Paleontology 28(1):21-33.

Shimada, K., S. L. Cumbaa, and D. Van Rooyen. 2006. Caudal fin skeleton of the Late Cretaceous lamniform shark, *Cretoxyrhina mantelli*, from the Niobrarra Chalk of Kansas. Bulletin of the New Mexico Museum of Natural History 35:185-192.

Shimada, K., and M. J. Everhart. 2004. Shark-bitten *Xiphactinus audax* (Teleostei: Ichthyodectiformes) from the Niobrarra Chalk (Upper Cretaceous) of Kansas. The Mosasaur 7:35-39.

Sigurjónsson, J. 1995. On the life history and autecology of North Atlantic rorquals. Pp. 425-441. *In* A. S. Blix, L. Walløe, and Ø. Ulltang, eds. Whales, Seals, Fish and Man. Elsevier Science.

Stacey, P. J., S. Leatherwood, and R. W. Baird. 1994. *Pseudorca crassidens*. Mammalian Species 456:1-6.

Stewart, B. E., and R. E. A. Stewart. 1989. *Delphinapterus leucas*. Mammalian Species 336:1-8.

Sun, Z., E. Lee, and S. W. Herring. 2004. Cranial sutures and bones: Growth and fusion in relation to masticatory strain. The Anatomical Record Part A: Discoveries in Molecular, Cellular, and Evolutionary Biology 276A(2):150-161.

Taylor, M. A. 1987. How tetrapods feed in the water: a functional analysis by paradigm. Zoological Journal of the Linnean Society 91:171-195.

Taylor, M. A. 1992. Functional anatomy of the head of the large aquatic predator *Rhomaleosaurus zetlandicus* (Plesiosauria, Reptilia) from the Toarcian (Early Jurassic) of Yorkshire, England. Philosophical Transactions of the Royal Society, London B 335:247-280.

Taylor, M. A., D. B. Norman, and A. R. I. Cruickshank. 1993. Remains of an ornithischian dinosaur in a pliosaur from the Kimmeridgian of England. Palaeontology 36(2):357-360.

Taylor, M. A. D., and A. R. I. Cruickshank. 1993. Cranial anatomy and functional morphology of *Pliosaurus brachyspondylus* (Reptilia: Plesiosauria) from the Late Jurassic of Westbury, Wiltshire. Philosophical Transactions of the Royal Society London. B 341:399-418.

Thomason, J. J. 1991. Cranial strength in relation to estimated biting forces in some mammals. Canadian Journal of Zoology 69:2326-2333.

Thulborn, T., and S. Turner. 1993. An elasmosaur bitten by a pliosaur. Modern Geology 18:489-501.

Turnbull, W. D. 1970. Mammalian masticatory apparatus. Fieldiana: Geology 18:149-356.

Welles, S. P. 1943. Elasmosaurid Plesiosaurs with description of new material from California and Colorado. Memoirs of the University of California 13(3):125-254.

Welles, S. P. 1962. A new Species of Elasmosaur from the Aptian of Colombia and a review of the Cretaceous Plesiosaurs.

Wroe, S., D. R. Huber, M. Lowry, C. McHenry, K. Moreno, P. Clausen, T. L. Ferrara, E. Cunningham, M. N. Dean, and A. P. Summers. 2008. Three-dimensional computer analysis of white shark jaw mechanics: How hard can a great white bite? J. Zoology Online.

Wroe, S., C. McHenry, and J. Thomason. 2005. Bite club: comparative bite force in big biting mammals and the prediction of predatory behaviour in fossil taxa. Proceedings of the Royal Society of London, Series B 272:619-625.

Young, M. T. 2007. Evolution and taxonomic revision of the Mesozoic marine crocodyliforms Metriorhynchidae, and phylogenetic and morphometric approach. University of London, M.Sc. Thesis.